INTERROGATION OF TELOMERASE STRUCTURE AND FUNCTION WITH TELOMERIC DNA

Ian K. Moon

A dissertation submitted to the faculty of the University of North Carolina at Chapel Hill in partial fulfillment of the requirements for the degree of Pharmaceutical Sciences in the School of Pharmacy (Division of Medicinal Chemistry and Natural Products).

Chapel Hill
2007

Approved by

Advisor: Michael B. Jarstfer, Ph.D.

Reader: Kenneth Bastow, Ph.D.

Reader: Scott Singleton, Ph.D.

Reader: Shawn Ahmed, Ph.D.

Reader: Clark Jeffries, Ph.D.

ABSTRACT

IAN K. MOON: Interrogation of Telomerase Structure and Function with Telomeric DNA
(Under the direction of Michael B. Jarstfer)

The studies described in this dissertation are directed toward understanding one of the components of a mechanism that cancer cells use to escape apoptosis and maintain genetic stability, resulting in cellular immortalization. Telomeres are nucleoprotein structures at the ends of eukaryotic chromosomes that are essential for safeguarding genomic stability and in regulating the lifespan of cellular replication. Telomerase is a specialized ribonucleoprotein complex that functions as a reverse transcriptase to extend the 3' end of the telomere, resulting in telomere conservation, and thus chromosomal stabilization. In greater than 85% of all cancer cells, telomerase is upregulated to rescue eroded telomeres and stabilize chromosomes, resulting in cellular immortalization. Because most somatic cells do not express detectable levels of telomerase, telomere-telomerase interactions are important in understanding cellular immortalization and aging, and developing specific anti-cancer therapeutics. Despite the great interest in telomerase, the mechanism of telomerase-catalyzed reverse transcription is not fully understood, and little is known about the structure of this intriguing enzyme.

Each chapter, herein, describes novel research that investigates telomerase oligomerization and interactions between telomerase and model telomeric structures. More specifically, Chapter II focuses on the characterization and visualization of cooperative *Euplotes aedicualtus* telomerase dimers by gel filtration chromatography and electron microscopy.

Chapter III details the formation, isolation, and characterization of G-quadruplex DNA structures by native gel electrophoresis, while Chapter IV documents novel interactions between a subset of G-quadruplex DNA structures and *Euplotes aediculatus* telomerase. Chapter V concludes the dissertation with a retrospective analysis of the research herein.

ACKNOWLEDGEMENTS

For the realization and culmination of this doctoral dissertation, I am indebted to the fine scientists and educators whom imparted their knowledge and encouragement, and more profoundly to my parents Keith and Emily Moon for their love and support.

TABLE OF CONTENTS

LIST OF TABLES

LIST OF FIGURES

CHAPTER I

INTRODUCTION

The Telomere

In life there are two general classes of chromosomes, linear and circular. Linear chromosomes pose a unique problem in that their ends, known as telomeres (in Latin: "telo" means "end" and "mere" means "part"), resemble double-stranded DNA breaks. If left unguarded, the telomeres are susceptible to an array of deleterious outcomes including erosion, due to incomplete DNA replication and nucleolytic degradation, and chromosomal end-to-end fusions that result in double-stranded DNA damage during meiosis (Blasco, 2005; de Lange, 2002; Smogorzewska and de Lange, 2004). To protect against these pitfalls, the eukaryotic cell has devised mechanisms, which require extra energy, to ensure proper telomere maintenance. Despite the problems inherent to linear chromosomes, all higher order organisms and some viruses and bacteria maintain their genetic information as linear DNA (Nosek *et al.*, 2006). The results of several studies suggest that linear chromosomes, and their telomeres, are essential for successful meiosis in eukaryotes and are therefore a requirement for sexual reproduction (Ishikawa and Naito, 1999; Jordan, 2006). This would further postulate that the advantages inherent to sexual reproduction must offset the disadvantages inherent to maintaining the ends of linear chromosomes.

Biological Roles of the Telomere

Telomeres are important factors that ensure chromosomal stability and integrity during various cellular processes (Blasco, 2005; de Lange, 2002; de Lange, 2005). Telomeres, the physical ends of the chromosome, are specialized protein-DNA complexes that conserve the genetic information during DNA replication, protect the chromosome ends from recognition as sites of DNA damage, and control the replicative capacity of cells. Foremost, telomeres protect the ends of eukaryotic chromosomes from recognition as regions of double-stranded DNA breaks, repress nonhomologous chromosomal end-to-end fusions and homologous recombination events, and control telomere processing post DNA replication. Telomere dysfunction due to the loss of telomeric DNA, mutations in the telomeric sequence, or mutations in or loss of telomere binding proteins results in improper telomere end-capping. Dysfunctional telomeres induce a telomere-specific DNA damage response that can lead to rapid cell growth arrest, chromosomal instability, and apoptosis.

While telomeres in part act as a steric blocks that safeguard the genetic information located within chromosomes, telomeres also serve as a substrate for the specialized reverse transcriptase, telomerase (Autexier and Lue, 2006). The normal DNA replication machinery is incapable of replicating the very 5' end of the chromosome resulting in the loss of DNA during every cell cycle. Several mechanisms to overcome this end replication problem have been observed, however elongation by the enzyme telomerase is the most frequently used mechanism. Thus, the telomeric 3' overhang is extended by telomerase while the complementary strand is replicated by the normal DNA replication machinery.

Beyond the scope of telomere maintenance, telomeres also serve as larger architectural elements in the nucleus that anchor chromosomes to the nuclear matrix (Luderus *et al.*, 1996), facilitate chromosomal organization (Chuang *et al.*, 2004; Lipps, 1980; Lipps *et al.*, 1982; Paeschke *et al.*, 2005), and in the case of replicatively quiescent human cells, telomeres are associated in nonrandom spatial arrangements during interphase (Nagele *et al.*, 2001). It has been proposed that the arrangement of such associations play a role in chromosome positional stability.

Furthermore, the clustering of telomeres that forms the telomeric bouquet, during zygotene, is important for pairing of chromosomes as well as the homologous recombination of chromosomes that occurs during meiosis. Mutations in *Saccharomyces pombe* (Chikashige and Hiraoka, 2001), *Saccharomyces cerevisiae* (Trelles-Sticken *et al.*, 1999), and maize (Golubovskaya *et al.*, 2002) that affect telomere structure and prevent proper telomere bouquet formation, exhibit faulty homologous chromosome pairing and abnormal chromosomal segregation (Cooper *et al.*, 1998; Nimmo *et al.*, 1998). In *Caenorhabditis elegans*, mortal germ line mutants showed progressive telomere shortening which resulted in chromosome fusions, the onset of senescence, and ultimately sterility, most likely do to meiotic non-disjunction and massive aneuploidy (Ahmed and Hodgkin, 2000). Similarly in telomerase negative mice, telomere shortening lead to a reduction in proliferation and an increase in apoptosis in germ line cells, further supporting a link between proper telomere maintenance and proper meiosis in mammals (Lee *et al.*, 1998).

In human physiology, the importance of proper telomere structure and function is evident in development (Bekaert *et al.*, 2004), aging (Geserick and Blasco, 2006), and

tumorigenesis (Blasco, 2005). Cellular stability and replication depend, in part, on the structure of the telomere, and in turn on telomere length, as the structure is length dependent. Thus, the telomere also serves as a mitotic clock, which regulates cellular senescence as telomeres naturally erode and approach the Hayflick limit (Hayflick, 1965). The limitation of cellular replicative capacity is postulated to protect healthy organisms against neoplastic growth associated with the onset of cancer.

Structures of the Telomere

Generally, the telomere is composed of noncoding, tandem repeats of short guanosine-rich (G-rich) sequence and telomere-specific proteins as well as canonical chromatin. Notably, the G-rich strand of telomeric DNA is oriented in the 5' to 3' direction pointing toward the end of the chromosome and is composed of two parts, a double-stranded DNA region followed by a single-stranded DNA region ending in a 3' overhang (Figure 1.1). The length of the double-stranded region, the length of the single-stranded region, and the sequence of the repeat unit are species dependent (Table 1.1). In *Euplotes aediculatus*, the 3' overhang is precisely 14 nucleotides long with the G-strand terminating in 5'-$G_2T_4G_2$-3' and the C-strand terminating in 3'-A_4C_4-5' (Klobutcher *et al.*, 1981). In *Tetrahymena thermophila*, the G-strand ends in 5'-TG_4T-3' and the C-strand terminates in 3'-CA_2C_3-5' or 3'-$C_2A_2C_2$-5' (Fan and Price, 1997; Jacob *et al.*, 2003; Jacob *et al.*, 2001). Due to the sequence variability in the 5' end, this suggests that the C- and G-strands are processed separately. While the lengths of the double and single-stranded telomeric regions are short and precisely maintained in ciliates, in humans these same lengths are much longer and more heterogeneous. Surprisingly, the 5' end of the C-strand of the human telomere was found to terminate precisely in the sequence 3'-CCAATC-5' in 80 percent of telomeres (Sfeir *et al.*, 2005). However, the G-strand was found to be less precise and telomerase-dependent. This suggests that after replication a highly specific nuclease or protein binding affects processing of the C-strand. One factor contributing to the C-strand end-sequence is the protection of telomeres 1 (POT1) protein, as RNAi knock down of POT1 resulted in the shortening of telomeres and the change of ending sequence to a random position within the 3'-A_2TC_3-5' repeat (Hockemeyer *et al.*, 2005).

Perhaps POT1 binds the single-stranded overhang during processing to affect the terminal sequence.

The telomere also consists of telomere-specific proteins and nucleosome arrays characteristic of heterochromatin (Garcia-Cao *et al.*, 2004), as telomeres are transcriptionally inactive. In humans, the telomere-associated heterochromatin is composed of the heterochromatin protein 1 (HP1) isoforms HP1α, HP1β, and HP1γ, and is enriched with histone modifications at histone 3 trimethylated at lysine 9 (H3-K9) and histone 4 trimethylated at lysine 20 (H3-K20) (Garcia-Cao *et al.*, 2004). Furthermore, the larger end-capping complex of the human telomere, known as shelterin (Figure 1.2.A), has several unique proteins that are important in forming proper telomere structure, known as the T-loop (Figure 1.2.B). Shelterin is composed of double-stranded telomeric DNA binding factors 1 and 2 (TRF1 and TRF2), the single-stranded binding protein protection of telomeres 1 (POT1), and the three inter-connecting proteins RAP1, TIN2, and TPP1 (Figure 1.2.A).

In ciliated protozoan, as was shown in *Stylonychia lemnae,* the short telomeric 3' overhang is capped with telomere binding proteins α and β (TeBPα and TeBPβ). Together, TeBPα and TeBPβ induce the formation of a terminal intermolecular G-quadruplex structure with neighboring telomeres (Figure 1.2.F) (Paeschke *et al.*, 2005).

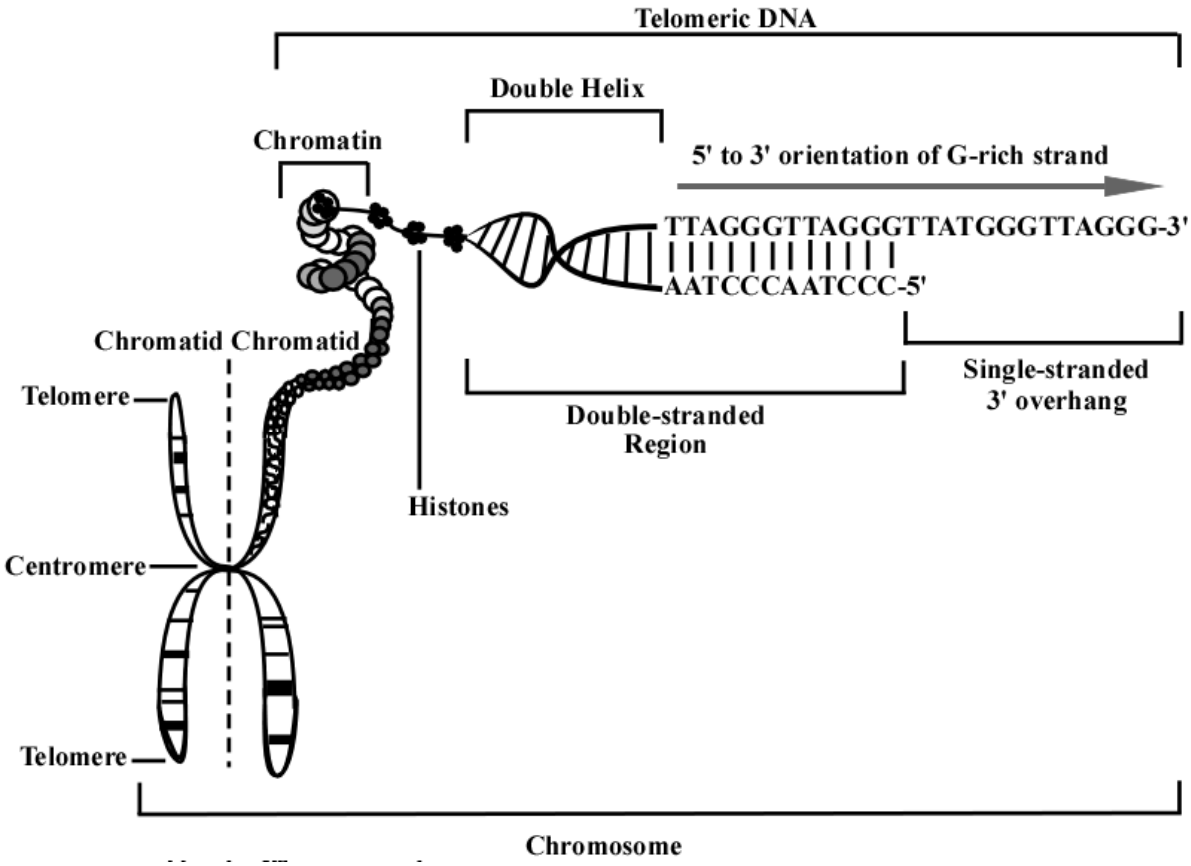

Figure 1.1. General structure of eukaryote chromosomes. The DNA portion of the telomere consists of a double-stranded region followed by a protruding single-stranded 3' overhang. The human telomeric repeat 5'-T_2AG_3-3' is depicted. Note the guanosine-rich strand runs 5' to 3' (grey arrow) toward the end of the chromosome. Telomeric proteins and telomere structure are not depicted.

Table 1.1. Description of the telomere lengths and sequence in telomerase-dependent organisms. Table from (Moon and Jarstfer, 2007).

Group	**Organism**	**Telomere length, dsDNA**	**Telomere Length, G-overhang**	**Telomere sequence (3' strand, orientated 5'-3')**
Vertebrate	Human	5 - 15 kb	60-600 nt	TTAGGG
Vertebrate	Lab mouse	~30 to 120 kb	150-200 nt	TTAGGG
Filamentous fungi	*Neurospora crassa*	~150 bp	ND	TTAGGG
Filamentous fungi	*Didymium*	100-400 bp	ND	TTAGGG
Kinetoplastid protozoa	*Trypanosoma brucei*	3 - 20 kb	< 30 nt	TTAGGG
Ciliate	*Tetrahymena*	250-400 bp	14-15 or 20-21 nt	TTGGGG
Ciliate	*Euplotes*	exactly 28 bp	exactly 14 nt	TTTTGGGG
Higher plant	*Arabidopsis thaliana*	2.5 - 5 kb	>20-30 nt	TTAGGG(T/C)
Green algae	*Chlamydomonas*	300-350 bp	ND	TTTAGGG
Insect	*Bombyx mori*	6 - 8 kb	ND	TTAGG
Roundworm	*C. elegans*	2-4 kb	ND	TTAC(A)(C)G(1-8)
Budding yeast	*Saccharomyces cerevisiae*	~300 ± 75 bp	12-16 nt (50 - 100 nt at the end of S phase)	G(2-3)(TG)(1-6)T
Budding yeast	*Candida albicans*	0.5 - 2.5 kb	ND	GGTGTACGGATGTCTAACTTCTT

The T-Loop

Electron microscopic examination of human and murine telomeric DNA showed that mammalian telomeres form a lasso-like structure, termed the T-Loop (Figure 1.2.B) (Griffith *et al.*, 1999). In these studies, the chromosomal DNA was psoralen cross-linked and subsequently stripped of its proteins to ensure that the native structure remained, without chance of dissociation upon protein removal. It was later shown that isolated telomeric chromatin from avian erythrocytes and murine lymphocytes exhibited the same lasso-like structure (Nikitina and Woodcock, 2004). It was proposed that the formation of the T-loop was due to the invasion of the single-stranded 3' overhang of the telomere into the double-stranded DNA region, which would result in a displacement loop. Using the single-stranded binding protein from *Escherichia coli* (SSB) as a probe, it was determined that a displacement loop (D-Loop) was evident at the T-Loop junction, ruling out the formation of a DNA triplex structure (Griffith *et al.*, 1999). Several structures can be imagined to form at the D-Loop (Figures 1.2.C-E). The most simple is the invasion and base pairing of the G-rich 3' overhang with the C-strand, thus displacing the G-strand from the double-stranded region (Figure 1.2.C). Another more stable structure would be the formation of a Holliday junction-like structure, where the 5' end of the C-strand base pairs with the displaced G-strand (Figure 1.2.D). An alternative structure would be the formation of an intermolecular G-quadruplex between the invading G-rich 3' overhang and the G-strand from the double-stranded region, thus displacing the C-strand (Figure 1.2.E). Furthermore these T-loop structures have been observed in the ciliated protozoan *Oxytricha fallax* (Murti and Prescott, 1999), the kinetoplastid protozoan *Trypanosoma*

brucei (Munoz-Jordan *et al.*, 2001), in the mitochondrial DNA of yeasts (Tomaska *et al.*, 2002), and in plants (Cesare *et al.*, 2003) highlighting their evolutionary conservation.

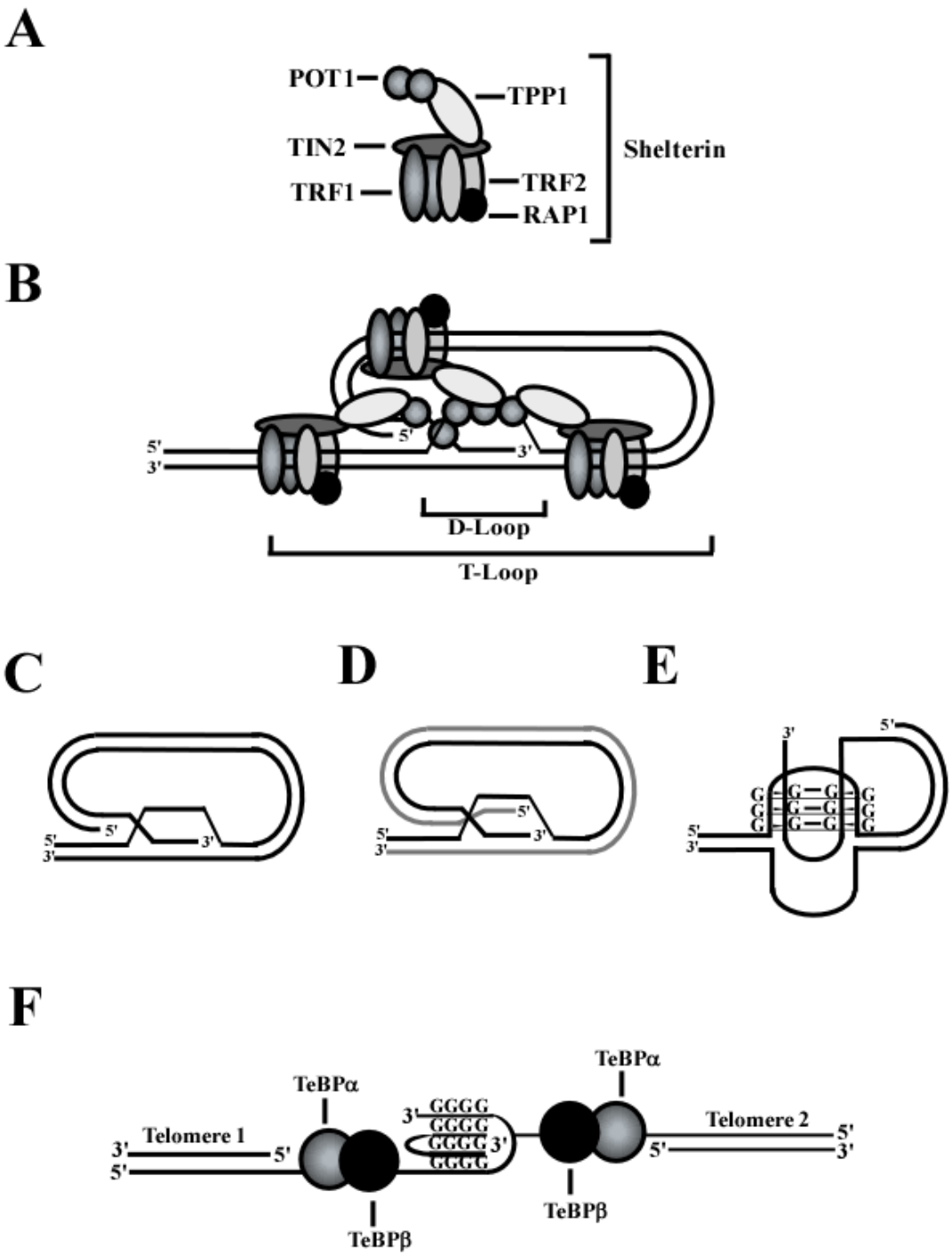

Figure 1.2. Telomere end-capping structures. (A) Shelterin complex. (B) T-Loop structure stabilized by shelterin. (C-D) Proposed D-loop structures. (F) Ciliate telomeres, with bound TeBPα and TeBPβ, joined by an intermolecular antiparallel G-quadruplex.

Single-stranded Telomeric DNA forms G-quadruplexes

Single-stranded guanosine-rich sequences that mimic telomeric DNA have the propensity to fold into higher order structures, termed G-quadruplexes (Figure 1.4), under physiological conditions *in vitro*. The guanosine residues in a G-quadruplex form a cyclic array stabilized through Hoogsteen hydrogen bonding and a centrally located monovalent or divalent cation, resulting in a G-quartet (Figure 1.3.A). These G-quartets can stack upon each other to form the unique nucleic acid structures known as G-quadruplexes (Figure 1.3.B and C). Diverse folding topologies have been observed for G-quadruplexes, as their variance depends on multiple factors including: strand stoichiometry, pattern of the strand orientation, the sequence intervening between the runs of guanosine, the identity of the stabilizing cation (typically sodium or potassium), and annealing conditions. Molecules containing one telomeric repeat are able to form four-stranded, parallel intermolecular G-quadruplexes, meaning the 5' to 3' orientation of the sugar-phosphate backbone of each molecule is facing the same direction in relation to the other molecules in the complex, and the glycosidic bond for each guanosine is positioned in the *anti* conformation. Molecules containing two telomeric repeats are capable of forming an array of dimeric, trimeric, and tetrameric G-quadruplexes. Furthermore, molecules that contain four telomeric repeats are able to fold into intramolecular G-quadruplexes or into various intermolecular G-quadruplexes depending on folding conditions.

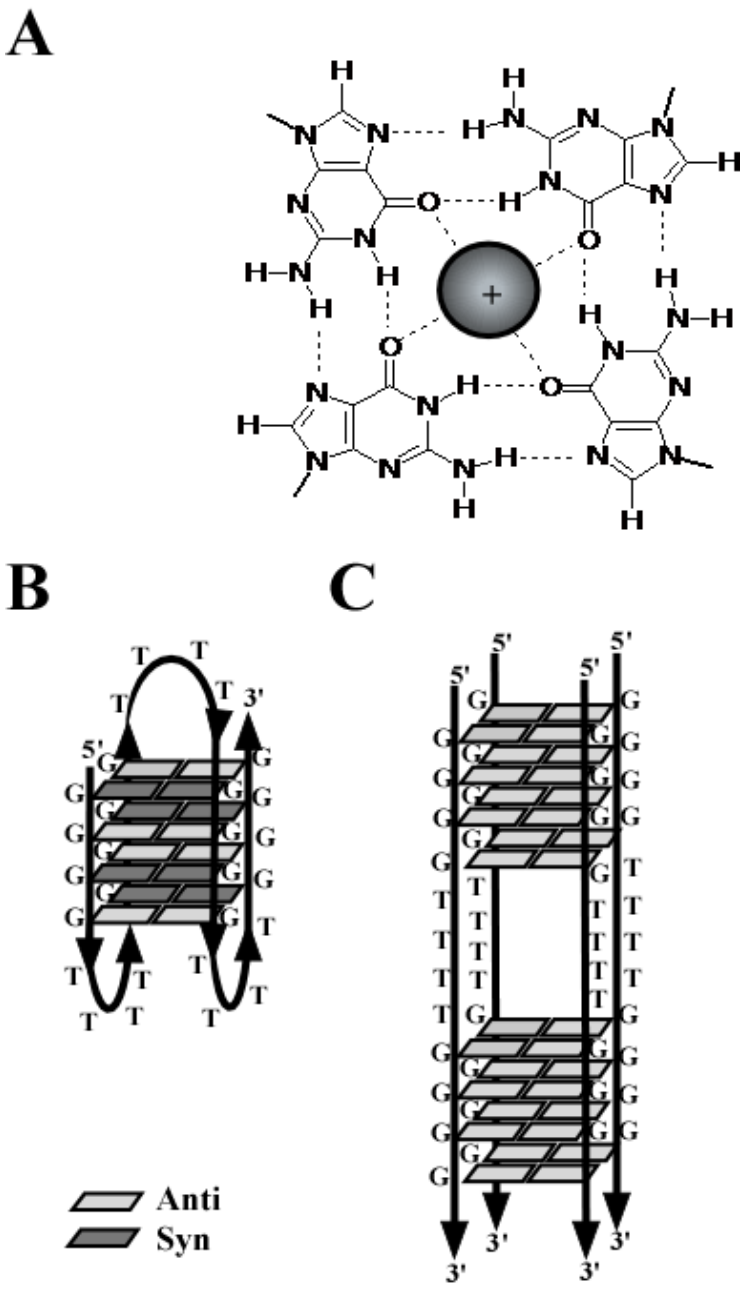

Figure 1.3. G-quadruplex DNA structures. (A) G-quartet where four guanine residues are coordinated by Hoogsteen hydrogen bonding accompanied by a centrally located cation. (B) An intramolecular antiparallel G-quadruplex (Smith *et al.*, 1995; Wang and Patel, 1995). (C) An intermolecular parallel G-quadruplex (Oganesian *et al.*, 2006).

G-quadruplex structures formed by DNA sequences consisting of one, two, and four telomeric repeats have been analyzed using biophysical techniques, such as NMR and X-ray crystallography. Usually the conditions used to form these G-quadruplexes are modeled using physiologic parameters such as salt concentrations, molecular crowding, and a biologically relevant pH.

Many G-quadruplex structures have been identified using various permutations of the telomeric repeats inherent to several organisms such as human, *Tetrahymena thermophila*, and *Euplotes aediculatus*. The following examples of G-quadruplexes do not serve as an exhaustive list, however they suitably illustrate the diversity of G-quadruplex structures formed by telomeric DNA. In solution, the human and *Tetrahymena* DNA single repeats of 5'-T_2AG_3-3' and 5'-T_2G_4-3' respectively, formed four-stranded parallel G-quadruplexes in the presence of potassium, and contained all *anti* glycosidic torsion angles (Figure 1.4.A and B) (Wang and Patel, 1992). Interrogation of the human two-repeat sequence 5'-$TAG_3T_2AG_3T$-3' revealed interconverting parallel and antiparallel dimeric G-quadruplexes in the presence of potassium in solution (Figure 1.4.C) (Phan and Patel, 2003). However, upon crystallization in potassium, the 5'-$TAG_3T_2AG_3T$-3' sequence only yielded the parallel dimeric G-quadruplex (Parkinson *et al.*, 2002). Further investigation by NMR of the *Tetrahymena* two-repeat sequence 5'-$TG_4T_2G_4T$-3' in sodium, exhibited the formation of two dimeric antiparallel G-quadruplexes, where the intervening loops were either at the same end or opposite ends of the G-tetrad core (Figure 1.4.D) (Phan *et al.*, 2004). The *Euplotes* two-repeat sequence 5'-$G_4T_4G_4$-3' has been observed to form a diagonal G-quadruplex dimer in potassium and sodium in solution (Figure 1.4.E) (Schultze *et al.*,

1994; Smith and Feigon, 1993), while crystallization in the presence of potassium resulted in the diagonal G-quadruplex dimer (Haider *et al.*, 2002) and in a separate study a G-quadruplex dimer with intervening loops at opposite ends of the G-tetrad core (Figure 1.4.F) (Kang *et al.*, 1992). An interesting and unusual (3+1) structure was observed for the human three-repeat sequence 5'-$G_3T_2AG_3T_2AG_3T$-3' in the presence of sodium in solution. A unique dimeric asymmetric G-quadruplex was formed, where the G-tetrad core consisted of three telomeric repeats from a single molecule and one telomeric repeat from a second molecule. The (3+1) denotes that the orientation of three telomeric repeats that make up the G-tetrad core are parallel while the remaining repeat is antiparallel (Figure 1.4.G) (Zhang *et al.*, 2005). Oligonucleotides that contain four-repeats form a variety of structures depending on the specific sequence contained by the repeat. The four-repeat sequence 5'-$AG_3(T_2AG_3)_3$-3', upon crystallization in potassium, formed a parallel propeller-like G-quadruplex (Figure 1.4.H) (Parkinson *et al.*, 2002). Furthermore, the mutated four-repeat sequence 5'-$T_2G_3(T_2AG_3)_3A$-3' revealed the formation of a mixed (3+1) G-quadruplex in solution in the presence of potassium (Figure 1.4.I) (Ambrus *et al.*, 2006; Luu *et al.*, 2006). The *Euplotes* four-repeat sequence 5'-$G_4(T_4G_4)_3$-3' formed a crossover basket antiparallel intramolecular G-quadruplex in the presence of sodium or potassium in solution (Figure 1.4.J) (Smith *et al.*, 1995; Wang and Patel, 1995).

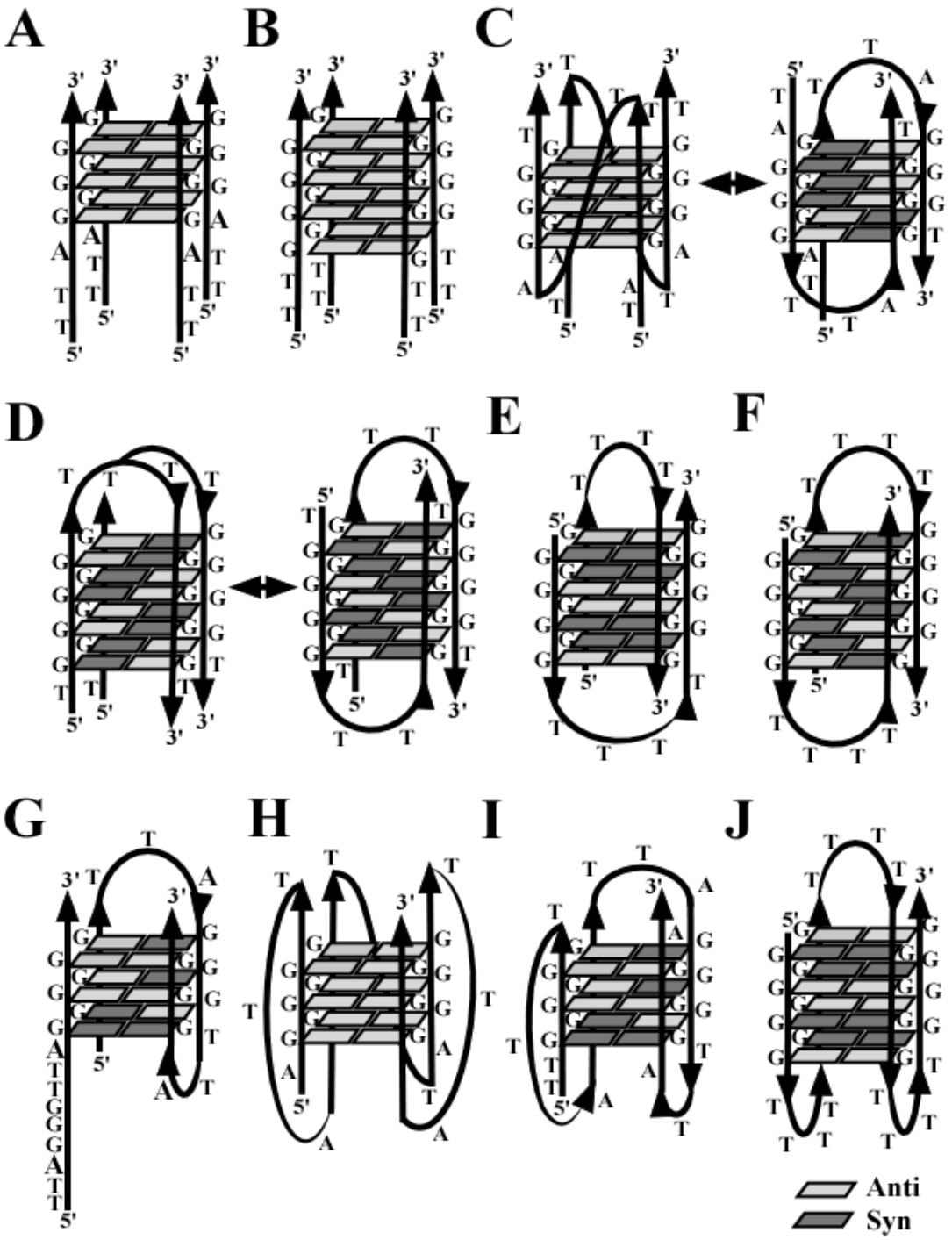

Figure 1.4. G-quadruplexes formed by telomeric DNA sequences. *Anti* and *syn* refer to the orientation of the glycosidic bond torsion angle of the guanosine residue within the G-quartets.

While the existence of G-quadruplex formation *in vitro* is well established, the evidence for these structures occurring *in vivo* and a description of their biological roles remain controversial. While proof that G-quadruplexes exist *in vivo* is not conclusive, mounting evidence supporting their existence originates from studies that investigate the effect that G-quadruplex-stabilizing agents have on cells, the development of structure-specific molecular probes for identifying G-quadruplexes in cells, and the identification and characterization of proteins that preferentially interact with G-quadruplex structures, which collectively suggest that these structures do form in certain situations in the cell (Cairns *et al.*, 2002; Neidle, 2001; Neidle and Read, 2000; Oganesian and Bryan, 2007).

The most convincing evidence that G-quadruplex structures exist at the telomeres comes from research conducted in the organism *Stylonichia lemnae* (Paeschke *et al.*, 2005; Schaffitzel *et al.*, 2001). The synthetic single-chain antibody fragments Sty49, which targets both parallel and antiparallel G-quadruplexes, and Sty3, specific only for parallel G-quadruplexes, were used to probe the macronucleus and micronucleus of vegetative *Stylonichia*. Only Sty49, but not Sty3, emitted a strong signal in the transcriptionally active macronucleus, but not the transcriptionally dormant micronucleus, supporting the existence of antiparallel G-quadruplexes *in vivo*. This result however does not dismiss the existence of parallel G-quadruplexes *in vivo*. Furthermore, the replication band, the region where DNA replication and telomere elongation take place, did not emit a signal suggesting that G-quadruplexes may be resolved for these processes to take place.

In other research, human chromosomal DNA was treated with a novel fluorescent ligand, 3,6-bis(1-methyl, 4-vinylpyridinium)carbazole diiodide (BMVC), which resulted

in G-quadruplex-specific fluorescence emissions in telomere-proximal sites, consistent with the presence of G-quadruplexes in human telomeres (Chang *et al.*, 2004). Autoradiography assays analyzing meta-phase spreads of normal human cells (peripheral blood lymphocytes) and cancer cells (T98G and CEM1301) that were treated with the radiolabeled, G-quadruplex specific ligand ^{3}H-360A, revealed that ^{3}H-360A preferentially bound G-quadruplex structure in chromosome terminal regions in all cell types (Granotier *et al.*, 2005).

While these studies do support G-quadruplex formation at the ends of chromosomes, through the preferential binding of G-quadruplex-specific antibodies or small molecule ligands, one caveat remains in that the respective ligands could be trapping G-quadruplex structure that would not intrinsically exist in the absence of ligand.

Presently, no functional roles for G-quadruplex DNA at the telomere have been established, however the fact exists that telomeric DNA can form G-quadruplexes under physiologic conditions *in vitro,* suggesting that these structures can arise within the cellular environment. Furthermore, if G-quadruplexes do exist *in vivo*, it is likely that the cell has developed mechanisms that recognize G-quadruplexes, such as proteins that bind to, resolve, cleave, or promote the formation of G-quadruplexes. As is the case, proteins that preferentially interact with G-quadruplex DNA have been identified.

Bloom's (BLM) and Werner's (WRN) syndrome helicases, both RecQ helicases, have been shown to unwind G-quadruplex DNA (Opresko *et al.*, 2004; Sun *et al.*, 1998). BLM and WRN helicases process G-quadruplexes with a 3' to 5' polarity and are dependent on ATP, Mg^{2+}, and a telomeric 3' tail (Mohaghegh *et al.*, 2001; Sun *et al.*, 1998). Furthermore, the telomere-specific binding protein TRF2 which guards and

shapes the end of the telomere, has been shown to bind WRN through the helicase's highly conserved RQC domain, resulting in co-localization at human telomeres and an increase in its unfolding activity of 2-3 fold (Opresko *et al.*, 2002). In the absence of WRN, the telomeres of sister chromatids that are replicated by lagging-strand synthesis are deleted, suggesting that WRN is important in resolving G-quadruplex structure for efficient telomeric DNA synthesis to occur (Crabbe *et al.*, 2004). Also concerning telomere maintenance, WRN is capable of resolving telomeric D-loops (Opresko *et al.*, 2004), of which the exact structure is currently unknown however a G-quadruplex structure has been suggested, supporting the facilitation of T-loop resolution for proper telomeric DNA synthesis. The BLM helicase has also been linked to the telomere through its interaction with telomeric DNA in the presence of telomere-associated proteins and by its association with telomeric DNA in chromatin immunoprecipitation experiments. Upon testing the BLM helicase's ability to unwind duplex telomeric DNA, the telomere-specific proteins TRF2 stimulated unwinding where as TRF1 inhibited it (Lillard-Wetherell *et al.*, 2004). Another telomere-specific protein protection of telomeres 1 (POT1) also exhibited a stimulatory effect on the unwinding of telomeric DNA by WRN and BLM helicases, further substantiating a role for these helicases in telomere maintenance (Opresko *et al.*, 2005).

POT1 has been observed to disrupt intramolecular telomeric G-quadruplexes *in vitro* allowing telomerase to catalyze extension of these otherwise inert primers (Zaug *et al.*, 2005). In these experiments POT1 may have been trapping the single-stranded G-quadruplex DNA and thus shifting the equilibrium toward the unfolded state, as opposed to actively unwinding the quadruplex. The heterogeneous nuclear ribonucleoproteins A1

(hnRNP A1) and D (hnRNP D) which are single-stranded DNA binding proteins have demonstrated G-quadruplex resolvase activity (Enokizono *et al.*, 2005; Fukuda *et al.*, 2002; Zhang *et al.*, 2006). Circular dichroism and chemical shift perturbation studies were used to show that hnRNP D utilizes its C-terminal BD2 domain to dissociate G-quadruplex structures formed by human telomeric DNA. While it was proposed that the BD2 domain could actively unfold the quadruplex (Enokizono *et al.*, 2005), it is possible that hnRNP D was trapping the dissociated single-stranded DNA in a passive manner, as previously mentioned for POT1. Likewise, hnRNP A1 has been shown to disrupt telomeric G-quadruplexes resulting in the stimulation of telomerase activity. This result prompted a model in which hnRNP A1 facilitates telomerase translocation by resolving guanosine-guanosine hairpins and G-quadruplex structures that may arise in the single-stranded telomeric DNA substrate (Zhang *et al.*, 2006). Using CB3 cells, a murine cell line deficient in hnRNP A1 that harbors shortened telomeres, hnRNP A1 was expressed using a retroviral vector resulting in an increase in telomere length (LaBranche *et al.*, 1998). Another single-stranded DNA-binding protein, replication protein A (RPA), was observed to expedite dissociation of telomeric G-quadruplex structure by 10 fold upon comparison with the complementary DNA strand. This activity was independent of ATP and a 3' single-stranded region, in contrast to the Bloom's and Werner's helicases (Salas *et al.*, 2006). However, like the WRN and BLM helicases, the SV40 large T-antigen helicase can unwind parallel four-stranded G-quadruplexes as well as antiparallel dimeric G-quadruplexes in the presence of ATP and a 3' tail (Baran *et al.*, 1997). Using tetrameric G-quadruplex affinity beads coupled with gel filtration chromatography, HeLa cell lysates were probed for tetrameric G-quadruplex resolvase activity which resulted in

the identification of the NTP-dependent DHX36 gene product, a DEXH type helicase (Vaughn *et al.*, 2005). A similar resolvase activity, which unwound four-stranded G-quadruplexes in a dNTP and Mg^{2+} dependent manner, was isolated from human placental tissue (Harrington *et al.*, 1997). The human nuclease GQN1 was observed to specifically cleave 5' single-stranded DNA regions before four- and two-stranded G-quadruplex regions, where G-quadruplexes were non-telomeric and telomeric models, in a sequence nonspecific manner under physiologic conditions (Sun *et al.*, 2001). Human topoisomerase I is able to bind prefolded intermolecular and intramolecular G-quadruplexes, as well as promote G-quadruplex formation from single-stranded G-rich DNA (Arimondo *et al.*, 2000). Additionally, this binding inhibits normal topoisomerase I DNA cleavage activity (Marchand *et al.*, 2002).

Further evidence for proteins that interact with G-quadruplexes has been obtained from studies with other eukaryotic species. The β subunit of the telomere binding protein (TeBP-β), from the organism *Oxytricha nova*, increased the rate of G-quadruplex formation from telomeric primers to 10^5-10^6 fold, and made the second order reaction first order under physiologic conditions *in vitro* (Fang and Cech, 1993). The crystal structure of TeBP in complex with the single-stranded telomeric substrate 5'-$G_4T_4G_4$-3' contained an intermolecular antiparallel G-quadruplex that co-crystallized with the protein-DNA complex (Horvath and Schultz, 2001). While this finding is compelling, it is uncertain if the formation of the G-quadruplex was an artifact of the crystallization process. Early studies in the ciliates *Oxytricha nova* and *Stylonychia mytilus* showed that the gene-sized chromosomes from the polyploidic macronucleus were tethered together in string-like and circular aggregates, and that both nucleic acid-nucleic acid and protein-

nucleic acid interactions were important for stabilizing this interaction of chromosomal organization (Lipps, 1980; Lipps *et al.*, 1982). More recent research in *Stylonychia lemnae* identified the formation of a proposed antiparallel intermolecular G-quadruplexes at the ends of the gene-sized chromosomes that facilitate the tethering of chromosomes *in vivo* (Paeschke *et al.*, 2005). One model suggests that the TeBP α subunit binds to telomeric DNA and in turn recruits the TeBP-β subunit, which through its basic C-terminus promotes G-quadruplex formation. The formation of the terminal G-quadruplex is dependent on TeBP-α and -β heterodimerization, while phosphorylation of TeBP-β dissociates the complex. The nucleic acid-nucleic acid (G-quadruplex) interaction, dependent on the TeBP heterodimer, and protein-protein (TeBP-α homodimer) interactions (Peersen *et al.*, 2002) from each contributing telomere are thought to sequester and promote chromosomal stability and organization.

In *Saccharomyces cerevisiae*, the repressor-activator protein 1 (RAP1), a double-stranded DNA binding protein, was observed to bind telomeric tails in a sequence specific manner and promote intermolecular G-quadruplex formation in the presence of potassium (Giraldo and Rhodes, 1994), while another study showed that RAP1 could promote parallel G-quadruplex formation and also bind preformed antiparallel and parallel G-quadruplexes *in vitro* (Giraldo *et al.*, 1994). Also in *Saccharomyces cerevisiae*, the Sgs1 helicase, a RecQ DNA helicase similar to the previously mentioned WRN and BLM helicases, unwinds telomeric G-quadruplexes with a 10 fold greater efficiency over duplex DNA *in vitro*, with a 3' to 5' polarity in an ATP and Mg^{2+} dependent manner (Sun *et al.*, 1999). Furthermore, a nuclease specific for cleaving 5' single-stranded regions upstream of four-stranded G-quadruplexes, much like the human

nuclease GQN1 previously mentioned, was also identified in partially purified fractions of *Saccharomyces cerevisiae* lysate (Liu *et al.*, 1993).

The nature of this ever expanding body of evidence provides substantial credence for the existence of G-quadruplex structure *in vivo*. However, future research is required to elucidate any biological roles these unique structures may elicit. Regarding this, Chapter III of this dissertation documents an important biochemical technique used to purify and partially characterize a single species of G-quadruplex structure from a mixture of quadruplex structures. This protocol facilitates the experimental testing of properties of lone G-quadruplex structures, excluding any bias that may occur in the presence of a mixture of G-quadruplex structures. Furthermore, Chapter IV of this dissertation investigates whether purified ciliate telomerase can utilize a library of diverse, purified G-quadruplex structures as substrates. This research reveals that telomerase has a novel affinity for a subset of G-quadruplexes structures. Therefore by demonstrating that telomerase interacts with some quadruplex structures preferentially, new insights are gained into telomerase functionality and its roles in cellular biology.

Replication of the Telomere

The conservation of eukaryotic chromosomes during each round of DNA replication is not absolute (Figure 1.5). Regarding this, two important matters concerning the replication of telomeres must be addressed. First, telomeres are partially defined by their inherent regions of single-stranded DNA that form the 3' overhangs; however these overhangs cannot be produced by leading strand synthesis (Lingner *et al.*, 1995). Second, lagging strand synthesis is incapable of conserving the very 5' ends of telomeric DNA, resulting in the "end-replication problem" (Olovnikov, 1973; Watson, 1972).

DNA replication is characterized by the progression of a replication fork along a chromosome, where coordinated synthesis of the leading and lagging strands produce newly formed sister chromatids. Because DNA replication progresses in a 5' to 3' direction, leading strand synthesis moves toward the replication fork, and unless prematurely terminated, continues to the end of the chromosome where it produces a blunt-ended, double-stranded DNA (Figure 1.5.A, B). The production of such an end is contrary to the single-stranded overhang that is inherent to telomeric structure.

The lagging strand, however, is synthesized in a discontinuous manner, moving 5' to 3' in the direction opposite the progression of the replication fork (Figure 1.3A). Lagging strand synthesis requires the synthesis of RNA primers by DNA primase, along the chromosome for use as DNA polymerase I substrates in the generation of short Okazaki fragments. The RNA primers are subsequently removed, the gaps are filled in by DNA polymerase, and the DNA segments are stitched together by DNA ligase. As lagging strand synthesis requires the successive placement of RNA primers upstream from DNA synthesis, it is impossible to generate an Okazaki fragment that conserves the very 5' end

of the telomere, as no RNA primer can be produced beyond the 3' end of the telomere (Figure 1.5B). Theoretically, if an RNA primer were to be placed complementary to the very 3' end of the telomere, later removal of the primer would result in a loss of 8 to 10 nucleotides, yielding an 8 to 10 nucleotide 3' overhang. This end-replication problem, along with compounding factors such as nucleolytic degradation and oxidative damage, results in the shortening of human telomeres by 50 to 200 nucleotides during each cell cycle. Interestingly, this rate of shortening is in proportion to the size of the telomeric 3' overhang (Huffman *et al.*, 2000).

In order to overcome these issues associated with telomere replication, the cell has devised a single mechanism that addresses the problems inherent to both leading and lagging strand syntheses (Autexier and Lue, 2006). Telomerase, a specialized reverse transcriptase, is able to use its integral RNA subunit to bind and extend the 3' end of the telomere. When considering the telomeric end produced by lagging strand synthesis, telomerase binds the G-rich 3' overhang and extends it, allowing for conservation of the complementary 5' end of telomeric sequence through further rounds of lagging strand synthesis. When considering the issue of the blunt end produced by leading strand synthesis, telomerase is able to synthesize G-rich single-stranded DNA allowing for the production of a 3' overhang. However the biochemical requirement of a single-stranded DNA primer for telomerase catalyzed extension suggests that the blunt end requires processing, the details of which have yet to be elucidated. Recently in telomerase negative normal human BJ fibroblasts, it was observed that the telomeres resulting from leading strand synthesis were, on average, half the length of the telomeres resulting from lagging strand synthesis (60-65 nucleotides versus 105-110 nucleotides) (Chai *et al.*,

2006). Further analysis in BJ fibroblasts overexpressing telomerase, revealed that leading strand telomeres were lengthened while lagging strand telomeres were virtually unchanged, suggesting that telomeres synthesized by leading and lagging strand synthesis are processed differently.

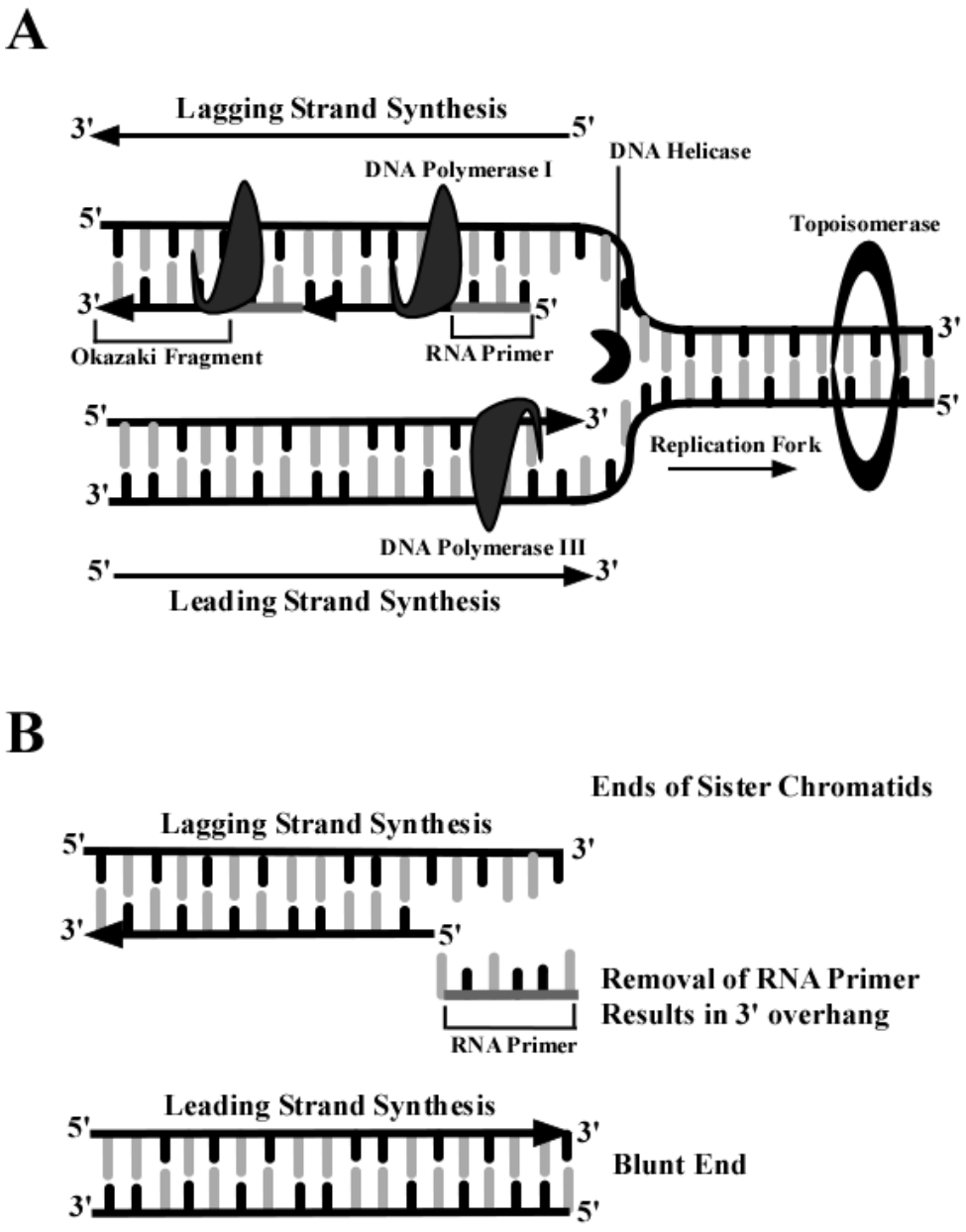

Figure 1.5. Chromosome-end replication. (A) As DNA helicase unwinds double-stranded DNA, leading strand synthesis follows 5' to 3' in the direction of the replication fork, while lagging strand synthesis follows 5' to 3' in the opposite direction. (B) Lagging strand synthesis can not conserve the very 5' end of the telomere, where as leading strand synthesis produces a blunt end, a structure not inherent to telomeres.

Telomerase

Telomerase is a specialized DNA polymerase that uses a short stretch of RNA sequence from the templating-region of its integral RNA subunit to bind and synthesize single-stranded telomeric DNA through reverse transcription. The *in vitro* reconstitution of a functional telomerase holoenzyme requires two subunits: the catalytic protein subunit, TElomerase Reverse Transcriptase (TERT); and the RNA subunit, Telomerase RNA (TR). However, other accessory proteins are required for proper telomerase assembly and nuclear localization *in vivo*.

Many of the details concerning the assembly of telomerase ribonucleoprotein (RNP) complexes *in vivo* have yet to be elucidated. However, the majority of studies have been conducted with telomerase from yeast, human and ciliates. In *Saccharomyces cerevisiae*, the telomerase RNA (tlc1) is synthesized by RNA polymerase II, polyadenylated, 5' end capped, and further processed to remove the adenosine tail (Chapon *et al.*, 1997; Singer and Gottschling, 1994). Furthermore, interaction between a uridine-rich consensus motif in the transcript and Sm proteins is important for stability and appears to facilitate biogenesis and nuclear import *in vivo* (Seto *et al.*, 1999). A complete description of telomerase assembly into a ribonucleoprotein complex, its nuclear export and import, and the mechanisms of biogenesis in yeast remain elusive. Currently, the holoenzyme for *Saccharomyces cerevisiae* is a complex thought to be comprised of TERT, EST1, EST3, Ku, and Sm proteins and the RNA subunit (Figure 1.6.A).

Similarly, human TR is transcribed by RNA polymerase II and subsequently undergoes several modifications, including the addition of a 5'-2, 2, 7-trimethyl guanosine (TMG) cap (Holt *et al.*, 1999; Zhu *et al.*, 2004), internal modifications, and 3’ end processing

(Collins and Mitchell, 2002; Feng *et al.*, 1995; Fu and Collins, 2006). In the 3' half of the TR lies an H/ACA motif that is responsible for its post-transcriptional maturation and association with the nucleolar proteins dyskerin (Cbf5), NHP2, and NOP10 (through direct interactions) and GAR1 (subsequently sequestered), which are known requirements for the accumulation of box H/ACA RNAs (Chen *et al.*, 2000; Dragon *et al.*, 2000; Fu and Collins, 2003; Mitchell *et al.*, 1999; Pogacic *et al.*, 2000). Each of these can be co-immunoprecipitated with telomerase activity but only dyskerin is part of the purified telomerase complex (Cohen *et al.*, 2007). While the H/ACA motifs are necessary for intracellular assemblage of the telomerase RNP (Fu and Collins, 2003), it is dispensable for reconstituting telomerase activity *in vitro* (Tesmer *et al.*, 1999). With a greater dimension of complexity than other H/ACA-motif RNAs, a loop in the H/ACA-motif 3' hairpin is necessary for cellular assemblage and accumulation by interacting with a yet to be determined biogenesis factor (Dragon *et al.*, 2000; Fu and Collins, 2003). Furthermore, the 3' loop is responsible for the RNP biogenesis and enrichment in subnuclear compartments, as both human TERT and TR co-localize in the nucleolus (Etheridge *et al.*, 2002; Lukowiak *et al.*, 2001; Mitchell *et al.*, 1999), and in Cajal bodies (Fu and Collins, 2006; Jady *et al.*, 2004). Most evidence points to Cajal bodies as the site of telomerase holoenzyme assemblage as human TR only accumulates in Cajal bodies in human TERT positive cells (Zhu *et al.*, 2004), while TERT accumulates in the nucleolus even when TR is absent (Etheridge *et al.*, 2002). Possibly, TERT may accumulate in the nucleolus awaiting a signal to assemble in Cajal bodies with TR. The functional human telomerase RNP is characterized by the assembly of TERT and dyskerin proteins with TR (Figure 1.6.B).

In contrast to yeast and human, ciliate TR is synthesized by RNA polymerase III and does not appear to undergo 3' end processing resulting in retention of the 3' polyuridine tail present at transcription termination. In *Euplotes aediculatus* and *Tetrahymena thermophila*, affinity purification of the telomerase complexes yielded a 43 kDa (p43) and 65 kDa (p65) proteins, respectively, that were identified as La homologs important in proper RNA folding and RNP assembly, processivity, and nuclear retention (Aigner and Cech, 2004; Aigner *et al.*, 2003; Mollenbeck *et al.*, 2003; O'Connor and Collins, 2006; Prathapam *et al.*, 2005; Richards *et al.*, 2006; Stone *et al.*, 2007; Witkin and Collins, 2004). The ciliate telomerase RNP consists of TERT and the La homolog proteins (p43 in *Euplotes* or p65 in *Tetrahymena*) and the TR subunit (Figure 1.6.C).

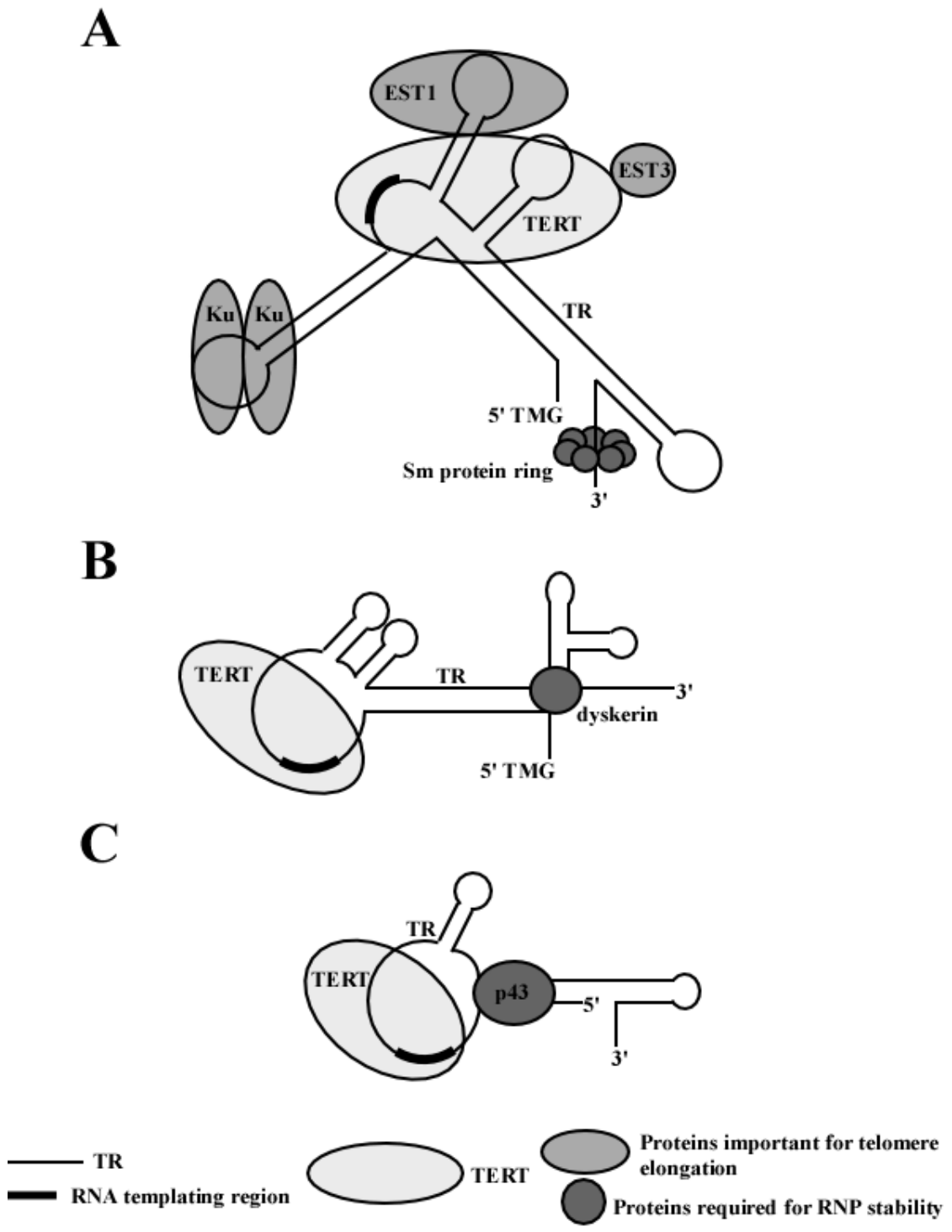

Figure 1.6. Telomerase ribonucleoproteins complexes. (A) *Saccharomyces cerevisiae*. (B) Human. (C) *Euplotes aediculatus*. Figure adapted from (Collins, 2006).

Telomerase has several biochemical activities that affect cellular biology. The foremost studied function is telomerase-catalyzed extension of telomeric DNA. The basic steps incorporated by telomerase elongation are substrate recognition, elongation, and translocation (Figure 1.7).

In vivo, telomerase is limited as to when it can extend the 3' end of telomeres, due to the cell cycle dependence of the end-capping of chromosomes by T-loops and G-quadruplex structures. *In vitro*, telomerase can recognize and extend most single-stranded G-rich sequences with a free 3' end (Greider, 1996), however it does not elongate blunt-ended double-stranded DNA (Lingner and Cech, 1996), 5' overhangs (Greider and Blackburn, 1987), nor some G-quadruplex structures (Oganesian *et al.*, 2006; Zahler *et al.*, 1991). Substrate recognition involves base pairing of the RNA subunit to a DNA substrate with complementary sequence at the 3' end (Harrington and Greider, 1991; Lingner and Cech, 1996; Wang *et al.*, 1998). There also appears to be separate primer binding site that binds an upstream portion of the primer. This allows extension of partially nontelomeric and short telomeric substrates, which would otherwise be inefficiently elongated with only the RNA template interaction (Hammond *et al.*, 1997; Moriarty *et al.*, 2005; Wyatt *et al.*, 2007). The catalytic site of telomerase synthesizes DNA, nucleotide by nucleotide, using dNTPs and magnesium. The affinity of different nucleotides for telomerase varies, as dGTP is preferred over other dNTPs, however telomerase can also incorporate ddNTPs as well as rGTP into its substrates (Collins and Greider, 1995). The concentration of dGTP influences the ability of telomerase to processively extend its DNA substrates (Bryan *et al.*, 2000; Collins and Greider, 1993; Collins and Greider, 1995; Hardy *et al.*, 2001), and it has been suggested

that the polymerase may contain a separate allosteric binding site for dGTP (Hammond and Cech, 1997; Hardy *et al.*, 2001).

As telomerase extends its substrate, the RNA template does not increasingly form base pairs with its ever nascent DNA product, rather distal RNA-DNA bonds are broken as proximal bonds are formed (Forstemann and Lingner, 2005; Hammond and Cech, 1998; Wang *et al.*, 1998). Human and ciliate telomerase undergo many rounds of extension while bound to the same telomeric DNA substrate (Greider, 1991; Morin, 1989; Prowse *et al.*, 1993), thus requiring a realignment or translocation step of the RNA template with respect to the catalytic site. Research aimed at investigating telomerase structure-activity relationships using substrate nucleotide analogues supported a dynamic model, in which the guanosines in the nascent DNA substrate assist translocation by forming guanosine-guanosine hairpins (Jarstfer and Cech, 2002; Shippen-Lentz and Blackburn, 1990). Some telomerase complexes are not processive, as murine telomerase is much less processive than human *in vitro* (Prowse *et al.*, 1993), and yeast telomerase is non-dissociative and non-processive *in vitro*, remaining bound to its substrate after one round of extension (Cohn and Blackburn, 1995; Prescott and Blackburn, 1997).

Interestingly, telomerase has also exhibited an evolutionary conserved nuclease activity. In ciliates, nuclease activity removes nontelomeric DNA that is 3' of a telomeric sequence or may remove a single telomeric nucleotide placed at the 5' end of the RNA template (Collins and Greider, 1993; Greene and Shippen, 1998; Melek *et al.*, 1996). Yeast telomerase-associated nuclease activity is triggered by RNA template-DNA base mismatches and noncanonical telomeric repeat sequences (Niu *et al.*, 2000; Prescott and Blackburn, 1997). It may be that the nuclease activity is inherent to the telomerase

complex, as it co-purifies with telomerase over several purification steps in both ciliates and yeast (Greene and Shippen, 1998; Melek *et al.*, 1996; Niu *et al.*, 2000). Although the possibility that the nuclease activity may be a contaminating factor has not been discounted, as the activity resembles that of a FLAP nuclease, of which there are no FLAP nuclease motifs found in the TERT gene. Furthermore, recombinant *Tetrahymena* telomerase, reconstituted with tTERT and tTR in rabbit reticulocyte lysate (RRL), exhibited nuclease activity (Collins and Gandhi, 1998). This was also observed in unpurified recombinant human telomerase, where products shorter than the input primer were generated (Huard and Autexier, 2004). Partially purified human telomerase, from recombinant and cell sources, removed 3' nontelomeric DNA from 5' telomeric-3' nontelomeric hybrid models, where the cut back point was dependent on the sequence of DNA 5' to the telomeric/nontelomeric boundary (Oulton and Harrington, 2004). Telomerase may harbor the nuclease activity for proofreading, reinitiating a stalled elongation complex (Collins and Greider, 1993; Melek *et al.*, 1996), or alternatively to promote chromosome healing (Bednenko *et al.*, 1997; Melek *et al.*, 1996).

Yet to be well characterized is telomerase's role in tumorigenesis. In one study using GM847 immortal human fibroblasts, which do not express telomerase but do express the alternative lengthening of telomeres (ALT) as a means for telomere maintenance, only cells transfected with both the human TERT protein and the H-Ras oncoprotein conferred tumorigenesis (Stewart *et al.*, 2002). Surprisingly, when an HA carboxy terminus-tagged TERT protein was substituted for wild-type TERT, as $TERT_{HA}$ has been shown to exhibit robust enzymatic activity *in vitro* (Counter *et al.*, 1998) but can not elongate telomeres *in vivo* (Ouellette *et al.*, 1999), tumorigenesis was also observed. The results of this study

showed that ATL cannot substitute for telomerase in the transformation of cells, and importantly that telomerase assumes an additional function that surpasses its ability to elongate telomeres in the passage of cells through tumorigenesis. Further research is required to tease out the details of this mechanism of telomerase.

Returning to the subject of telomerase's ability to extend telomeric primers, scientists have further characterized this activity by identifying two contributing factors. The first factor, nucleotide addition processivity, is the activity associated with telomerase that incorporates nucleotides onto the telomeric primer until the end of the telomerase RNA template is reached. The second factor, repeat addition processivity, is the result of realigning the telomeric primer with the alignment region of the telomerase RNA template, following the completion of a nucleotide addition event, allowing for multiple rounds of nucleotide addition processivity to commence successively. In an effort to further understand and characterize these processivities and thus telomerase's activity as a whole, various studies have been conducted using TERT and TR mutants, and by evaluating cofactors, chaperoning proteins, and telomerase oligomerization. Concerning telomerase oligomerization, many studies support the existence of telomerase as a cooperatively functional dimer. Chapter II of this dissertation addresses whether purified *Euplotes aediculatus* telomerase functions as a cooperative oligomer or as a lone monomer by using size exclusion chromatography and electron microscopy as the methods of measurement. The results of this research provide the first visualization of intact telomerase bound to a telomeric DNA substrate and thus the highest resolution structure of telomerase to date. Furthermore, the findings also provide the first direct evidence for telomerase oligomerization in *Euplotes aediculatus*, which impart new

insights into the mechanism of telomerase catalyzed extension of telomeric DNA via cooperative telomerase dimers.

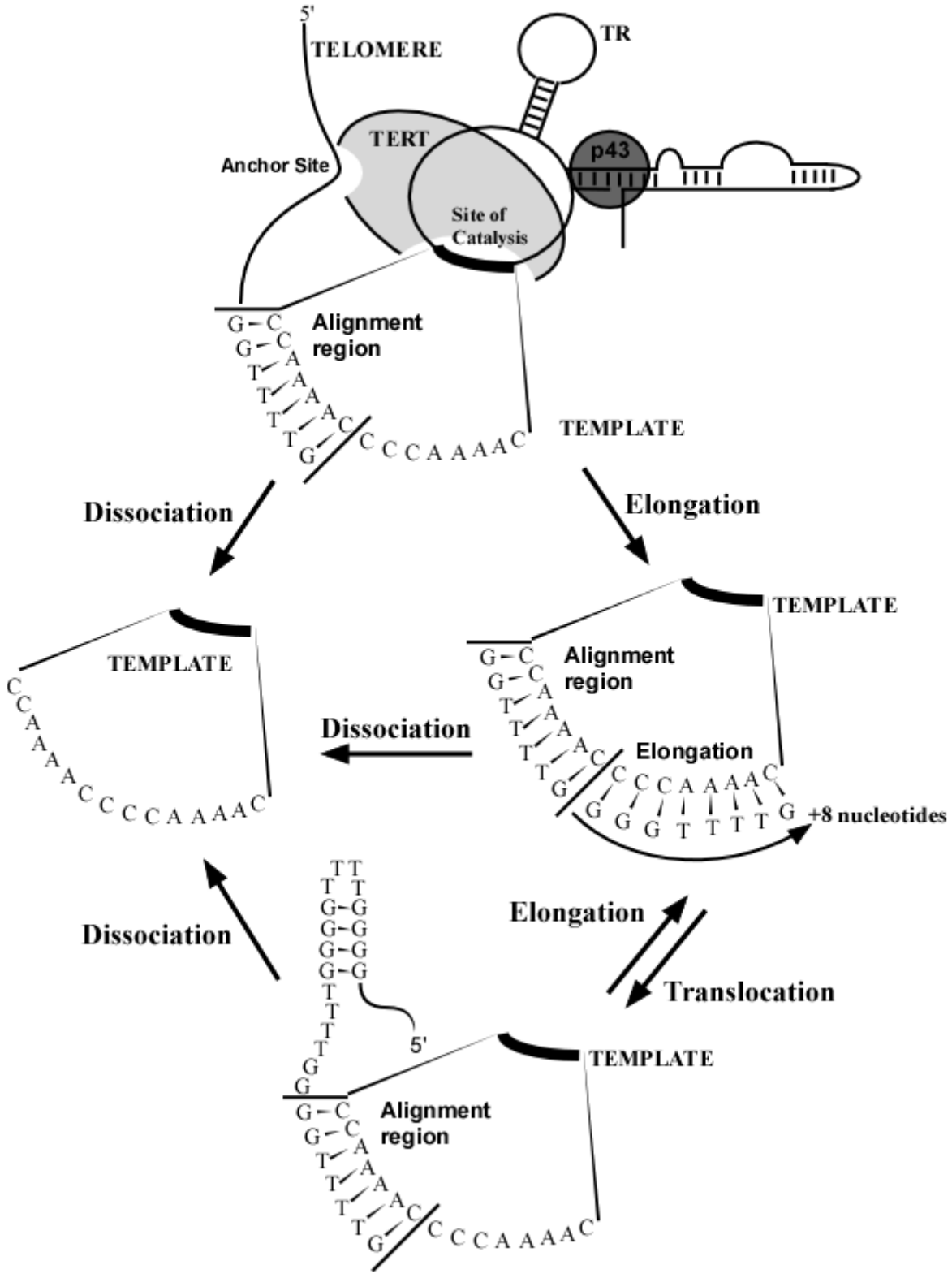

Figure 1.7. *Euplotes aediculatus* telomerase extension cycle.

CHAPTER II

ELECTRON MICROSCOPE VISUALIZATION OF TELOMERASE FROM *EUPLOTES AEDICULATUS* BOUND TO A MODEL TELOMERE DNA

Adapted from (Fouché *et al.*, 2006)

The unique mechanism by which telomerase extends the telomere, by adding multiple copies of telomeric repeats following a single initial binding event, has been the focus of numerous studies in an effort to fully understand the holoenzyme's activity. Telomerase can catalyze two types of processive elongation of a primer: Type I or nucleotide addition processivity, and Type II or repeat addition processivity. Nucleotide addition processivity refers to the synchronous movement of the telomerase RNA-telomeric DNA duplex relative to the active site of the enzyme upon addition of each deoxynucleotide phosphate during reverse transcription. Repeat addition processivity refers to the unpairing of the telomerase RNA-telomeric DNA duplex followed by a translocation and realignment of the telomerase RNA with the DNA substrate, relative to the 3'-region of the RNA template, thus allowing for further rounds of nucleotide addition processivity. Mutations in both the telomerase RNA and the reverse transcriptase subunits, and the probing of cofactors and chaperones that interact with telomerase, are direct methods of inquiry that have been used to examine the structure, function and processivity relationships inherent to the telomerase reaction cycle. Another feature of telomerase that may play an important role in telomerase processivity, and further elucidate aspects

fundamental to telomerase catalyzed reverse transcription, is the ability of telomerase to form dimeric and oligomeric complexes.

Several studies indicate that oligomerization may be a conserved feature of telomerase in various model organisms. Using two component mixtures of truncated hTERT protein with overlapping and non-overlapping regions and with a catalytically inactive full-length mutant, Beattie *et al.* was able to form functionally cooperative oligomers in cell lysate and when reconstituted *in vitro* (Beattie *et al.*, 2001). Complementing this observation, Wenz *et al*. used gel filtration chromatography to indicate that active human telomerase exhibited an elution profile similar to that expected for a dimeric telomerase complex (Wenz *et al.*, 2001). Glycerol gradient profiles and nano-liquid chromatography-tandem mass spectrometry analyses of purified human telomerase isolated from an array of cancers (breast, lung, colon, bone, connective tissue, and embryonic kidney cells) resulted in the identification of the integral components of the catalytically active telomerase: hTERT (127 kDa), hTR (153 kDa), and dyskerin (57 kDa), which made up half of the observed dimeric complex (650-670 kDa) (Cohen *et al.*, 2007). Wild type and template mutant forms of the human telomerase RNA (hTR) subunit were used to characterize the activities of homodimeric versus heterodimeric telomerase ribonucleoprotein complexes. When a DNA primer specific for the wild type hTR was added to two separate direct telomerase assays containing either the affinity purified wild type-wild type hTR homodimer or the wild type-mutant hTR heterodimer, the activity observed from the heterodimer was approximately 40 fold less (not 50%) than the activity of the homodimer, suggesting that dimeric complexes cooperate in *trans* during telomerase catalyzed extension (Wenz *et al.*, 2001). Furthermore, Moriarty *et al*. observed that a mutation in the RNA interaction domain 1 (RID1) of hTERT impaired

repeat addition and weakened human telomerase RNA dimerization, while addition of mutant hTERT proteins with wild type RID1 domains acted in *trans* to restore repeat addition processivity (Moriarty *et al.*, 2004). However, Bryan *et al*. performed gel filtration chromatography on recombinant *Tetrahymena thermophila* telomerase and partially purified cellular extracts. They found that the recombinant telomerase complex was catalytically active as a monomer, but that data for the native telomerase model was inconclusive. The native telomerase elution profile favored possible dimer formation (however a single telomerase RNP with other associated proteins cannot be discounted) while the biochemical experiments using co-immunoprecipitation were consistent with a monomeric RNP (Bryan *et al.*, 2003). In *Saccharomyces cerevisiae*, Prescott and Blackburn utilized glycerol gradient centrifugation to confirm a single telomerase species from fractionated whole-cell extracts, and conducted biochemical pulldown experiments that resulted in the identification of at least two active sites supporting telomerase oligomerization (Prescott and Blackburn, 1997). Using a multi-step purification procedure ending with glycerol gradient centrifugation, Lingner and Cech observed that purified *Euplotes aediculatus* telomerase from cell extract (229 kDa) had a sediment coefficient similar to that of catalase (~232 kDa) suggesting that it was active as a monomeric RNP complex (Lingner and Cech, 1996). Aigner *et al*. purified nuclear extract as detailed by Lingner and Cech (Lingner and Cech, 1996), however used gel filtration to analyze the telomerase RNP without further purification. The apparent molecular mass of the telomerase complex was observed to be between 450-500 kDa, consistent with the formation of a telomerase dimer (458 kDa) (Aigner *et al.*, 2003). From the organism *Euplotes crassus*, Wang *et al.* prepared nuclear extracts and isolated active fractions by gel filtration. The active fractions were subjected to biochemical pulldown

assays which confirmed at least two active sites in the RNP complex. Further probing using radiolabeled, T7 tagged recombinant hTERT truncated mutants in conjunction with untagged full length hTERT, yielded the identification of two independent regions in the N- and C-termini (amino acids 186-354 spanning the CP motif, and 755-857 spanning the C, D, E, and RT motifs) sufficient for oligomerization *in vitro* (Wang *et al.*, 2002).

Mounting evidence supporting the tenet that telomerase exists in multimeric form suggests that two or more telomerase ribonucleoprotein complexes work in concert during processive elongation to simultaneously extend one or more telomeric DNA substrates. To address this hypothesis, three models that incorporate a cooperative and coordinated telomerase dimer have been proposed (Kelleher *et al.*, 2002; Prescott and Blackburn, 1997; Wenz *et al.*, 2001). In the "Parallel Extension" model, two active sites within two different yet associated telomerase ribonucleoproteins simultaneously extend two separate chromosome 3' overhangs (Figure 2.1.A) (Prescott and Blackburn, 1997; Wenz *et al.*, 2001). It has been proposed that this mechanism of elongation could occur to the leading and lagging strands of telomeres following DNA replication of sister chromatids. In the "Template Switching" model, the two active sites within a telomerase dimer sequentially extend a shared chromosome's 3' end. Following the addition of the initial telomeric repeat by the first telomerase RNP, the DNA substrate upon translocation is realigned with the RNA template of the second telomerase RNP, where a second telomeric repeat is synthesized (Figure 2.1.B) (Wenz *et al.*, 2001). In the "DNA Anchor Site" model, one telomerase RNP acts as an anchor by base pairing to the telomeric DNA substrate upstream from the second telomerase RNP, which binds the very 3' end of the substrate and is responsible for telomeric elongation (Figure 2.1.C) (Kelleher *et al.*, 2002). It is also conceivable that combinations of these three models may exist, until

future research elucidates the exact mechanism. In this chapter, the study of the oligomeric structure of telomerase from the ciliate *Euplotes aediculatus* is reported.

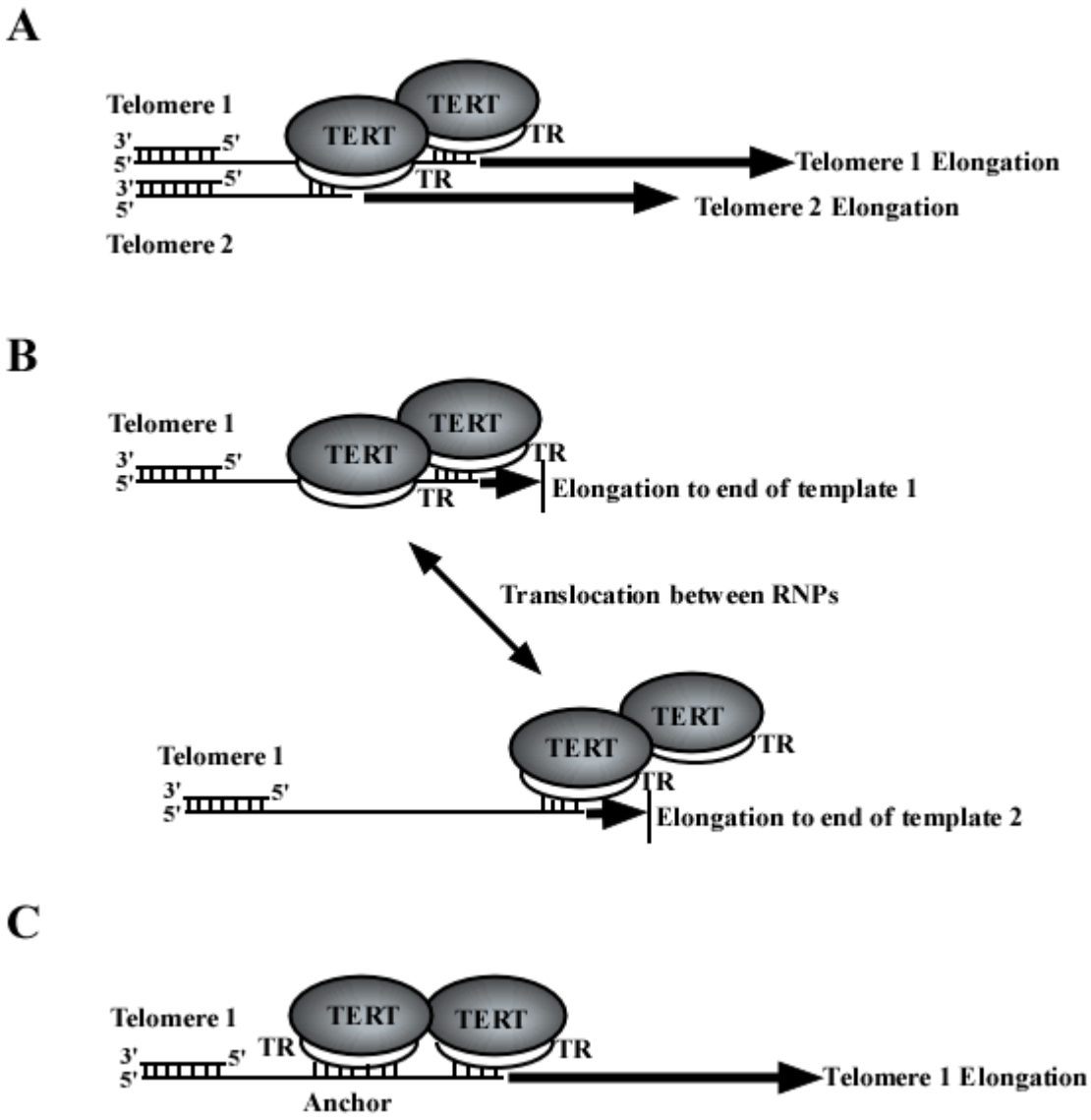

Figure 2.1. Models for cooperative and coordinated telomere elongation by telomerase dimers. (A) Parallel extension model. (B) Template switching model. (C) DNA anchor model.

Euplotes aediculatus

Euplotes aediculatus is a hypotrichous ciliate with a polyploidic macronucleus containing approximately 50,000,000 gene-sized chromosomes, which correlates to 100,000,000 telomeres (Prescott, 1994). The telomeres in *Euplotes aediculatus* are very short and well defined, with a total telomere length of 42 nucleotides: 28 base pairs in the double stranded portion of the telomere and a single-stranded 3' overhang of 14 nucleotides (Klobutcher *et al.*, 1981). Due to the large number of very short telomeres present in these cells, constant chromosomal maintenance is necessary for survival. Telomerase is present at much higher levels in ciliates than other eukaryotes, approximately 300,000 ribonucleoproteins per cell (Lingner and Cech, 1996), and is instrumental in ensuring chromosomal stability and thus cellular proliferation. Due to the potential for isolating larger yields of endogenous telomerase compared to other native and recombinant sources, and because it was the first telomerase model for which all the subunits were identified following biochemical purification, *Euplotes aediculatus* is an excellent model for interrogating telomerase oligomerization.

Euplotes aediculatus telomerase consists of three subunits that copurify: the 123 kDa reverse transcriptase (*Ea*TERT), the 64 kDa (189 nucleotide) RNA subunit, and a 43 kDa accessory protein (a La homologue that is important for nuclear retention, proper RNA folding, and anchorage to an end-replication complex) (Aigner *et al.*, 2000; Lingner and Cech, 1996). Assembly of these three components constitutes the functional telomerase RNP complex (~230 kDa for the monomeric form) *in vivo*.

Purification of *Euplotes aediculatus* Telomerase

Euplotes aediculatus telomerase was purified by the method described by Lingner and Cech (Lingner and Cech, 1996). The total fold-purification of the affinity-purified fractions could not be determined due to very low yields as well as the large amount of BSA used in the purification procedure. However, the telomerase purity was estimated to be approximately 50%, as was reported previously for the purification of a much larger culture with much higher yields (Lingner and Cech, 1996). The quality of the purified telomerase was analyzed by silver staining of SDS-PAGE gels (Figure 2.2). Bands corresponding to all known *Euplotes aediculatus* subunits were observed (120 kDa *Ea*TERT, 64 kDa *Ea*TR, p43 doublet) as well as bands for known polypeptide contaminants (67 kDa BSA, and previously observed polypeptides 35 kDa and 37 kDa) (Lingner and Cech, 1996). The presence of Telomere-end Binding Protein (TeBP) subunits α (56 kDa) and β (41 kDa) were not observed. The stacking interface, the interface between the stacking and separating gels, is shown as a possible site of protein precipitation. Additionally observed bands were likely polypeptide contaminants, however due to very dilute samples the stoichiometry of these contaminating proteins with respect to telomerase was undetermined. Nevertheless these proteins did not appear to interfere with telomerase, as telomerase activity was robust in all assays and no protein was observed by EM to bind to non-telomeric DNA templates. Thus it is believed that these contaminants should not interfere with the telomerase EM binding experiments (results discussed below). In support of this, when Hammond *et al.* cross-linked partially purified *Euplotes aediculatus* to a ^{32}P-radiolabeled primer, only one type of protein-primer product was observed (Hammond *et al.*, 1997).

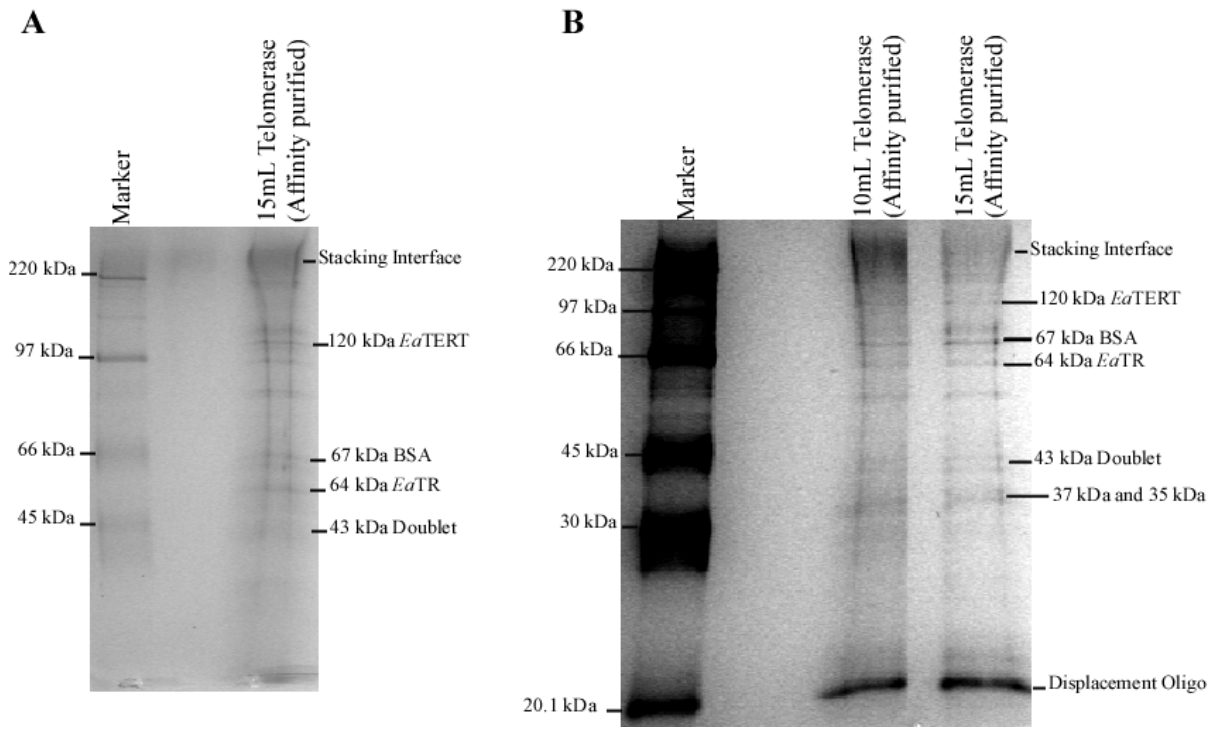

Figure 2.2. Silver stain analysis of purified *Euplotes aediculatus* telomerase. (A) Gel with longer running time separates out higher molecular weight proteins. (B) Gel with shorter running time and increased intensity to exhibit all bands present. Figure adapted from (Fouché *et al.*, 2006).

Analysis of Telomerase by Gel Filtration Chromatography

The oligomeric state of the affinity purified telomerase was determined by gel filtration chromatography using a Superdex 200 column. The retention volume of telomerase was compared to that of four marker proteins with known molecular weights: aldolase (158 kDa), catalase (232 kDa), ferritin (440 kDa), and thyroglobulin (669 kDa). The fractions were subsequently assayed for *Euplotes aediculatus* telomerase RNA (*Ea*TR) content as well as telomerase activity using a direct telomerase assay (Figure 2.3). The *Ea*TR content peaked in retention volume 11.6 ml, corresponding to an approximate molecular weight of 400 kDa, whereas the telomerase activity peaked in retention volume 11.2 ml, corresponding to an approximate molecular weight of 457 kDa. If the shape of the telomerase particle does not greatly deviate from spherical, then this result would be consistent with the predicted mass of a telomerase dimer of ~460 kDa (the molecular weight of a telomerase monomer is ~230 kDa), a result that is in agreement with gel filtration chromatography of *Euplotes aediculatus* nuclear extracts done previously by Aigner *et al.* (Aigner *et al.*, 2003). The slight offset between the peak RNA content and the peak telomerase activity could then be due to some dissociation of telomerase subunits during the gel filtration experiments, which could also account for the lower activity of the fractions with smaller apparent molecular weight. This data suggests, therefore, that *Euplotes aediculatus* telomerase is active as a dimer in solution.

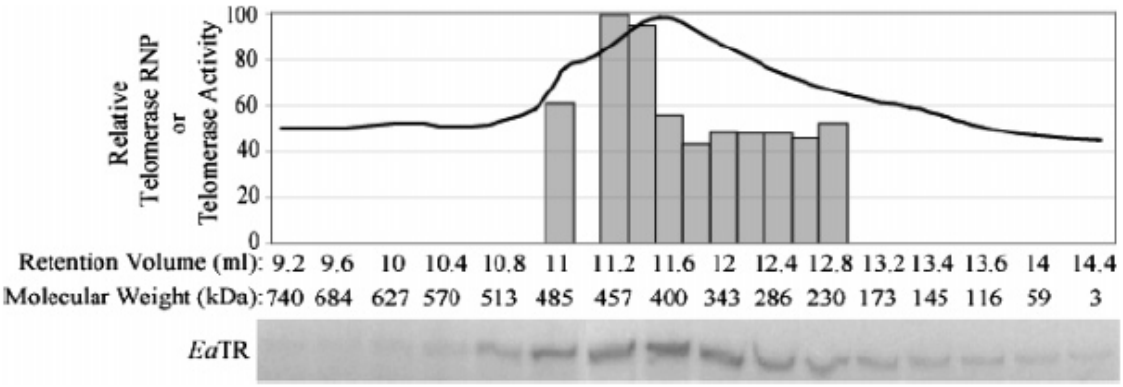

Figure 2.3. Elution profile of telomerase ribonucleoprotein complex and activity supporting dimerization. The amount of telomerase (line graph) in each fraction was determined by detecting the RNA subunit, *Ea*TR. The fraction containing the highest detectable level of *Ea*TR was assigned a relative 100%, giving fractions with background density an approximate 40% baseline. Telomerase activity (bar graph) of the fractions was determined using a direct telomerase extension assay, as detailed in Experimental Procedures. Only fractions that exhibited activity above background are shown, and relative amounts of *Ea*TR and activity were normalized to the highest value, set at 100%. Figure from (Fouché *et al.*, 2006).

Synthesis, Extension, and Determination of K_m of Model Telomeres

To examine the structure of affinity-purified *Euplotes aediculatus* telomerase bound to a model chromosome, synthetic model telomeres consisting of telomeric and nontelomeric DNA were constructed for *in vitro* analyses (Figure 2.4.A). The plasmid pRST5 was linearized by digestion with *BsmB*1 followed by fill in with the Klenow fragment of DNA polymerase and dCTP and dTTP to yield a double-stranded DNA, containing one blunt end and the other end with 550 base pairs of 5'-TTAGGG-3'/5'-CCCTAA-3' repeats terminating in a 5'-CCCT single-stranded overhang. A single-stranded 26 nucleotide DNA, containing a 4 nucleotide complementary sequence to the linearized pRST5 single-stranded overhang and 22 nucleotides of the *Euplotes aediculatus* telomeric repeat 5'-$(T_4G_4)_2T_4G_2$-3', was ligated onto pRST5 to create the model telomere Ea_CM_22. As a negative control, a 26 nucleotide nontelomeric sequence, containing the same 4 nucleotide complementary sequence, was ligated to pRST5. The ligation reactions yielded approximately 65-70% ligation efficiency.

Direct telomerase activity assays were conducted using affinity-purified telomerase in the presence of Ea_CM_22, the nontelomeric control, or pRST5 (Figure 2.4.B). The reaction products were electrophoresed on polyacrylamide gradient gels and analyzed for the incorporation of [α-^{32}P] dGTP into the DNA substrates. Of the three possible substrates, only the Ea_CM_22 model telomere was efficiently extended by telomerase. The nontelomeric control and linearized pRST5, which does not contain a telomeric single-stranded 3' overhang, were not substrates for telomerase. Furthermore, the K_m for the binding of telomerase to Ea_CM_22 was determined to be 4 nM, and was compared to the K_m for the single-stranded control sequence 5'-$(T_4G_4)_2T_4G_2$-3' which was 14 nM. The

reactivity between telomerase and Ea_CM_22 is comparable to the reactivity of other primers with any of the other possible permutations of the telomeric sequence (Hammond and Cech, 1997; Jarstfer and Cech, 2002).

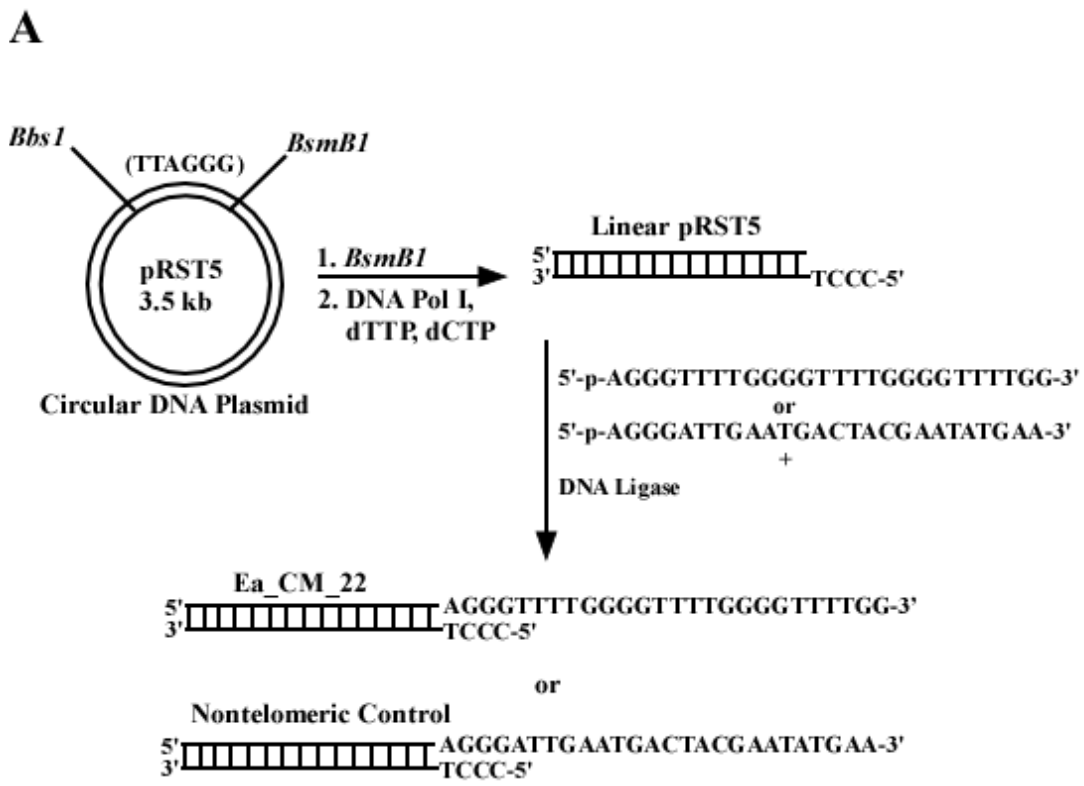

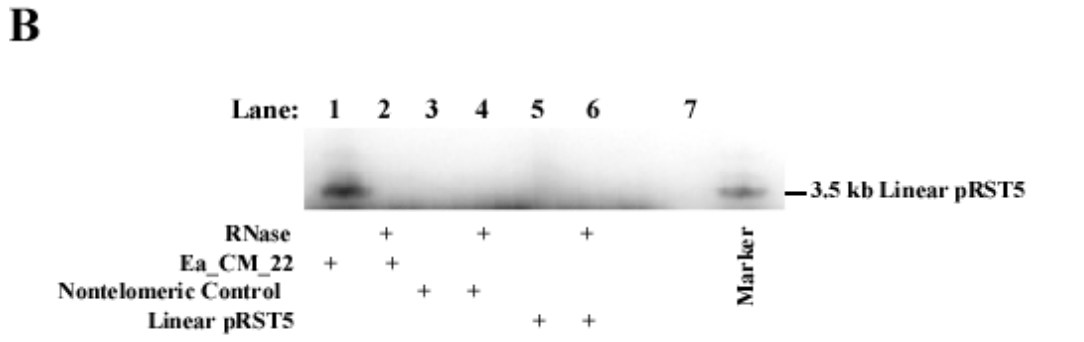

Figure 2.4. Telomerase can extend a model chromosome. (A) Synthesis of model chromosomes containing the *Euplotes aediculatus* telomeric sequence (Ea_CM_22) and the nontelomeric control sequence, as detailed in Experimental Procedures. (B) Affinity-purified telomerase was incubated with DNA substrates: Ea_CM_22, nontelomeric control, and linear pRST5 in direct telomerase activity assays, as detailed in Experimental Procedures. RNase was added to specified reaction mixtures as a negative control. Adapted from (Fouché *et al.*, 2006).

Electron Microscopy

In preparing samples for the visualization of telomerase bound to a model telomere, the affinity-purified telomerase was incubated with Ea_CM_22, using reaction conditions that were consistent with the direct telomerase activity assays with slight modifications to achieve the best conditions for visualizing protein-DNA complexes by electron microscopy (EM). Alternative permutations of the *Euplotes aediculatus* telomeric sequence were not studied, as it has previously been shown that, while telomerase processivity is affected, the activity of *Euplotes* telomerase is not sensitive to the primer sequence as long as it is a telomeric sequence (Hammond and Cech, 1998). Telomerase binding reaction parameters were varied with respect to time (1-20 minutes), temperature (4, 25, and 37ºC), molar ratio of telomerase to DNA substrate (5:1 – 14:1), and in the presence or absence of polyethylene glycol (PEG), a molecular crowding agent. The optimum binding conditions were determined as using a 7.5:1 molar ratio of telomerase to DNA when incubated for 10 minutes at 37ºC in the presence of 8% PEG. Reactions were fixed with glutaraldehyde and examined by EM.

Upon examination, an array of telomerase-telomere complexes was observed (Figure 2.5). The most common species consisted of a telomerase complex bound to the end of a single model telomere (Figure 2.5.A-C). Also present were two or more model telomeres bound at their ends by a telomerase complex (Figure 2.5.D-G). Less frequently observed were telomerase complexes bound internally to the model telomeres (not shown).

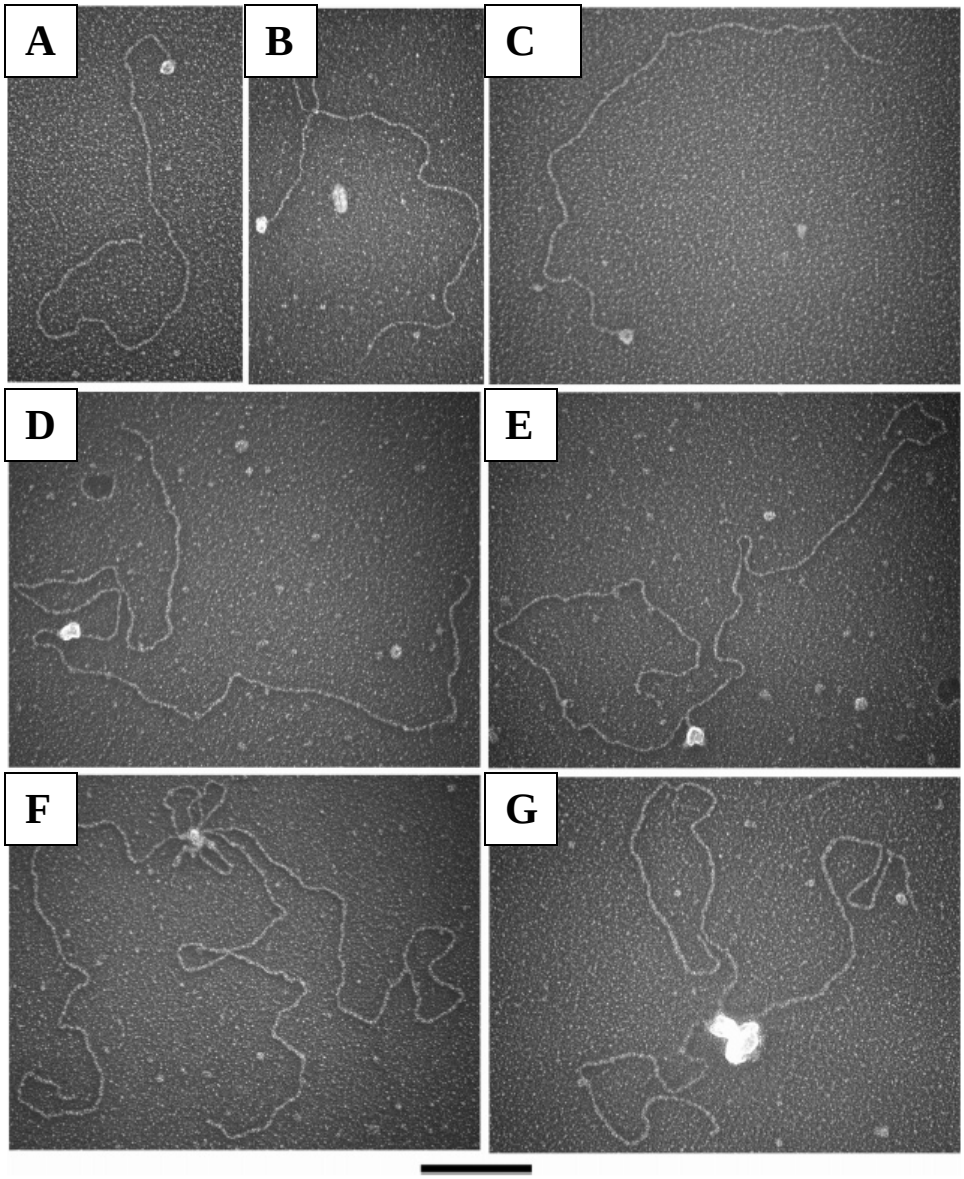

Figure 2.5. EM of *Euplotes aediculatus* telomerase bound to a model telomere. *Euplotes aediculatus* affinity-purified telomerase was incubated with a 3 kb model telomere (Ea_CM_22) and was fixed with glutaraldehyde, mounted on carbon-coated EM grids, and rotary shadowcasted with tungsten (Experimental Procedures). Evidence of telomerase complexes binding the ends of one (A-C), two (D and E), and three (F and G) model telomeres was observed. Images are shown in reverse contrast. The bar is equivalent to 500 bp. Figure from (Fouché *et al.*, 2006).

To further examine telomerase specificity for the model telomere, 5 separate binding reactions were conducted and were scored with an average of 71 molecules counted per experiment (Table 2.1). In total, 46% of all telomere models revealed a telomerase complex bound at one end. When using the nontelomeric control model (Figure 2.4.A), only 4% of the ends showed a protein bound. Thus the telomeric 3' overhang of Ea_CM_22 is specifically bound by telomerase. Further quantification of the protein bound DNA molecules revealed that an average of 45% represented a telomerase complex bound to the end of a single telomere model. An average of 22% and 21% represented two and three model telomeres, respectively, bound at their ends by a large telomerase complex, likely in an oligomeric state. Only 12% represented telomerase complexes bound nonspecifically to internal DNA sequences of the telomere models. Occasionally, large protein-DNA aggregates were observed and were disregarded in the scoring. While decreasing the concentration of telomerase in the binding reactions alleviated this problem, optimum conditions for binding required that the telomerase concentration not be to low.

From these observations it is evident that affinity-purified *Euplotes aediculatus* telomerase binds specifically to the 3' end of the model telomeres and can self-associate sequestering the ends of multiple DNA molecules.

Table 2.1. Percent of model telomeres bound at their end by a telomerase complex. Table adapted from (Fouché *et al.*, 2006).

Reaction	Number of Molecules Counted	Percentage of End-Bound Complexes to Telomeric Ea_CM_22	
1	104	52	
2	109	47	
3	45	40	
4	43	42	
5	54	50	
Average	71	46	Specificity
Average Percentage of End-Bound Complexes to Non-telomeric Control		4	

Quantification of Protein-Bound DNA Molecules

Percent	# of Model Telomeres Bound
45	1
22	2
21	3
12	nonspecifically to internal regions

The size of the telomerase bound complexes was determined using a variation of a method employed in previous studies by the Griffith lab (Allen *et al.*, 1997; Griffith *et al.*, 1998). More specifically, a large protein standard of known mass is mixed with the sample and the size (projected area on the micrograph) is compared to the projected area of the protein, in this case telomerase, bound to DNA. If the projected areas are of similar size and shape, then molecular mass estimates can be used to differentiate with certainty between oligomeric states of the protein bound to DNA. In this study, there were significant amounts of free telomerase present in the background on the grids, so the molecular mass standard was adsorbed onto separate grids and the sample and standard were processed for EM, side by side. In the side by side comparison, a negligible amount of measurement error is expected when viewing two separate slides simultaneously.

The telomerase complexes on DNA were observed to be globular and further inspection showed that the protein apoferritin (443 kDa) most closely resembled the size (projected area) of the telomerase complexes most frequently seen bound at the ends of single telomere models, suggesting the telomerase complexes may be dimers. Photographs of fields of apoferritin molecules were taken (Figure 2.6.E), and the mean projected area of 30 samples was measured and the average projected area of apoferritin was set to an arbitrary value of 100 units. Using the equation:

$$\textbf{(Mass of Telomerase)/(Mass of Apoferritin)} = \textbf{((Area of Telomerase)/(Area of Apoferritin))}^{3/2}$$

and the molecular mass of a monomeric telomerase RNP, the predicted projected area for a telomerase monomer would be 64 units. Similarly, a dimer would have a predicted projected area of 102 units, a trimer 134 units, a tetramer 162 units, and a pentamer 188 units. These values were then compared to the measurements made for the projected areas of telomerase complexes bound to single model telomeres (Figure 2.6.A-D), and the calculated mass

derived from these measurements is represented as a histogram in Figure 2.7. The mean projected area of the complex was calculated to be 101 $\pm$ 23 units corresponding to a mean projected mass of 455 $\pm$ 160 kDa (n = 34). To account for mass of the consensus sequence bound by telomerase, assuming it only bound the 3'telomeric overhang 5'-$(T_4G_4)_2T_4G_2$-3', 8.6 kDa was subtracted from this value to give a final projected mass of 447 $\pm$ 151 kDa. Although, the distributions may have been broadened by the oblong shape of the telomerase and thus by variations in projections of the telomerase particles, these data suggest that telomerase bound the telomere end most commonly as a dimer. This finding is consistent with the size of telomerase as determined in the gel filtration analysis in this study (Fouche *et al.*, 2006) and previously reported (Aigner *et al.*, 2003).

The class of telomerase complexes that bound to two model telomeres (Figure 2.6.F-H) was also analyzed. The protein mass was frequently much larger than that of apoferritin. The projected areas of a subset (n = 19) of the smallest particles were measured revealing a broad distribution of calculated mass values. Upon comparison to apoferritin (set to 100 units), the mean projected area of these particles was 176 $\pm$ 64 units. After the subtraction of approximately 17 kDa, accounting for DNA content, the mean calculated mass was 1061 $\pm$ 569 kDa. While this value is sufficiently broad enough to include a telomerase trimer (690 kDa) or a pentamer (1150 kDa), the data more likely suggest, at a minimum, that two dimers of telomerase, each associated with a model telomere, bind to form a tetramer (920 kDa) *in vitro*. As it happens, reports made in this study suggest that within this class of particles, occasionally a region of separation was distinguishable between two globular particles, each the size of a dimer, consistent with a dimer of dimers (Figure 2.5.D-E, Figure 2.6.F-H).

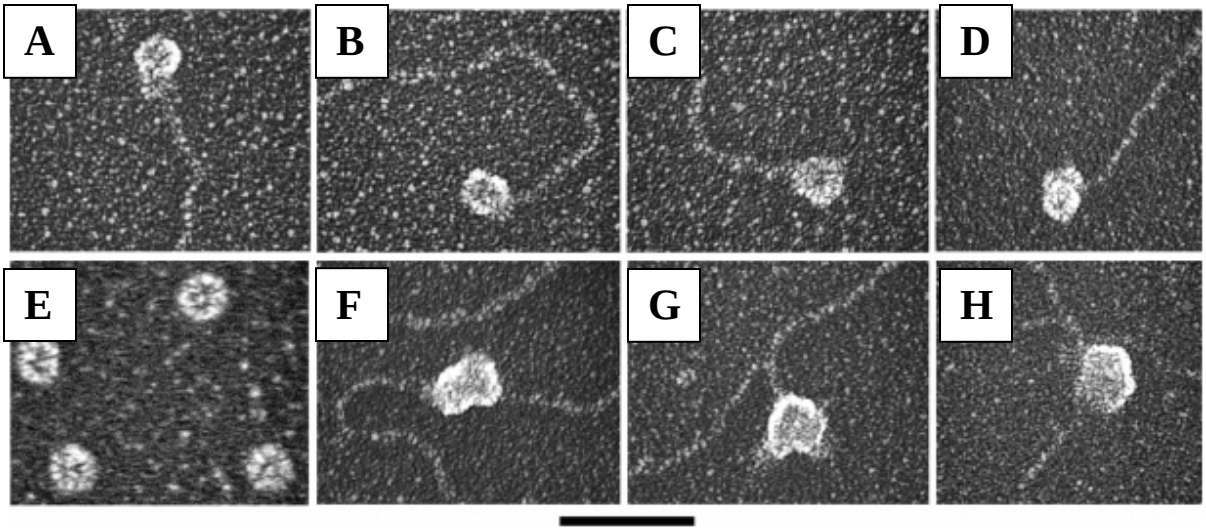

Protein	Number of Samples	Projected Area (units)	Predicted Projected Areas	Molecular Mass (kDa)	Designation
Apoferritin	30	100		443	
Monomer			64	230	
Dimer			102	460	
Trimer			134	690	
Tetramer			162	920	
Pentamer			188	1150	
Protein bound to single telomere	34	101 ± 23		447 ± 151	Dimer
Protein bound to two telomeres	19	176 ± 64		1061 ± 569	Trimer Tetramer Pentamer

Figure 2.6. Estimation of the oligomeric state of DNA-bound telomerase by direct size comparison. Telomerase complexes at the ends of single-model telomeres (A-D), or joining two-model telomeres (F-H), were compared to apoferritin particles (E). The telomerase-model telomere complexes and apoferritin were prepared on separate EM supports for side by side analysis. Images are shown in reverse contrast. The bar is equivalent to 500 bp. The table summarizes the averaged measurements of projected areas and corresponding masses for the standard apoferritin and the protein bound to single and two model telomeres. Figure adapted from (Fouché *et al.*, 2006).

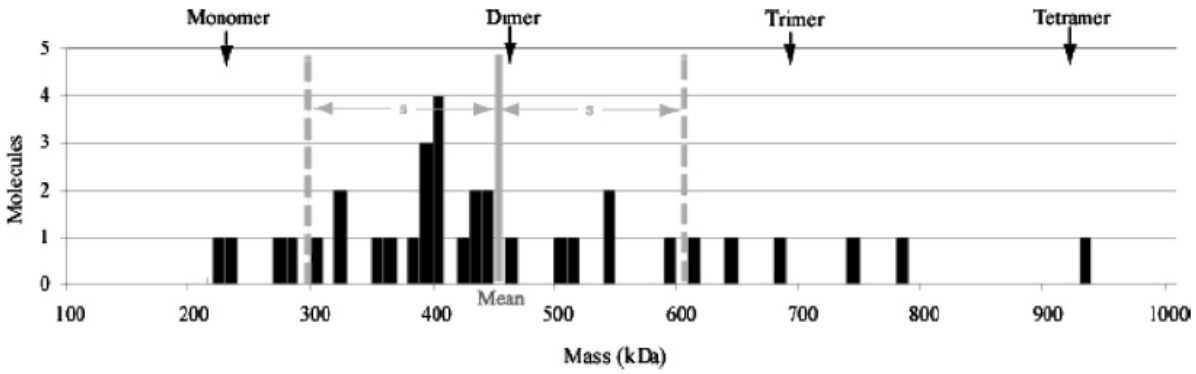

Figure 2.7. Histogram of the calculated mass of the telomerase complex bound to the end of a single-model telomere. The calculated mass values derived from the projected areas of telomerase complexes bound to the end of a single-model telomere are shown. The mean calculated mass value (solid gray bar) was determined to be 447 kDa with a standard deviation of 151 kDa (s, dashed gray lines). The molecular masses of a monomer (230 kDa), dimer (460 kDa), trimer (690 kDa), and tetramer (920 kDa) of telomerase are denoted with arrows. Figure from (Fouché *et al.*, 2006).

Discussion

In this study, *Euplotes aediculatus* telomerase was isolated from nuclear extracts and purified using an affinity chromatography approach. Analysis of the quality of telomerase revealed some contaminants in addition to all the previously characterized subunits of the telomerase RNP. The contaminants did not affect telomerase activity, as activity was robust in all assays, nor EM experiments, where telomerase specifically bound telomeric DNA and was not observed to bind model telomeres with nontelomeric overhangs.

The molecular mass of the affinity-purified telomerase was determined using gel filtration, resulting in RNP and activity elution profiles that were consistent with the formation of a telomerase dimer. Upon examination by EM, telomerase was found to be mostly globular, while calculations of its projected mass supported the observation that telomerase dimers predominantly bound the ends of the synthetic model telomeres. Together these findings support the conclusion that functional *Euplotes aediculatus* telomerase is a dimer in solution and can bind telomeric DNA in an oligomeric form, most commonly as a dimer. Furthermore, when two model telomeres were bound at their ends by a telomerase complex, the data supported likely formation of a telomerase tetramer, or dimer of dimers.

These findings lend support to both the "Template Switching" and "DNA Anchoring" models where two telomerase RNPs cooperatively extend one telomeric substrate. Although, Rivera *et al.* showed that a dimeric human telomerase could processively utilize a single template, devaluing the validity of the "Template Switching" model (Rivera and Blackburn, 2004). Nevertheless, *Euplotes aediculatus* is an evolutionary distant species from human, and it may be possible that each model or combinations there of exist *in vivo*. It does not however support the traditional "Parallel Extension" model where two telomeres are

extended by each telomerase RNP in the dimeric complex. Although, it is possible to extrapolate the "Parallel Extension" model to where each dimer of a tetrameric telomerase complex could extend adjacent yet different chromosome ends, which this research supports.

This study detailed the first visualization of intact telomerase bound to a telomeric DNA substrate, yielding the highest resolution structure of telomerase, and providing the first direct evidence for telomerase oligomerization in *Euplotes aediculatus*. Future studies aimed at defining telomerase dimerization motifs, either in the TERT subunit or in the La homolog accessory protein are needed to identify the driving force behind this interaction.

Acknowledgements

I would like to thank Nicole Fouché, Ph.D. for her work conducting the EM studies; Michael Jarstfer, Ph.D. and Brian Keppler, Ph.D. for their work in the synthesis, primer extension, and K_m studies of model telomeres; Funda Sar, Ph.D. for her assistance in conducting the gel filtration chromatography; and Sezgin Ozgur, Ph.D. for his suggestions concerning silver staining analysis.

Experimental Procedures

Growth of *Euplotes aediculatus* and Preparation of Nuclear Extracts

Euplotes aediculatus was grown under nonsterile conditions using Chlorogonium as the food source as previously described. Cultures were grown in 5 gallon flasks with continuous aeration (Swanton *et al.*, 1980). Nuclei were isolated by sucrose cushion gradient centrifugation, and nuclear extracts were prepared by Dounce homogenization, as previously described (Lingner *et al.*, 1994).

Purification of *Euplotes aediculatus* Telomerase

Telomerase was purified from nuclear extracts following the procedure described by Lingner and Cech (Lingner and Cech, 1996). In short, nuclear extracts (15 ml from 1×10^9 cells) were chromatographed over a heparin sepharose column (Amersham Biosciences, Piscataway, NJ) using a linear gradient of increasing potassium glutamate, and the telomerase containing fractions were pooled and concentrated using an Amicon stirred cell concentrator (Millipore, Billerica, MA). Telomerase was purified from these enriched fractions by affinity chromatography using a bait oligonucleotide, 5'-biotin-TAGACACCTGTTA-$(rmeG)_2$-$(rmeU)_4$-$(rmeG)_4$-$(rmeU)_4$-(rmeG)-3' to trap telomerase onto Ultralink Neutravidin beads (Pierce Biotechnology, Inc., Rockford, IL). Telomerase was displaced by a chase oligonucleotide that is complementary to the bait, and the chase was removed by extensive dialysis against reaction buffer (20 mM Tris Acetate (pH 7.5), 10 mM $MgCl_2$, 50 mM potassium acetate, and 1 mM DTT) and concentrated. The quality of the purified telomerase was analyzed by silver staining of SDS-PAGE gels using standard procedures.

Gel Filtration Analysis

An AKTA FPLC system equipped with a Superdex 200 10/300 GL column (Amersham) was used. The column was equilibrated with 20 mM Tris-HCl pH 7.5, 200 mM potassium acetate, 10 mM $MgCl_2$, 1 mM EDTA, 10% glycerol and 1 mM DTT. Affinity-purified telomerase was injected and the column was run at a rate of 0.4 ml/min at 4 ºC. After 7 ml of void volume had passed through the column, 200 µl fractions were collected. The column was calibrated three times using the high molecular weight calibration kit from Amersham ($R^2 = 0.9978$). Aldolase (158 kDa), ferritin (440 kDa) and thyroglobulin (669 kDa) were run at the same time on the Superdex 200 column and their retention volumes were determined twice, in two separate runs, and fit to the curve y = -148.18x + 2124.4. The marker protein catalase (232 kDa) was run as a separate control to validate the calibration curve, since it has a retention volume that would be similar to that of a telomerase monomer.

Telomerase Quantification

The telomerase was quantified by analysis of the RNA subunit by solution hybridization with a ^{32}P-labeled probe for the *Euplotes aediculatus* telomerase RNA. Quantities were normalized to RNA standards and the amount of telomerase RNP was determined according to the calculation: ng RNP = ng RNA / 64 kDa x 230 kDa, where the mass of the RNA subunit is known to be 64 kDa and the mass of the telomerase RNP monomer is 230 kDa (Aigner *et al.*, 2000; Lingner and Cech, 1996). We assumed the telomerase RNA was equimolar with the telomerase RNP monomer, and that the majority of the RNA was contained within an intact telomerase complex.

Formation of Model Telomeres

Model telomeres were synthesized by a modification of the method described by Stansel *et al.* (Stansel *et al.*, 2001). In short, the plasmid pRST5 (10 μg), was digested with BsmB1 to generate a 5′ overhang with the sequence TCCC. The linearized DNA was incubated with the Klenow fragment of DNA polymerase 1, 33 μM dTTP, and 0.4 mM dCTP to create a blunt end on one side of the linear DNA. A 3' overhang was generated by ligating either a telomeric DNA Ea_CM_22 (5'-AGGG$T_4G_4T_4G_4T_4G_2$-3') or non-telomeric DNA (5'-AGGGATTGAATGACTACGAAGATGAA-3') oligomer onto linearized pRST5. Ligation reactions contained 5 μg linearized pRST5, 5-fold molar excess of 5' phosphorylated oligonucleotide, T4 DNA ligase (200 U, New England Biolabs, Inc., Ipswich, MA) and T4 DNA ligase buffer (New England Biolabs) and were incubated at 25º C for 30 min. Excess oligonucleotide was removed by size exclusion chromatography using Sephacryl-400 (Promega). DNA was deproteinized by the addition of 80 μg/ml proteinase K in 1% SDS followed by extraction with phenol/chloroform and concentration by ethanol precipitation. DNA was resuspended in 10 mM Tris-HCl (pH 7.6), 1 mM EDTA to give a final concentration of ~20 ng/μl. Ligation efficiency was determined by treating ligated and unreacted linearized pRST5 with the Klenow fragment of DNA polymerase 1 and [α-^{32}P]-dGTP and dATP and comparing the percent of incorporated dGTP. Typically, we achieved 70% ligation efficiency.

Direct Telomerase Activity Assay and Catalyzed Extension of Model Telomeres

The ability of telomerase to extend telomere model DNAs was determined by a modification of a primer extension assay (Jarstfer and Cech, 2002). Each 10 μl DNA extension assay contained 20 ng of DNA (see Figure 2.5.B for details), 2 fmol of purified

telomerase, 2 μCi [α-^{32}P]-dGTP (3000 Ci/mmol), 10 μM dGTP, 50 μM dTTP, 20 mM Tris-acetate (pH 7.5), 50 mM potassium acetate, 10 mM $MgCl_2$, and 1 mM DTT. Reaction mixtures were incubated at 25ºC for 30 min and quenched by the addition of 20 mM Tris-acetate (pH 7.5), 10 mM EDTA, 1% SDS and 80 μg/ml proteinase K. Extension products were recovered by ethanol precipitation and analyzed by electrophoresis on a 10 cm x 10 cm 4-12% acrylamide gradient gel containing 7 M urea. Dried gels were imaged by phosphorimaging (Molecular Storm 860) and quantified using ImagQuant version 5.2. The activity of telomerase in fractions eluted from the gel filtration column was similarly determined using a primer extension assay, where 50 μl of each fraction was reacted with 1 μM of the primer 5'-AATGAATGACTACGATTTT-3' at 25º C for 20 h. The radiolabeled primer [α-^{32}P]-T_{10} was added to the quenching solution as a work up and loading control and extension products were analyzed by electrophoresis on a 20 cm x 20 cm denaturing PAGE gel.

Determination of Primer K_m

K_m for telomerase binding to the telomere model DNA Ea_CM_22 or to a short, single stranded DNA primer, pEA22 (5'-$T_4G_4T_4G_4T_4G_2$-3') were determined by a DE81 filter-binding assay. Affinity purified telomerase (0.5 nM) was incubated with varying concentrations of primer (either pEA22, or Ea_CM_22), 50 μM dTTP, 10 μM dGTP, and 0.33 μM [α-^{32}P]-dGTP (3000 Ci/mmol) in telomerase reaction buffer for 30 min at 25º C. Reactions were quenched by the addition of 50 mM EDTA and spotted onto DE81 filter paper. Unincorporated [α-^{32}P]-dGTP was washed away with 0.5 M sodium phosphate, pH 7.0. Filters were counted by liquid scintillation counting and the data was corrected by the

subtraction of background binding to the filter using a telomerase negative reaction. Data were fit to the Michaelis-Menten equation using Sigma Plot.

Electron Microscopy

Model telomeric DNA was diluted to 1 μg/ml in 10 mM HEPES pH 7.5, 50 mM potassium acetate, 8% PEG, 2 mM magnesium acetate followed by addition of *E. aediculatus* telomerase to 0.7 μg/ml for 10 min at 37ºC. Proteins were fixed onto the DNA with 0.6% glutaraldehyde and the mixtures were filtered through 2 ml columns of Bio-Gel A-5m (Bio-Rad Laboratories, Inc., Hercules, CA) that had been equilibrated with 0.01 M Tris-HCl (pH 7.6), 0.1 mM EDTA. Addition of spermidine to 2.5 mM and $MgCl_2$ to 1 mM allowed for sample adsorption onto copper grids supporting thin, glow-charged carbon foils. The samples were washed stepwise with 25%, 50%, 75% and 100% ethanol for 5 min followed by air-drying and rotary shadowcasting with tungsten (Griffith and Christiansen, 1978). An FEI Tecnai 12 electron microscope was used at an accelerating voltage of 40 kV to photograph images on plate film or a Gatan 4K x 4K CCD camera. Micrographs for publication were captured from plate film negatives using a Nikon SMZ1000 digital camera and morphometry measurements were done using ImageJ version 1.29 (National Institutes of Health).

CHAPTER III

METHODS FOR THE PREPARATION AND DETECTION OF G-QUADRUPLEX STRUCTURES BY NATIVE GEL ELECTROPHORESIS

Interest in G-quadruplexes lies in the functionality associated with the various unique structures that these guanosine-rich oligonucleotides can form. While initial interest expressed by biologists in G-quadruplexes stemmed from studies of telomere biology, new potential functions and applications for G-quadruplexes are emerging in the areas of gene regulation, therapeutics, biotechnology, and nanotechnology.

Early research directed at investigating the structures formed by G-rich DNA was dominated by the development and characterization of chemical and biological agents that preferentially interact with G-quadruplexes. These have been sought to probe telomere biology *in vitro* and to act as anticancer therapeutics by inhibiting telomerase-mediated telomere maintenance in cancer cells. A wide variety of small molecules, most commonly aromatic cations, have been explored as telomerase inhibitors by virtue of their G-quadruplex stabilizing properties (Neidle, 2001; Neidle and Read, 2000). More recently, these have been found to directly affect telomere structure and function by preventing telomere binding proteins like Pot1 from associating with the telomere (Gomez *et al.*, 2006). Evidence supporting a role for G-quadruplexes as *cis*-acting regulatory elements in gene regulation has been computationally examined, and greater than 40% of human gene promoters were

predicted to contain one or more G-quadruplex motif (Huppert and Balasubramanian, 2007). The ability of promoter regions to fold into G-quadruplex structures has been substantiated for promoters of several oncogenes including c-*Myc* (Siddiqui-Jain *et al.*, 2002), k-*RAS* (Cogoi and Xodo, 2006), and *VEGF* (Sun *et al.*, 2005). A functional role for these G-quadruplex structures has been tested biochemically using G-quadruplex-stabilizing ligands to bind the c-*Myc* and k-*RAS* promoters in cell-based assays, resulting in suppression of transcriptional activation (Cogoi and Xodo, 2006; Siddiqui-Jain *et al.*, 2002).

Therapeutic applications for G-quadruplexes rely on the defined tertiary structures that recognize specific binding sites on the therapeutic target. Generation of G-quadruplex based ligands has been accomplished by modeling based on inherent gene regulatory elements or by using selective evolution of ligands by exponential enrichment (SELEX). Connor *et al*. utilized a G-quadruplex DNA, containing a two repeat sequence of the insulin-linked polymorphic region of the human insulin gene promoter region, to capture insulin (Connor *et al.*, 2006); while Tasset *et al*. performed SELEX to isolate a potent thrombin binding DNA aptamer, containing a highly conserved G-quadruplex structure that inhibits clot formation (Tasset *et al.*, 1997). In the areas of biotechnology and nanotechnology, G-quadruplexes have been designed as sensors and mechanical devices which incorporate fluorescence resonance energy transfer (FRET) as the reporter. He *et al*. used a cationic, conjugated polymer in combination with a fluorescein chromophore labelled G-quadruplex DNA as a platform to detect for potassium ions in solution (He *et al.*, 2005). Alberti *et al*. constructed a DNA-fuelled nanodevice by utilizing the quadruplex-duplex cycling of the human telomeric sequence 5'-$G_3(T_2AG_3)_3$-3' (Alberti *et al.*, 2006).

Mounting evidence supporting the existence of DNA structures containing G-quadruplexes *in vivo* makes these unique and diverse nucleic acid structures an important research subject, and future investigations aimed at elucidating their biological roles are expected. Purification and characterization of G-quadruplex structures can be challenging because their inherent structural diversity, complexity, and stability are sensitive to an array of variables. The stability of G-quadruplex structures depends on many factors including: number of DNA strands involved in G-quartet formation, the identity of the stabilizing cation(s), the number and sequence context of the guanosines involved in stacking, the presence of single-stranded overhangs, the intervening loop size, and the identity of nucleosides in the loop.

This chapter details important biochemical techniques used to purify and partially characterize single G-quadruplex species from a mixture of quadruplex structures. This direct and readily adaptable protocol is important because it facilitates the experimental testing of the properties of lone G-quadruplex structures, excluding any bias that may occur in the presence of a mixture of G-quadruplex structures.

Methodology

During the assembly, isolation and characterization of G-quadruplex structures, much care must be taken to ensure that the integrity of the structures is not compromised if a homogenous G-quadruplex sample is desired. After the initial denaturing/folding of the guanosine rich DNA, the conditions in the workup must allow for maintaining maximum stability of the G-quadruplex. Factors that contribute to G-quadruplex instability are: diluting stabilizing cation concentrations, warming of native gels during electrophoresis, using unchilled buffers, and leaving G-quadruplexes at room temperature for extended time periods. To avoid these issues, the native gels and buffers used in electrophoresis, extractions, and reconstitution of G-quadruplexes should contain the same components as the initial folding buffer. These processes should also be performed at 4ºC, and samples should be kept on ice. For long term storage between experiments, samples should be stored at -20ºC. The overall work-up scheme for this chapter is represented in Figure 3.1.

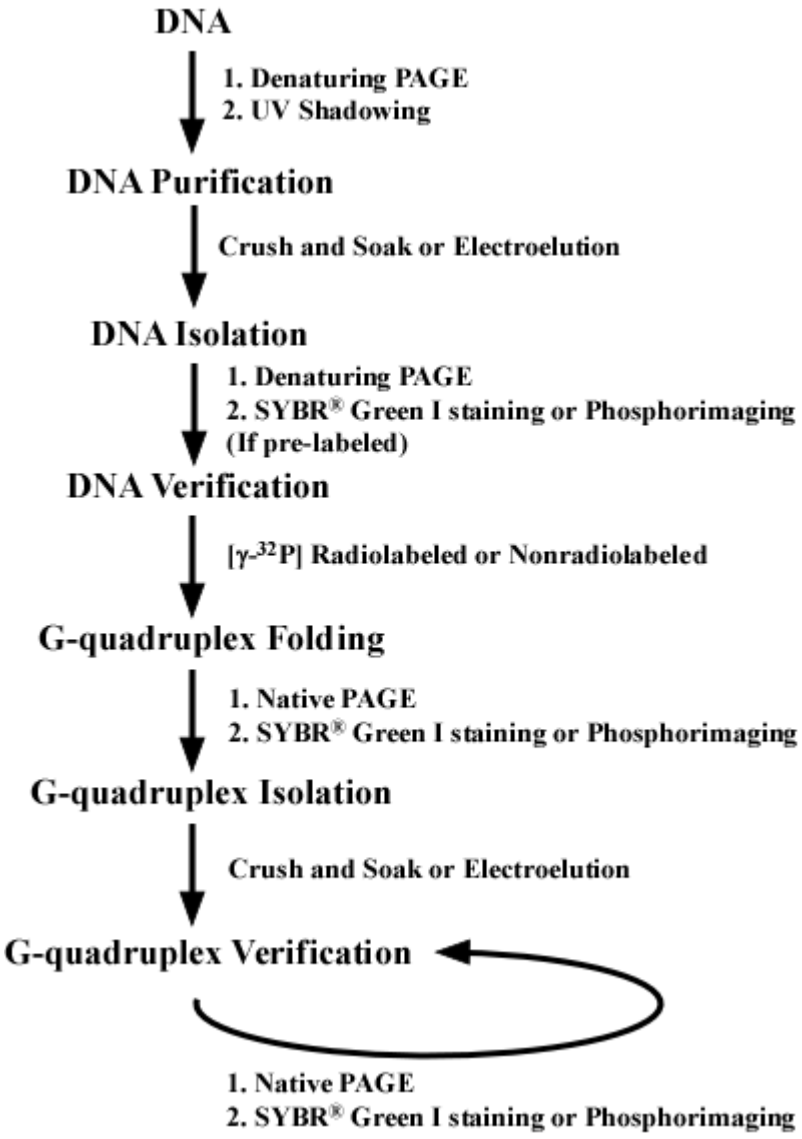

Figure 3.1. Flowchart for the formation, isolation, characterization, and detection of G-quadruplex DNA by native gel electrophoresis.

Purification of Guanosine Rich DNA and DNA Markers

The initial purification of DNA is important to ensure that contaminating DNA from incomplete synthesis, degradation or other sources of contamination is removed, yielding a single oligonucleotide species. Upon synthesizing or receiving DNA from a commercial source, the DNA should be resuspended in an appropriate buffer and at an appropriate stock concentration that maintains oligonucleotide stability and is compatible with future experimental conditions (e.g. 1 mM DNA using 1X Tris-EDTA, pH 7.4 buffer). To ensure that the DNA has dissolved, the sample should be vortexed well and briefly centrifuged. The DNA should then be purified by HPLC or polyacrylamide electrophoresis. Generally, approximately 20 nmoles of DNA is sufficient to load onto a 1.5 mm-thick, 20cm x 20cm polyacrylamide denaturing gel in order to observe the major DNA product by UV shadowing (discussed below), and to protect against overloading issues that result in overlap of the desired product band and other contaminants. Therefore, approximately 20 μL of each stock DNA (at a 1 mM concentration) should be added to an equal volume of formamide-loading buffer in new microcentrifuge tubes. To ensure homogeneity the sample is vortexed well and briefly centrifuged followed by denaturation of the samples by heating at 95ºC for 3 minutes using a heat block or boiling water bath. Again, the denatured samples are removed from the heat source, briefly centrifuged, and placed on ice to capture the DNA species in solution in a denatured state.

It is efficient to pre-cast the denaturing polyacrylamide gel before the DNA work-up, in preparation for prompt loading of the denatured DNA samples. A 20 cm x 20 cm, 1.5 mm-thick 10% denaturing polyacrylamide gel should be prepared by mixing 35 mL of 20% denaturing acrylamide solution, 35 mL dilution solution, 700 μL 10% APS, and 25 μL of

Temed. A gel comb with wide wells should be used to minimize overloading effects. These effects, such as streaking, can make purifying a single DNA species from contaminating species difficult. In the absence of wide-welled combs, tape can be applied to gel combs to create the desired well width. The gel should polymerize within 45 minutes.

Once the gel has polymerized, the comb is carefully removed to ensure the wells remain intact and a 3 mL syringe fitted with a 22-gauge needle is used to flush the wells with 1X running buffer. The gel is then placed into the electrophoresis apparatus, and 1X running buffer is added to the upper and lower reservoirs of the apparatus to the appropriate levels so that running buffer makes contact with the top and bottom of the gel and any air bubbles trapped in the wells are again flushed with 1 X running buffer. The assembly of the electrophoresis unit is completed and connected to a power supply. The gel is equilibrated by pre-running for 10 minutes at 800 V. Prewarming a gel before running samples equilibrates the gel and removes any charged species that might be generated during the polymerization process, minimizing artifacts that may arise. Upon completion of the pre-run, the cover of the electrophoresis unit is removed and the wells are reflushed using 1X running buffer from the top reservoir to remove any urea that may have accumulated.

Each denatured DNA sample is loaded into individual wells and the electrophoresis cover is replaced and programmed to run for 30 minutes at 800 V. The amount of time needed to run all of the DNA samples on a single gel can be optimized by comparing the known sizes of your DNA sequences with the migration of xylene cyanol (an approximately 12 nucleotide DNA sequence on a 10% denaturing polyacrylamide gel) and bromophenol blue (an approximately 55 nucleotide DNA sequence on a 10% denaturing polyacrylamide gel) dyes that should be loaded, using the same loading buffer, into a vacant well. Upon completion,

the electrophoresis unit is disconnected from the power source and disassembled. The gel is removed from its casting, and the upper left corner of the gel is cut to track its orientation. The gel is then placed onto a clear plastic wrap covered fluor-coated surface such as a TLC plate or an intensifying screen.

By carefully exposing the gel to a shortwave UV lamp in the dark, DNA bands should appear as shadows in the gel which should then be excised using a clean razor blade. Importantly, UV light damages DNA so it is important to use the lamp sparingly when UV shadowing. It is equally important to take care in excising full length DNA from lower migrating degradation products, to ensure complete removal of contaminants. Each slice of gel containing a unique DNA fragment should then be passed through a 3 mL syringe into a 2 mL round-bottom snap-cap eppendorf tube to efficiently crush the gel, and all tubes should be labeled with names and dates. To extract the DNA from the crushed polyacrylamide gel, 1X TEN buffer is added to each eppendorf tube at a ratio of 2 mL per 1 mL of gel. The DNA extractions should be incubated overnight at 4ºC on an orbital shaker.

The DNA extractions should then be briefly centrifuged, and the extraction buffer is removed and placed into a Handee™ spin cup column that rests in a collection microcentrifuge tube. This column is useful for quick separation of solid polyacrylamide from the extraction buffer. The crushed gel is usually retained if a second extraction is necessary to improve upon the yield of DNA. A second extraction can improve an initial poor yield; however it need not go overnight. The crushed gel can be resuspended in 1X TEN buffer, placed on dry ice for 5 minutes and then heated at 95ºC for 5 minutes. Alternating these extreme temperatures aids to maximize the second extraction yield. The spin columns are then centrifuged at room temperature for 2 minutes at a maximum speed of

≥10,000 RCF. Each flow-through is then transferred in ~500 μL aliquots to labeled 2 mL pelleting microcentrifuge tubes. To efficiently precipitate the DNA from the extraction buffer, 2.5 volumes of absolute ethanol, prechilled at -20 ºC, are added to each sample and the mixtures are vortexed well. The DNA mixtures are then incubated on dry ice for 5 minutes or until the mixture becomes syrupy. The precipitated DNA is then collected at the bottom of the tubes by centrifuging, with hinges up, for 25 minutes at maximum speed of ≥10,000 RCF at 4ºC. During ethanol precipitations, the hinges of the microcentrifuge tubes are placed in the up position to allow the user a simple guide for the location of the oligonucleotide pellet on the surface of the tube.

Each supernatant is then removed carefully, making sure not to disturb the DNA pellet. If excessive salt precipitates during the first precipitation, a second rinse with chilled 70% ethanol (-20ºC) can be used followed by a second precipitation, to assist in further removal of salts. To ensure the removal of residual moisture, the microcentrifuge tubes are placed on the bench top with caps open for 5 minutes to air-dry. When samples are determined to be dry, the DNA pellet in each tube is redissolved by adding a small volume (≤ 100 μL) of 1X TE buffer, and the mixture is vortexed well and briefly centrifuged. The new concentration for each sample should be determined by observing the absorbance at 260 nm using a UV spectrophotometer. Furthermore, it is important to confirm that a single oligonucleotide species of the correct size has been isolated. This can be accomplished by re-running 100 ng of each DNA sample on a 10 cm x 10 cm, 0.75 mm-thick 15% denaturing polyacrylamide gel to validate that only a single band of DNA is present. The detection of DNA species can be accomplished using SYBR® Green I staining or radiolabeling as detailed below.

Assembly of G-quadruplex Structures

Initially, purified guanosine rich DNA should be stored in a 1X TE buffer at a high micromolar concentration. Next, the user must determine the parameters for the folding conditions. The folding mixture can contain any component at any concentration that the user desires. A mixture of one or more monovalent or divalent cations at different concentrations is acceptable, as is the determination of the final concentration of guanosine rich DNA in the mixture. The guanosine rich DNA concentration will depend on the type of G-quadruplex that the user wishes to form. Higher concentrations of DNA favor intermolecular interactions, while lower concentrations favor intramolecular interactions, if the sequence permits intramolecular structures. Irrespective of the care taken in folding, more than one type G-4 DNA species may be present. The following are examples of the formation of two different G-quadruplex structures in the same folding buffer (Figure 3.2) (Oganesian *et al.*, 2006).

(A) A final concentration of purified 1 μM 5'-$(G_4T_4)_3G_4$-3' Oxy3.5 DNA was added to a folding buffer containing 20 mM TrisOAc (pH 7.5), 50 mM KGlu, 10 mM $MgCl_2$, and 1 mM DTT.

(B) A final concentration of purified 200 μM 5'-$G_4T_4G_4$-3' Oxy1.5 DNA was added to a folding buffer containing 20 mM TrisOAc (pH 7.5), 50 mM KGlu, 10 mM $MgCl_2$, and 1 mM DTT.

Each mixture (A and B) of guanosine rich DNA in folding buffer was heated at 95ºC for 5 minutes. The heat block was subsequently removed from the heat source and was allowed to cool ~2ºC/min to 25ºC. Each sample was then removed from the heat block, briefly centrifuged, and was placed on ice to preserve G-quadruplex structure. The concentration for

each sample was determined by observing the absorbance at 260 nm using a UV spectrophotometer, and 100 ng of each sample (A and B) was electrophoresed on a 10 cm x 10 cm, 0.75 mm-thick 20% native polyacrylamide gel to validate successful G-quartet formation. The DNA species were detected using SYBR® Green I staining or radiolabeling as detailed below.

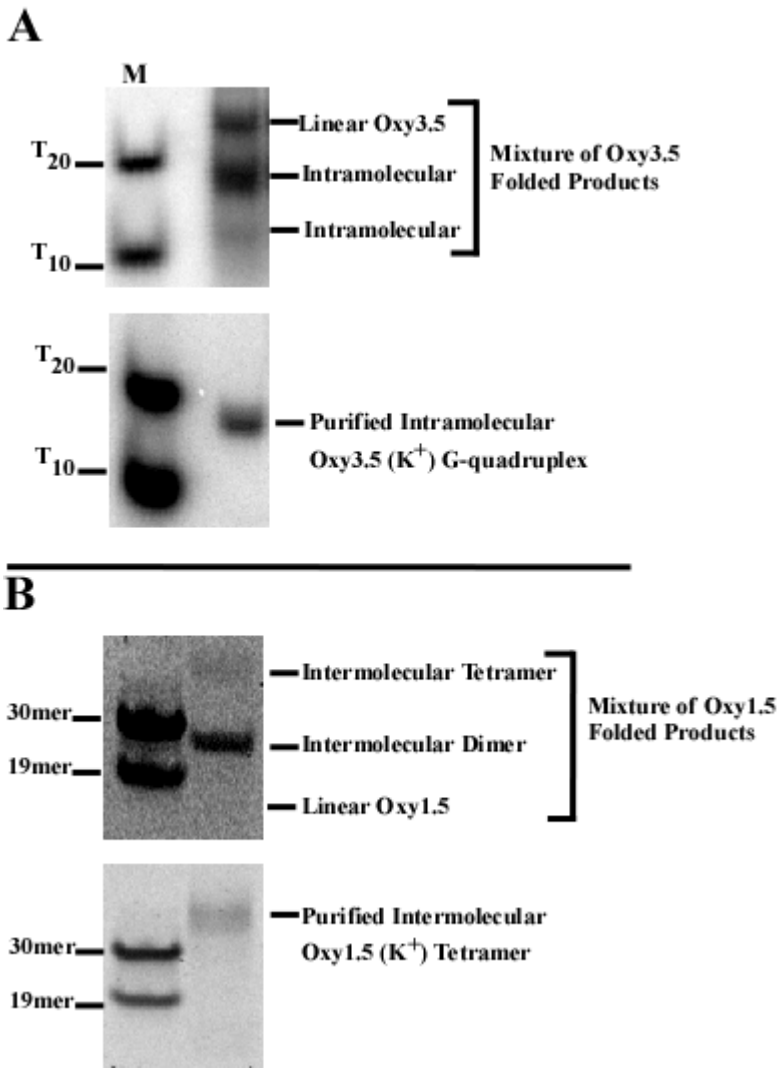

Figure 3.2. Assembly and purification of G-quadruplex structures (Oganesian *et al.*, 2006). Oligonucleotides were 5'-[^{32}P] end labeled **(A)** or stained with SYBR® Green I **(B)**. Lane designated "M" denotes molecular weight markers: T_{20}, T_{10}, unstructured 30mer, and unstructured 19mer oligonucleotides. An intramolecular Oxy3.5 G-quadruplex **(A)** and an intermolecular tetrameric Oxy1.5 G-quadruplex **(B)** were purified from a mixture of structures.

Native Polyacrylamide Gel Electrophoresis

During native gel electrophoresis, the conditions for separating individual G-quadruplex species should mimic folding conditions and be maintained throughout the process, so as to minimize any change in the oligonucleotide structure. Therefore, salts used during G-quadruplex formation, should be included at the same concentrations in the buffer used during polymerization of the native gel and added to the running buffer. The type and amount of salt to be used is dependant on the given application. 20-150 mM concentrations of sodium or potassium are generally reported for G-quadruplex studies in the literature. Mixtures of monovalent and/or divalent cations such as Mg^{2+} are also sometimes added, however it should be noted that during electrophoresis, $MgCl_2$ can be associated with excessive heat and emission of chlorine vapors.

A 10 cm x 10 cm, 1.5 mm-thick (for quadruplex purification) or 0.75 mm-thick (for quadruplex verification and assays) 20% nondenaturing polyacrylamide gel should be prepared by mixing 12.5 mL 40% acrylamide solution, 2.5 mL 10X TBE, 10 mL water, appropriate concentration of cation salt, 25 μL 10% APS, and 5 μL Temed. The gel should polymerize within 45 minutes. Once the gel has set, the comb is carefully removed and a 3 mL syringe fitted with a 22-gauge needle is used to flush the wells with 1X running buffer containing appropriate salt concentrations. The gel is placed into the electrophoresis apparatus, and 1X running buffer is added, again containing the appropriate concentration of salt, to the upper and lower reservoirs of the electrophoresis apparatus. The apparatus is cooled to 4ºC in a cold room or using a refrigerated circulating pump. By maintaining the native gel and running buffer at 4 ºC the denaturing effects of gel heating, which could arise during electrophoresis, are minimized.

An equal volume of chilled (4ºC) native loading buffer should be added to each DNA sample, prepared in new microcentrifuge tubes. The samples should be mixed to homogeneity by pipetting up and down, and subsequently samples should be loaded into individual wells. The assembly of the electrophoresis unit is completed and is connected to a power supply. The samples will need to run for 4-5 hours, judging DNA migration using the dye markers xylene cyanol (an approximate 12 nucleotide DNA sequence on a 20% native polyacrylamide gel) and bromophenol blue (an approximate 45 nucleotide DNA sequence on a 20% native polyacrylamide gel) which are to be loaded in loading buffer free of sample DNA in a separate well, and run at 100 V at 4ºC. Upon completion, the electrophoresis unit is disconnected from the power source and disassembled. The gel is then removed from its casting, and the upper left corner of the gel is cut to track its orientation. At this point the detection of G-quadruplex DNA and DNA markers can be achieved using a scanning phosphorimager.

If the user is imaging the gel for radiolabeled G-quadruplex DNA isolation, the gel can be placed between two pieces of clear plastic wrap and imaged for a short time in a phosphorimaging cassette. The image of the gel and its DNA products should be scaled to actual size. The actual size image, obtained by the phosphorimager, can then be printed and placed under the gel and the regions containing G-quadruplex DNA can be excised for isolation. The G-quadruplexes are then extracted either using the crush and soak or electroelution methods discussed below. Alternatively, radiography film can be used to produce an image of the radioactive samples.

If the user is imaging the gel for the detection of non-radiolabeled G-quadruplexes, the SYBR® Green I staining procedure should be used, followed by the aligning of an actual-

sized image with the gel and excision as previously described for radiolabeled G-quadruplex isolation. Likewise, the extraction procedure then follows using the crush and soak or electroelution methods.

If the user is imaging the gel for G-quadruplex verification or for an assay, the SYBR® Green I staining procedure may be used to detect nonradiolabeled structures, while phosphorimaging may be used for radiolabeled structures. If the user wishes to detect radiolabeled structures, the 20% native gel should be placed on a gel drier under vacuum and at high heat for $\geq$ 4 hours (prematurely removing the gel before it completely dries can result in the gel cracking). When the gel has dried, it is removed from the drier and is placed into a phosphorimaging cassette and exposed overnight.

Extraction of G-quadruplex Structures

Crush and Soak

Each slice of gel containing a unique G-quadruplex structure is passed through a 3 mL syringe into a labeled 2 mL round-bottom snap-cap eppendorf tube to efficiently crush the gel. To the crushed acrylamide sample, 1-1.5 mL of extraction buffer, prechilled to 4ºC, is added. The extraction buffer is usually a modified 1X TE buffer, containing the same salt concentrations as those in the folding and electrophoresis protocol. The DNA extractions are then incubated overnight at 4ºC on an orbital shaker.

The DNA extractions are briefly centrifuged to clarify the solution, and the supernatant is removed and placed into a Handee™ spin cup column that rests in a collection microcentrifuge tube. Just as with the initial removal of solid acrylamide in the DNA purification work-up, this step accomplishes the same goal by facilitating the isolation of G-quadruplex structures in extraction buffer free of solid acrylamide. The spin columns are then centrifuged for 2 minutes at a maximum speed of $\geq$10,000 RCF at 4ºC. Subsequently, each flow-through is then transferred in ~500 μL aliquots to 2 mL pelleting microcentrifuge tubes and placed on ice. A secondary extraction for obtaining G-quadruplex DNA is usually impractical, as a second extraction would need to incubate overnight at 4ºC (increasing the amount of time for potential unfolding) and because less DNA is used in the folding process than in the initial oligonucleotide purification (yielding a more dilute secondary extraction). Rather, we have found that it is more effective to reassemble G-quadruplexes in a second separate reaction and pool the like structures after isolation and characterization. The extracted DNA is precipitated with 2.5 volumes of absolute ethanol, prechilled at -20ºC. The DNA mixtures are then incubated on dry ice for 5 minutes or until the mixtures become

syrupy. The precipitated DNA samples are then centrifuged for 25 minutes at a maximum speed of ≥10,000 RCF at 4ºC. Each supernatant is then removed carefully, making sure not to disturb the DNA pellet. If the G-quadruplex being isolated is radiolabeled, precipitation efficiency can be gauged using a Geiger counter to follow counts/minutes that remain in the pellet or the supernatant. The microcentrifuge tubes are then placed on the bench top for 5 minutes to air-dry.

After the samples dry, a small volume (≤ 50 μL) of prechilled folding buffer is added to each tube to reconstitute the DNA pellet. The G-quadruplex samples are then homogenized by pipetting the buffer up and down, followed by a brief and gentle centrifugation. The concentrations for each G-quadruplex sample are determined by observing the absorbance at 260 nm using a UV spectrophotometer. It is imperative to re-run 100 ng of each sample on a 10 cm x 10 cm, 0.75 mm-thick 20% nondenaturing polyacrylamide gel to validate successful G-quadruplex isolation. Reiterative verification of the samples' G-quadruplex structure by native gel electrophoresis may be necessary over the lifetime of experimental use, as the structures may change with time. Depending on the nature of the G-quadruplex, the user will image using SYBR® Green I staining or phosphorimaging as discussed in the detection section.

Electroelution

Electroelution can be a useful method for isolating G-quadruplex structures when the extraction and precipitation conditions used in the "crush and soak" method do not allow for efficient yields. One example of this is when using short lengths of guanosine rich DNA to form tetrameric structures. Tetrameric structures formed by short oligonucleotides, such as 5'-$G_4T_4G_4$-3', prove to be more difficult to precipitate than structures formed by longer guanosine rich DNA, such as 5'-$(G_4T_4)_3G_4$-3'. Electroelution allows smaller G-quadruplexes to be directly eluted from a piece of polyacrylamide gel into a concentrating chamber containing a small volume (200 μL – 3.6 mL) of the folding buffer, provided the complex is larger than the membrane molecular weight cut-off. It is important however, as in gel electrophoresis, to keep the process at 4ºC.

Detection of G-quadruplexes Utilizing Electrophoresis

SYBR® Green I Staining

Staining with SYBR® Green I is an efficient detection method for most linear and structured oligonucleotides, as is the case with guanosine rich DNA and G-quadruplexes, and serves as an alternative to using radioactive nuclei. However, poly T and A DNA used as molecular weight markers are best used as 5'-[^{32}P] labeled markers, as SYBR® Green I staining does not efficiently stain A and T rich sequences. Once a denaturing or native polyacrylamide gel is ready for processing, 50 mL of 1X TBE is added to a shallow plastic tray and an aliquot of SYBR® Green I is thawed in hand and 5 μL is added to the 1X TBE. The remaining SYBR® Green I aliquot is placed back in the freezer. The gel is removed from its casting, and the upper corner of the gel is cut to track its orientation. The gel is then placed into the tray containing the 1X SYBR® Green I solution, and is incubated on an orbital shaker at room temperature for 20 minutes while being protected from exposure to light. The gel is then imaged using an appropriate scanner (Molecular Dynamics Storm 860 set to chemiluminescence/blue fluorescence) and is imaged using ImageQuant or similar software.

Radiolabeling

The 5' end radiolabeling of oligonucleotides is a powerful method for oligonucleotide detection, including the quantitation of breakdown products and the observation of changes in structure. However, as with most quantitative techniques there are considerations to be made. When [^{32}P] 5'-end radiolabeling oligonucleotides for the purpose of forming intermolecular G-quadruplexes, the user must consider the possible destabilizing effects resulting from the positioning of multiple phosphate groups at guanosine termini on the same end of the quadruplex (Uddin *et al.*, 2004). For example, if the user desired to form an intermolecular, four-stranded, parallel G-quadruplex using the sequence 5'-G_5-3', gel staining would be preferred as the 5'-terminal phosphates would compromise quadruplex stability. Using SYBR® Green I to detect this subset of G-quadruplexes bypasses this limitation of radiolabeling.

If 5' end radiolabeling is the best method for detection, 4 μL of 25 μM purified DNA, 4 μL of 10X kinase buffer, 10 μL of [γ-^{32}P] ATP, 20 μL of water, and 2 μL of T4 polynucleotide kinase are incubated at 37 ºC for 45 minutes. During the incubation, a MicroSpin™ G-25 column (Amersham Biosciences) is prepared by resuspending the resin by vortexing gently. The cap to the column is then loosened one-fourth turn and the bottom is snapped off. The column is placed into a 1.5 mL microcentrifuge tube and is centrifuged for 1 min at 735 RCF at room temperature to remove the resin storage buffer. The column is then placed into a new 1.5 mL microcentrifuge tube and the reaction mixture is loaded drop-wise onto the center of the column, taking care not to disturb the resin. The reaction mixture is centrifuged for 2 min at 735 RCF at room temperature. The radiolabeled oligonucleotide present in the flow-through is quantified using a scintillation counter. A Geiger counter can be used to

determine if most the radioactivity pasted through the resin, or if most of it was retained, indicating the efficiency of the labeling reaction. After running PAGE analysis on radiolabeled oligonucleotides, gels can be imaged using a Molecular Dynamics Phosphorimaging scanner.

Experimental Procedures

G-quadruplex Folding

Water for all buffers is deionized water purified through a Barnstead NANOpure DIamond™ purifier. Folding buffer components include but are not limited to: stock buffers of 10X Tris-EDTA (100 mM Tris-Cl pH 7.4, 10 mM EDTA pH 8.0), 1 M $MgCl_2$, 1 M DTT, 500 mM TrisOAc pH 7.5, 2 M KGlu, and 2M NaGlu. These should be sterile filtered and stored at room temperature. Oligonucleotide(s): guanosine rich DNA and marker DNA containing the desired sequences and lengths can be purchased (IDT) and purified by denaturing polyacrylamide gel electrophoresis (PAGE) followed by extraction and precipitation procedures as detailed in this chapter.

Denaturing Polyacrylamide Gel Electrophoresis (PAGE)

The following are buffers and components necessary for denaturing PAGE: **denaturing acrylamide solution**: 20% Acrylamide/7 M Urea/1X Tris-Borate-EDTA (store at 4ºC); **dilution buffer**: 7 M Urea/1X Tris-Borate-EDTA (store at 4ºC); **ammonium persulfate (APS)**: prepare a 10% (w/v) in water and store at 4ºC; **N, N, N', N'-Tetramethylethylenediamine** (Temed, SIGMA) and store at 4ºC; **running buffer**: 10X Tris-Borate-EDTA (Fisher): dilute to 1X in water and store at room temperature; **formamide-loading buffer** (80% (w/v) deionized formamide, 10 mM EDTA pH 8.0, 1 mg/mL xylene cyanol FF, and 1 mg/mL bromophenol blue (store at room temperature); **extraction buffer**: prepare a stock of 10X Tris-EDTA-Sodium (100 mM Tris-Cl pH 7.4, 10 mM EDTA pH 8.0, 1 M NaCl) TEN buffer and store at room temperature or alternatively, if potassium is used to form G-quadruplexes, substitute NaCl with KCl and dilute to 1X in

water before use; **Handee™ spin cup columns**: cellulose acetate membrane (Pierce) and store at room temperature.

Native Polyacrylamide Gel Electrophoresis (PAGE)

The following are buffers and components necessary for native PAGE: **40% Acrylamide solution** (Acrylamide: BisAcrylamide, 19:1) and store at 4ºC; **ammonium persulfate (APS):** prepare a 10% (w/v) in water and store at 4ºC; **N, N, N', N'-Tetramethylethylenediamine** (Temed, SIGMA) and store at 4ºC; **running buffer**: 10X Tris-Borate-EDTA (Fisher): dilute to 1X in water (store at room temperature) and the components that are in the folding buffer (i.e. NaCl or KCl) should be added to the running buffer at appropriate concentrations; **DNA markers**: poly T DNA or other DNA that is not expected to fold in the presence of cations may be used to compare changes in migration patterns of guanosine rich DNA; **loading buffer**: 50% (v/v) glycerol, 2X Tris-Borate-EDTA (store at room temperature).

5'-end Radiolabeling of Oligonucleotides

The following are components necessary for 5' end labeling DNA: **T4 Polynucleotide Kinase** (Promega) and store at -20ºC; **adenosine 5'-triphosphate**, [γ-^{32}P] (1 mCi, 6000 Ci/mmol, Perkin Elmer) and store at -20ºC in a radiation designated freezer; **MicroSpin™ G-25 column** (Amersham Biosciences) and store at room temperature.

Oligonucleotide Staining

The following are components necessary for oligonucleotide staining: **SYBR® Green I** (10,000X concentration in DMSO, Invitrogen): aliquot into 50 µL volumes and store at -20ºC; shallow plastic tray (13 cm x 11 cm x 4 cm)

CHAPTER IV

EXTENSION OF G-QUADRUPLEX DNA BY CILIATE TELOMERASE

Adapted from (Oganesian *et al.*, 2006)

The single-stranded 3' overhang of telomeric DNA has been observed to adopt higher order structures under physiological conditions *in vitro*. Theses structures are characterized by the coordination of four guanine residues in a cyclic array (G-quartet) that are stabilized by Hoogsteen hydrogen-bonding and a centrally located cation (Figure 4.1.A) (Williamson *et al.*, 1989). Furthermore, multiple layers of G-quartets can stack upon each other to form G-quadruplexes (Figure 4.1.B-E). As discussed in Chapter 1, G-quadruplexes exhibit extensive structural polymorphism resulting in a multitude of diverse folding topologies (Simonsson, 2001). G-quadruplexes can form intramolecularly (Figure 4.1.B and E) or intermolecularly (Figure 4.1.C and D), and strand orientation of the G-rich DNA can be parallel (Figure 4.1.C and D), antiparallel (Figure 4.1.B), or a hybrid of these (Figure 4.1.E).

While the subject is controversial, evidence supporting the existence of G-quadruplex structures *in vivo* is gaining momentum, fueled by a mounting body of biological observations. In *Oxytricha nova*, the telomere binding protein β (TeBP-β) expedites the formation of dimeric and tetrameric G-quartet structures (Fang and Cech, 1993). Similarly in *Saccharomyces cerevisiae*, the double-stranded telomeric DNA binding protein RAP1 was capable of binding to G-quadruplexes (Giraldo and Rhodes, 1994), and in a separate study promoting the formation of parallel G-quadruplexes *in vitro* (Giraldo *et al.*, 1994). Furthermore, just as there are proteins that promote the formation of G-quadruplex structures,

there are also numerous factors that promote the resolution of G-quadruplex structures (Baran *et al.*, 1997; Enokizono *et al.*, 2005; Harrington *et al.*, 1997; Sun *et al.*, 1999; Sun *et al.*, 1998), and the specific cleavage of G-quadruplex proximal DNA (Liu *et al.*, 1993; Sun *et al.*, 2001). Direct probing *in vivo* revealed that single-chain antibody fragments specific for G-quadruplex structures reacted with the telomeres in the transcriptionally active macronuclei of *Stylonychia lemnae* (Schaffitzel *et al.*, 2001). Further investigation elucidated that the telomere binding proteins α and β (TeBPα and TeBPβ) are necessary for the formation of the G-quadruplex structures at telomeres in *Stylonychia lemnae in vivo* (Paeschke *et al.*, 2005).

Telomerase is a ribonucleoprotein that acts as a specialized reverse transcriptase, using its integral RNA subunit to synthesize the G-rich strand of telomeric DNA. This activity results in chromosomal stabilization (Greider and Blackburn, 1985). Importantly, telomerase is expressed in greater than 85% of all cancer cells; however its protein (TERT) levels and activity are undetectable in normal somatic cells. The role of telomerase in promoting cellular immortalization, coupled with its presence in most cancers and absence in most normal cell types, has attracted significant attention as an anti-cancer target (Shay and Bacchetti, 1997). Seminal research investigating telomerase catalyzed extension of G-quadruplex DNA structures determined that telomerase does not require any secondary structure of its DNA substrate for elongation and found that telomerase could not extend stable G-quadruplex DNA (Zahler *et al.*, 1991). These results lead to the hypothesis that G-quadruplex stabilization *in vivo* may be an effective means for telomerase inhibition (Hurley *et al.*, 2000; Zahler *et al.*, 1991). Thus, telomerase inhibition via the development of G-quadruplex-stabilizing agents became a novel anticancer approach. However, one caveat in

this seminal research was the use of crude extracts containing telomerase, in which G-quadruplex interacting-proteins, such as TeBPβ, and potentially crude mixtures of G-quadruplex DNA could have been present, thus biasing the experimental results. Furthermore, the G-quadruplexes tested in this study were present in mixtures, not as individually purified species, disallowing the characterization of substrate specificity for each unique quadruplex structure.

In the following research, purified telomerase isolated from *Euplotes aediculatus* and purified recombinant telomerase from *Tetrahymena thermophila* was used to reevaluate telomerase's ability to extend G-quadruplex DNA. Telomeric DNA substrates capable of forming intramolecular and intermolecular G-quadruplexes, in the presence of sodium or potassium, were used as substrates for telomerase. As the folding of these DNA oligonucleotides routinely yielded a mixture of conformations, individual G-quadruplex species were isolated by native gel purification and the structures were subsequently characterized by circular dichroism (CD), native gel electrophoresis, and thermal denaturation studies. Our results show that telomerase interacts with subsets of G-quadruplexes differently. In the case of intramolecular antiparallel G-quadruplexes, our study validated the original observation that increasing stabilization of these telomeric secondary structures inhibited telomerase's ability to utilize them as a substrate, deterring telomerase catalyzed extension (Zahler *et al.*, 1991). However, more interestingly is the interaction between telomerase and intermolecular parallel G-quadruplexes. Telomerase was able to extend these structures to a much greater extent than would be predicted by their slow dissociation kinetics and high thermal stabilities.

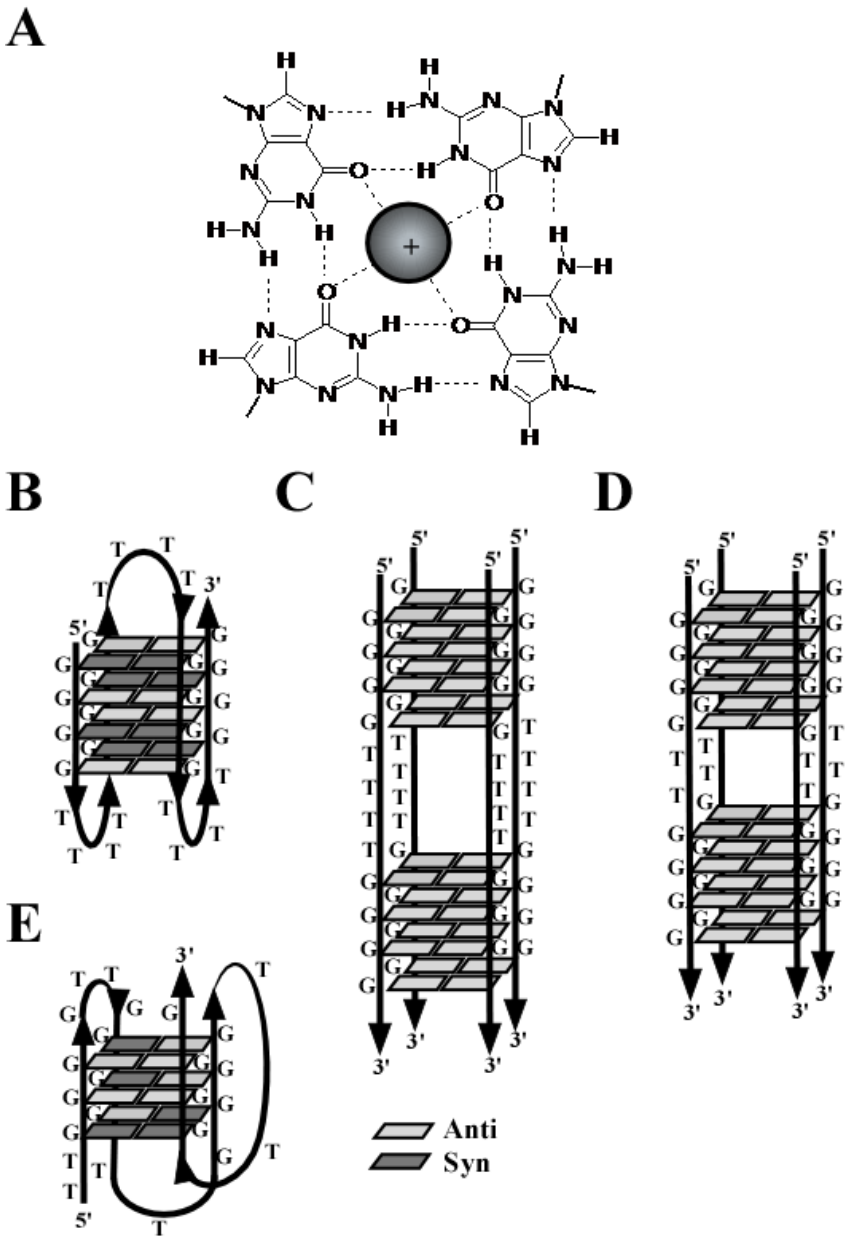

Figure 4.1. G-quadruplex DNA structures. (A) G-quartet where four guanine residues are coordinated by Hoogsteen-hydrogen bonding accompanied by a centrally located cation. (B) Model structure of the Oxy3.5 G-quadruplex in sodium (Wang and Patel, 1995) and potassium (Smith *et al.*, 1995). Predicted structures for the Oxy1.5 G-quadruplex in potassium (C) and 12GT G-quadruplex in sodium (D) (Oganesian *et al.*, 2006). Solution structure of the (3+1) mixed 24GG G-quadruplex in sodium (Wang and Patel, 1994). Figure adapted from (Oganesian *et al.*, 2006).

Folding and Characterization of G-quadruplex DNA

Euplotes Sequences

Initially, gel-purified single-stranded telomeric DNA representing permutations of *Euplotes aediculatus* and *Tetrahymena thermophila* telomeric repeats (Table 4.1) were folded, either in the presence of Na^+ or K^+. As expected, a heterogeneous population of structures was observed after the folding process, as the structures formed by G-rich DNA are highly polymorphic. Each desired structure was excised and extracted from native gels, and the resultant purified G-quadruplex structure was characterized. Before use, the stability of each structure was verified using biochemical and spectroscopic methods.

Oligonucleotides containing either one and one half (Oxy 1.5) or three and one half (Oxy 3.5) of the *Euplotes* telomeric repeat, were used to study the interaction of *Euplotes* telomerase with G-quadruplexes. These oligonucleotides are known to form well characterized G-quadruplexes (Smith and Feigon, 1993; Smith *et al.*, 1995; Wang and Patel, 1995). The 12 nucleotide Oxy1.5 oligonucleotide is a more accurate model of the 3' overhang of the *Euplotes* telomere, which is exactly 14 nucleotides long (Klobutcher *et al.*, 1981). Two folded structures of Oxy3.5 oligonucleotide, one folded in the presence of 50 mM Na^+ and the other 50 mM K^+, exhibited a major compact species which migrated below the T_{20} marker, suggesting intramolecular G-quadruplex formation (Figure 4.2.A and B). The Oxy1.5 oligonucleotide folded in 50 mM K^+ showed two slower migrating major products, one a dimeric intermolecular G-quadruplex migrating around a 24mer, the other likely a tetrameric intermolecular G-quadruplex (~48 nucleotides) migrating well above a 30 nucleotide marker (Figure 4.2.C). Due to instability associated with the isolation of the dimeric Oxy1.5 structure, only the supposed tetrameric Oxy1.5 structure was purified.

Further verification and characterization of these structures was accomplished using CD spectroscopy (Figure 4.2.D). Parallel G-quadruplexes exhibit a positive CD peak at ~265 nm and a negative CD peak at ~240 nm, while antiparallel G-quadruplexes exhibit a positive CD peak at ~295 nm and a negative CD peak at ~260 nm (Keniry, 2000; Williamson, 1994). The Oxy3.5 structures, folded in either Na^+ or K^+, exhibited positive and negative CD peaks of 291/262 nm and 296/264 nm respectively (Figure 4.2.D), supporting the formation of intramolecular antiparallel G-quadruplexes as previously characterized by NMR spectroscopy (Petraccone *et al.*, 2004; Smith *et al.*, 1995; Wang and Patel, 1995). In contrast, the Oxy1.5 structure folded in K^+ exhibited positive and negative CD peaks of 262 and 238 nm, supporting the formation of a four-stranded intermolecular parallel G-quadruplex (Figure 4.2.D).

Table 4.1. Oligonucleotides used in this study. Adapted from (Oganesian *et al.*, 2006).

Nomenclature	Sequence	Length
***Euplotes* oligonucleotides**		
Oxy1.5	5'-GGGGTTTTGGGG-3'	12
Oxy3.5	5'-GGGGTTTTGGGGTTTTGGGGTTTTGGGG-3'	28
Ea 23	5'-TTTTGGGGTTTTGGGGTTTTGGG-3'	23
Ea TR	5'-CAAAACCCCAAAACC-3' (RNA)	15
***Tetrahymena* oligonucleotides**		
6TT	5'-GGGGTT-3'	6
6GG	5'-TTGGGG-3'	6
12GT	5'-TGGGGTTGGGGT-3'	12
24TT	5'-GGGGTTGGGGTTGGGGTTGGGGTT-3'	24
24GG	5'-TTGGGGTTGGGGTTGGGGTTGGGG-3'	24
21GG	5'-GGGGTTGGGGTTGGGGTTGGG-3'	21
48CC	5'-$(AACCCC)_8$-3'	48
48AA	5'-$(CCCCAA)_8$-3'	48
30AA	5'-$(CCCCAA)_5$-3' (RNA)	30
Biot-24TT	5'-Biotin-GGGGTTGGGGTTGGGGTTGGGGTT-3'	24
Biot-24GG	5'-Biotin-TTGGGGTTGGGGTTGGGGTTGGGG-3'	24
Nontelomeric oligonucleotides		
T_{10}	5'-TTTTTTTTTT-3'	10
T_{15}	5'-TTTTTTTTTTTTTTT-3'	15
T_{20}	5'-TTTTTTTTTTTTTTTTTTTT-3'	20
Biot-PBR	5'-Biotin-AGCCACTATCGACTACGCGATCAT-3'	24
19mer	5'-AATGAATGACTACGAATGG-3'	19
30mer	5'-TGTCGATAGTCTTTTGTCCCGCATTACCAC-3'	30

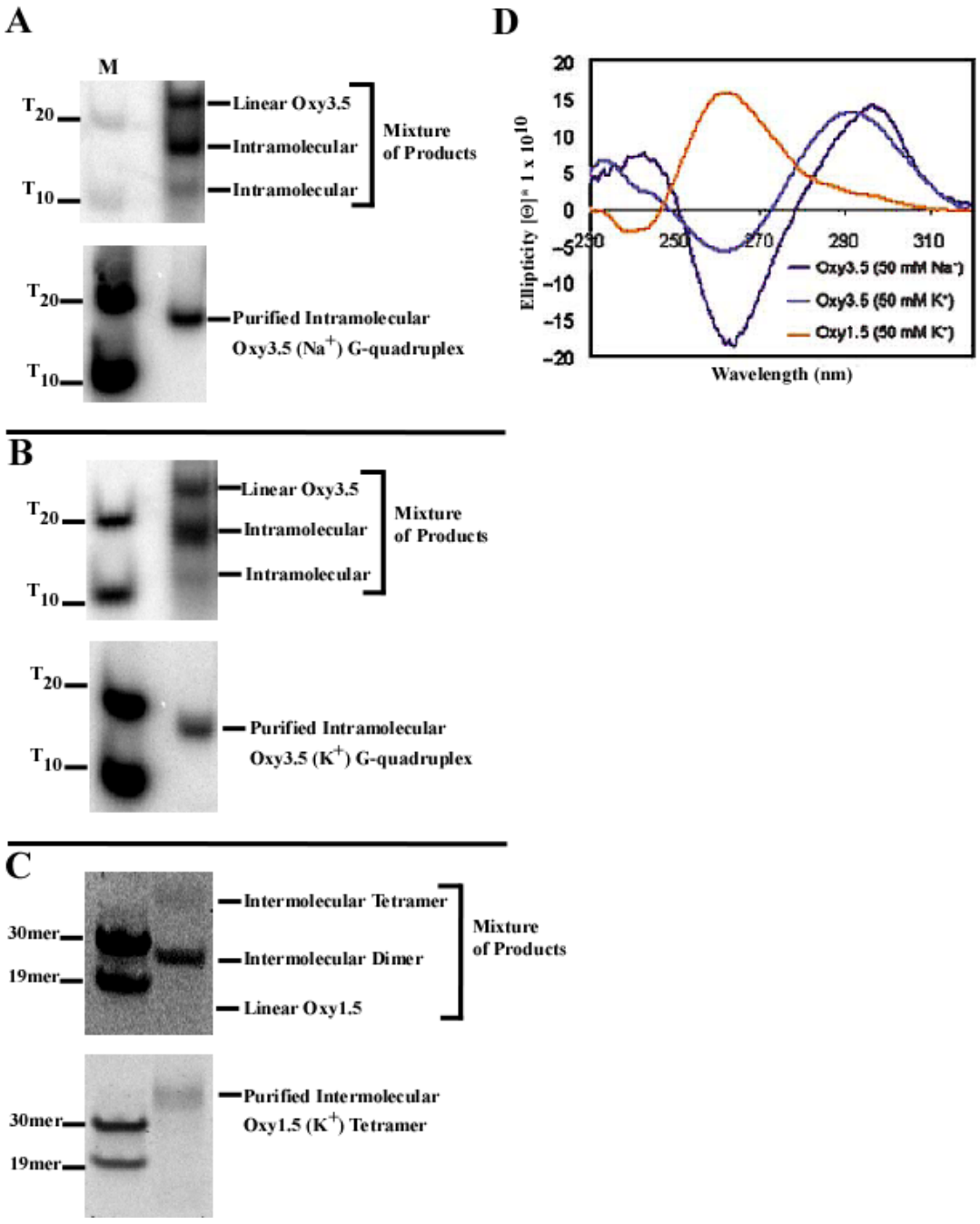

Figure 4.2. Characterization of gel-purified *Euplotes* G-quadruplexes. Folding and purification of antiparallel intramolecular (Na^+) Oxy3.5 (A), antiparallel intramolecular (K^+) Oxy3.5 (B), and parallel intermolecular (K^+) Oxy1.5 G-quadruplexes (C). CD analysis of all three gel-purified *Euplotes* G-quadruplexes (D). 'M' denotes molecular weight markers. Figure adapted from (Oganesian *et al.*, 2006).

Tetrahymena Sequences

Of the *Tetrahymena* oligonucleotides, a large portion of the 21 and 24 nucleotide sequences migrated faster on the native gels in the presence of Na^+ or K^+ (Figure 4.3.B-D), suggesting the formation of compact intramolecular G-quadruplex structures as previously observed (Williamson *et al.*, 1989). In the presence of K^+, the 24TT and 21GG oligonucleotides also exhibited a slower migrating species indicative of an intermolecular G-quadruplex (Figure 4.3.C and D). The 24GG oligonucleotide did not exhibit a prominent intermolecular interaction in K^+, although it has previously been reported that an intermolecular G-quadruplex can form in the presence of K^+ (Hardin *et al.*, 1991). Furthermore, the 12GT oligonucleotide exhibited a slower migrating species in the presence of Na^+ (Figure 4.3.E); it was subsequently determined by cross-linking analysis that this structure was a four-stranded intermolecular G-quadruplex (Figure 4.4).

Using CD analysis, the intermolecular 24TT, 21GG, and 12GT G-quadruplexes were confirmed to be parallel by exhibiting the characteristic positive and negative peaks at 265 nm and 240 nm, respectively (Figure 4.3.F). Furthermore the intramolecular 24TT G-quadruplex exhibited an antiparallel profile, with positive and negative peaks at 295nm and 260nm, respectively. Previously, an intramolecular antiparallel G-quadruplex structure, formed in the presence of Na^+, for the 24TT has been observed (Redon *et al.*, 2001; Wang and Patel, 1994), however the other *Tetrahymena* G-quadruplex structures have yet to be solved.

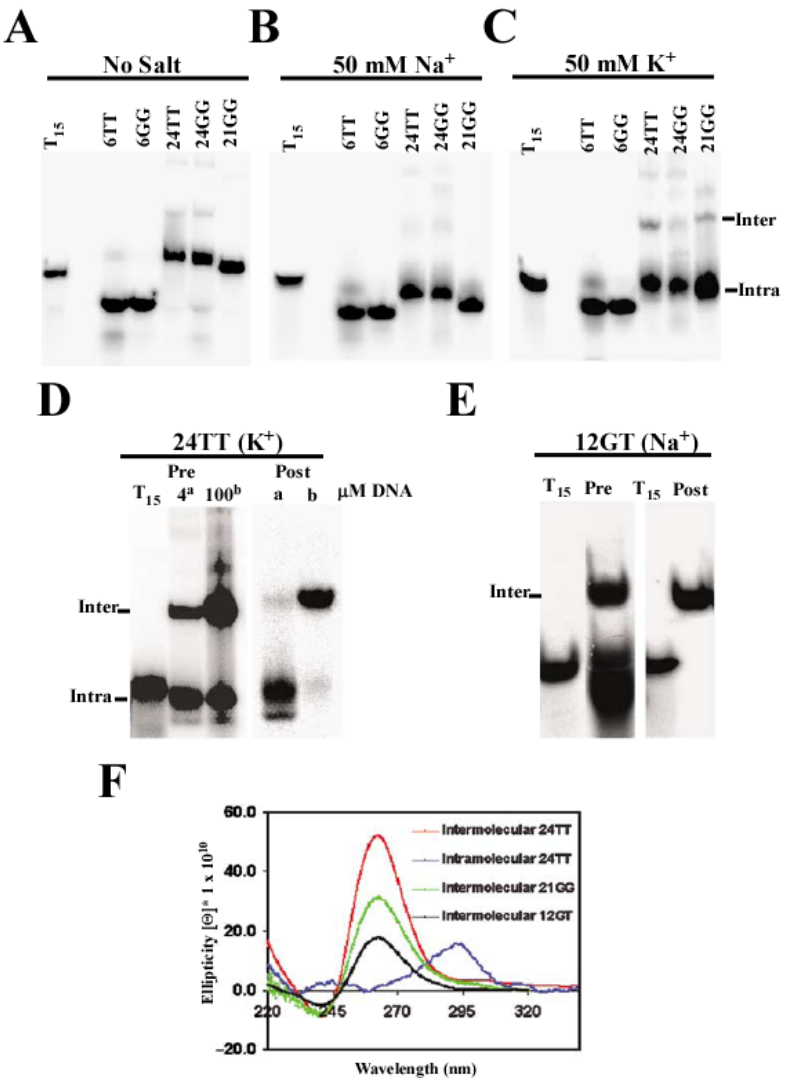

Figure 4.3. Characterization of gel-purified *Tetrahymena* G-quadruplexes. *Tetrahymena* oligonucleotides (1 µM) with no salt (A), 50 mM NaGlu (B), and 50 mM KGlu (C). Gel-purified intra- and intermolecular 24TT G-quadruplexes ([a] isolated from 4 µM DNA; [b] isolated from 100 µM DNA) in the presence of 50 mM KGlu (D), and intermolecular 12GT in the presence of 100 mM NaCl (E). T_{15} is an unstructured molecular weight marker. CD analysis of gel-purified *Tetrahymena* G-quadruplexes (F). Intermolecular 24TT, 21GG, and 12GT are parallel, while intramolecular 24TT G-quadruplex is antiparallel. Figure adapted from (Oganesian *et al.*, 2006).

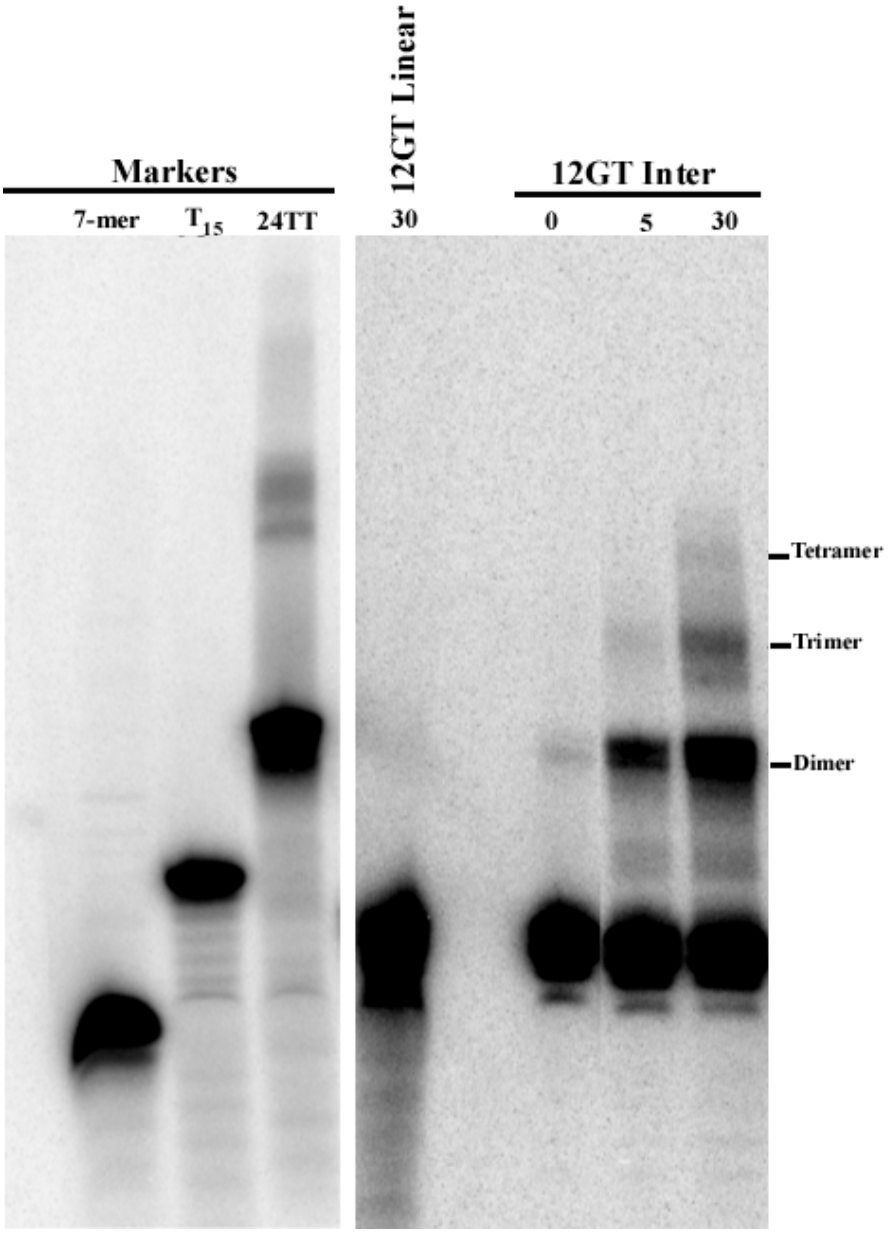

Figure 4.4. UV crosslinking of intermolecular 12GT stabilized in Na^+ to determine strand stoichiometry. ^{32}P-labelled intermolecular 12GT G-quadruplex (99% pure; 43 μM) was crosslinked at 254 nm for 0-30 min. at 25ºC. Linear counterpart was crosslinked for 30 min. as a negative control. 7-mer, T_{15}, and 24TT were used as size markers. The crosslinked products were electrophoresed on a 14% denaturing polyacrylamide gel. Figure adapted from (Oganesian *et al.*, 2006).

Stability of G-quadruplexes

The stability of each gel-purified G-quadruplex species was assessed using two methods. First, thermal denaturation studies were used to determine the melting temperature (T_m) of each folded structure (Table 4.2). Second, a complementary strand "trap" assay (Raghuraman and Cech, 1990) was conducted, in which an excess concentration of the C-strand was used to Watson-Crick base pair with any dissociated G-quadruplex molecules, indicating the rate of dissociation over time. The observed rates of G-quadruplex dissociation were independent of the concentration of the C-strand, supporting the passive trapping of the dissociated quadruplex by the C-strand and discounting an active invasion of the quadruplex by the C-strand.

In the case of the *Euplotes* intramolecular G-quadruplexes, the 15 nucleotide telomerase RNA template sequence (EaTR) was used as the complementary strand in the trap assay, to more effectively mimic the conditions present in the telomerase extension assay. In the case of the Oxy1.5 intermolecular G-quadruplex, the trap assay proved unsuccessful as 5' end radiolabelling of the telomeric sequence interfered with G-quadruplex assembly (Uddin *et al.*, 2004). Importantly though, this quadruplex was quite stable as the melting temperature was quite high (Table 4.2) and any dissociation of the complex observed over the use of the experiments was negligible.

Table 4.2. T_m values for *Euplotes* and *Tetrahymena* gel-purified G-quadruplexes. The UV melting curves were monitored at 295 nm in the appropriate folding buffer. Heating and cooling curves were superimposable with only slight hysteresis. [a] 10 μM strand concentration. [b] 20 μM strand concentration. Figure adapted from (Oganesian *et al.*, 2006).

G-quadruplex	Cation	Strand Orientation	Strand Stoichiometry	T_m(°C)[a]	T_m(°C)[b]
Oxy3.5	Na^+	Antiparallel	Intramolecular	60	-
Oxy3.5	K^+	Antiparallel	Intramolecular	85	-
Oxy1.5	K^+	Parallel	Intermolecular	88	-
21GG	K^+	Parallel	Intermolecular	82	88
24TT	K^+	Parallel	Intermolecular	77	90

Complementary Strand Trap Assay for *Euplotes* G-quadruplexes

The intramolecular Oxy3.5 K^+-stabilized G-quadruplex was incubated in the presence of increasing equivalents of EaTR in K^+ reaction buffer (Figure 4.5.A). The lone intramolecular G-quadruplex exhibited a single band, while preannealed Oxy3.5-EaTR showed multiple band shifts indicating that several higher order species had formed. The presence of these higher order species is likely due to several different binding modes of the RNA template to the DNA primer in 1:1 and 2:1 stoichiometries. These higher order interactions were not characterized individually, but were treated as contributors to the total amount of shifted DNA species. In order to determine if the total amount of shifted species changed with time, time course incubations with 1 and 100 molar equivalents of EaTR at 1 and 30 minute time points were conducted. At 1 minute with 100 equivalents of EaTR, 78% of the K^+-stabilized Oxy3.5 G-quadruplex was conserved, while at 30 minutes with 100 equivalents of EaTR, 76% of the quadruplex was conserved. This limited gain in hybridization over a 29 minute time lapse indicated that the purified G-quadruplex structure contained two populations of quadruplex. The first population of G-quadruplex (22%) rapidly bound to EaTR, while the second population of G-quadruplex (2%) hybridized over a longer time period. While the G-quadruplex is expected to be a single species, as demonstrated by CD analysis and native gel electrophoresis, this phenomenon has been previously reported in the literature and further research is required to accurately explain this interaction (Raghuraman and Cech, 1990).

The Na^+-stabilized intramolecular Oxy3.5 G-quadruplex time course revealed that at 1 minute with 100 equivalents of EaTR, 45% of the quadruplex was conserved, while at 30 minutes with 100 equivalents of EaTR, 35% of the quadruplex remained intact (Figure 4.5.B). Again, the purified G-quadruplex exhibited a rapidly hybridizable population

followed by a second population of quadruplex that hybridized slowly to the complementary strand. Furthermore, the observation that the Oxy3.5 intramolecular antiparallel G-quadruplex is less stable in Na^+ than in K^+ buffer was evident, a trend that has also been documented in the literature (Balagurumoorthy and Brahmachari, 1994; Dominick and Jarstfer, 2004; Hardin *et al.*, 1991; Raghuraman and Cech, 1990; Risitano and Fox, 2003).

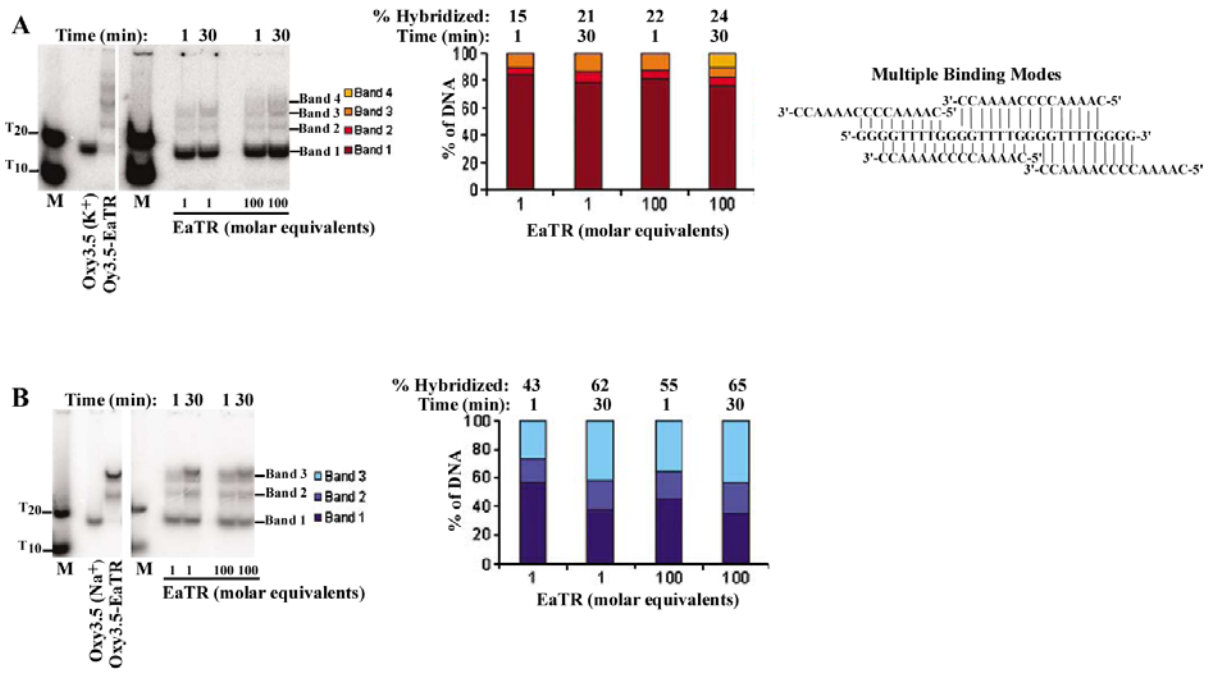

Figure 4.5. *Euplotes* complementary strand trap assays used to determine G-quadruplex stability in the presence of telomerase RNA template (EaTR). 5' end-labelled 10 μM Oxy1.5 intramolecular G-quadruplexes in 50 mM KGlu (A) or NaGlu (B) were incubated with 1 or 100 equivalents of unlabelled EaTR for 1 or 30 minutes at 25°C and electrophoresed on 20% nondenaturing polyacrylamide gels (in 50 mM K^+ (A) or NaGlu (B)). In lane 1: 5' end-labelled unstructured poly-T markers (M). Lane 2: lone G-quadruplex. Lane 3: preannealed Oxy3.5-EaTR polymorphic species. Figure adapted from (Oganesian *et al.*, 2006).

Complementary Strand Trap Assay for *Tetrahymena* G-quadruplexes

For the *Tetrahymena* G-quadruplexes, a 10 fold excess of the complementary strand (48CC) was added to the Na^+-stabilized 24TT and 21GG intramolecular G-quadruplexes, where by 98 and 100% of the quadruplexes, respectively, hybridized to the C-strand within 1.5 minutes (Figure 4.6.A). This suggests that the 24TT and 21GG intramolecular G-quadruplexes are highly unstable in Na^+, due to rapid unfolding. The monophasic mode of unfolding for both these quadruplexes exhibited half-lives ($t_{1/2}$) of less than 1.5 minutes.

The K^+-stabilized intramolecular 21GG G-quadruplex exhibited approximately 40% hybridization after 1 minute, and an additional 30% after 60 minutes (Figure 4.6.B, row 2). The biphasic unfolding kinetics for this G-quadruplex yielded an unfolding rate of $0.95 \pm 0.13\ h^{-1}$ ($t_{1/2}$ of 0.7 ± 0.1 h) for the slower unfolding population, and a $t_{1/2}$ of less than 1 minute for the initial hybridizable population. Likewise, the K^+-stabilized intramolecular 24TT G-quadruplex also demonstrated biphasic unfolding, with an initial unfolding of 32% of the quadruplex at 1.5 minutes ($t_{1/2} < 1$ minute) followed by slower unfolding at a rate of 0.15 ± 0.2 h which corresponds to a half life of 4.8 ± 0.8 h (Figure 4.6.B, row 1). Thus, for these two quadruplexes there are two distinct species: one that is readily hybridizable to the complementary strand and one that is not (Raghuraman and Cech, 1990).

The K^+-stabilized intermolecular 21GG and 24TT, and Na^+-stabilized intermolecular 12GT G-quadruplexes followed a monophasic unfolding trend (Figure 4.6.C). The intermolecular 21GG G-quadruplex exhibited less than 6% hybridization after 62 minutes; however the majority of hybridization can be attributed to the contaminating intramolecular 21GG counterpart (Figure 4.6.C, row 2). Similarly, less than 7% of the intermolecular 24TT G-quadruplex hybridized with the complementary strand after 63 minutes of incubation

(Figure 4.6.C, row 1). More impressively, the intermolecular 12GT G-quadruplex did not exhibit any detectable hybridization with the complementary strand over a 60 minute incubation time (Figure 4.6.C, row 3). For all three of these intermolecular G-quadruplexes, the unfolding was too slow to accurately fit to a single exponential equation.

The observed stabilities for the intermolecular parallel 21GG and 24TT G-quadruplexes in the complementary strand trap assays were further supported by their high melting temperatures (Table 4.2). As the strand concentration was increased from 10 to 20 μM the T_m increased, a property indicative of intermolecular G-quadruplexes. Overall the parallel intermolecular G-quadruplexes appear to be highly stable.

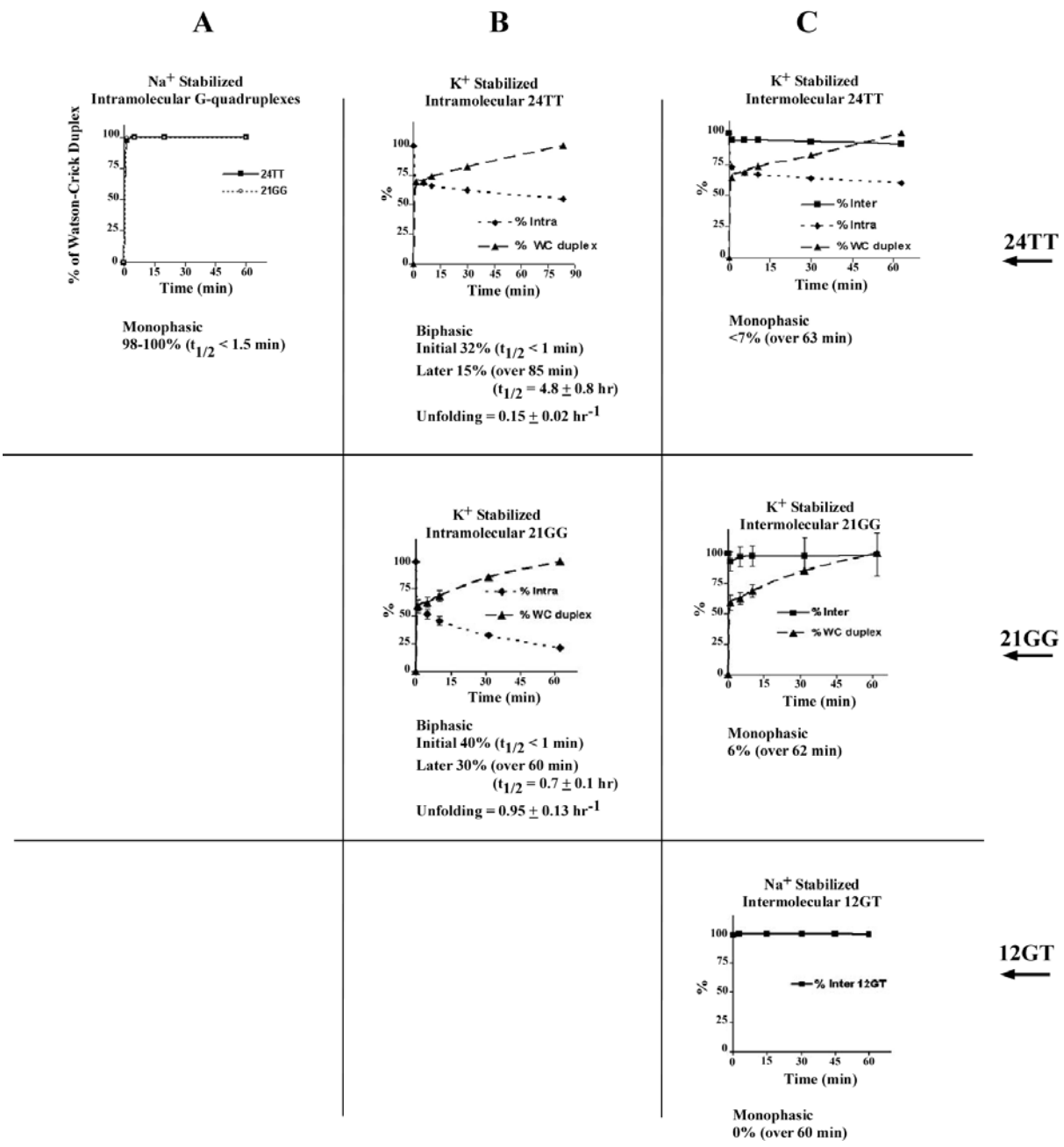

Figure 4.6. Complementary strand trap assay for gel-purified *Tetrahymena* G-quadruplexes. The plots show percentage of DNA that exists as G-quadruplex and hybridized Watson-Crick duplex over time; error bars represent the average of at least two experiments. (A) Unfolding of ^{32}P-labeled intramolecular Na^+-stabilized 24TT and 21GG G-quadruplexes. (B) Unfolding of ^{32}P-labeled intramolecular K^+-stabilized 24TT and 21GG G-quadruplexes. (C) Unfolding of ^{32}P-labeled intermolecular G-quadruplexes. Figure adapted from (Oganesian *et al.*, 2006).

Extension of Purified G-quadruplexes by Ciliate Telomerase

Euplotes Telomerase

Purified native *Euplotes* telomerase was tested for its ability to extend the G-quadruplexes formed from the Oxy3.5 and Oxy1.5 sequences. In all telomerase extension assays, the denatured control primer Ea23 and the corresponding denatured Oxy3.5 or Oxy1.5 counterpart was present for comparison with the respective G-quadruplex. The Ea23 primer, a sequence that is unable to form an intramolecular G-quadruplex, was used to gauge telomerase activity from batch to batch.

The K^+-stabilized intramolecular Oxy3.5 G-quadruplex (Figure 4.7) was a poor substrate for telomerase. The increased stability of the quadruplex's secondary structure in K^+ resulted in an increase in K_m, thus telomerase had a lower affinity for this structure as a substrate (Table 4.3).

In contrast, The Na^+-stabilized intramolecular Oxy3.5 G-quadruplex acted as a better substrate for telomerase-catalyzed extension (Figure 4.7). The lower K_m value for this quadruplex supports the trend that Na^+ stabilizes the same G-quadruplex less effectively than K^+, resulting in a more accessible primer.

Interestingly, the K^+-stabilized intermolecular Oxy1.5 G-quadruplex exhibited a lower K_m, an increased affinity, by comparison to the control Ea23 primer and the K^+-stabilized intramolecular Oxy3.5 G-quadruplex (Figure 4.7). Furthermore, despite an approximate 2 fold increase in K_m (Table 4.3), the overall activity observed with the quadruplex mirrored that of the denatured Oxy1.5 primer (Figure 4.7). This finding counters the thermodynamic data the where the intermolecular Oxy1.5 G-quadruplex exhibited the highest stability of all quadruplexes tested (Figure 4.2). One would postulate from the thermodynamic data that the

intermolecular Oxy1.5 G-quadruplex would yield the highest K_m and lowest overall activity of all the *Euplotes* G-quadruplexes tested, however this is not the case. Therefore, this experiment showed that the tetrameric G-quadruplex was available as a substrate for telomerase to a greater extent than what would have been expected from its measured stability.

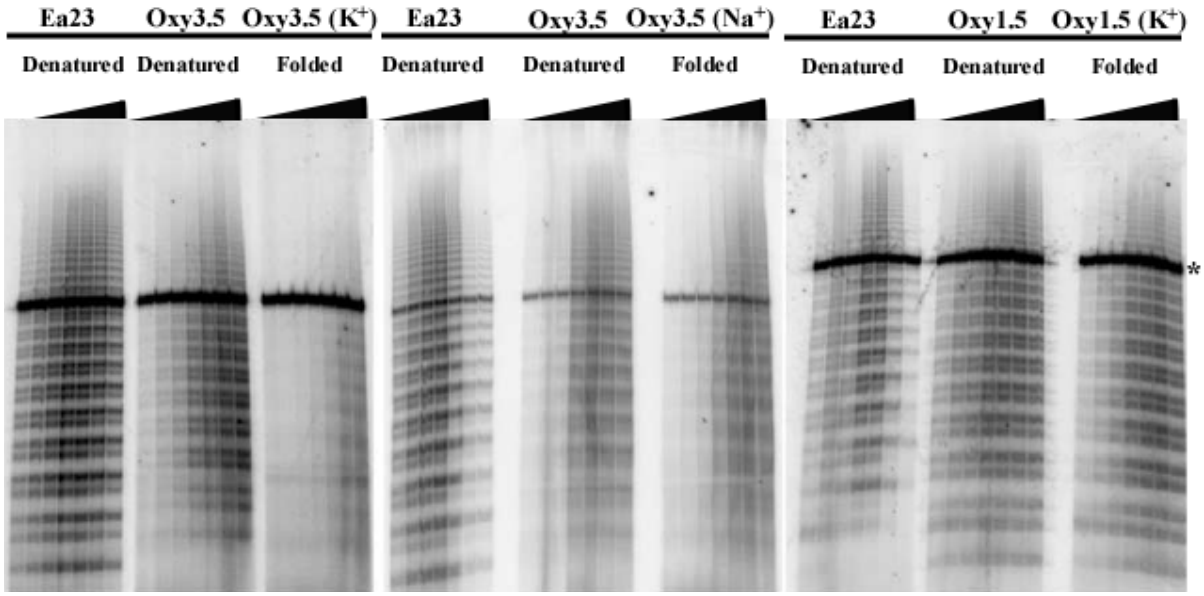

Figure 4.7. *Euplotes* telomerase can extend some G-quadruplexes. Denatured control primers (Ea23, Oxy3.5, and Oxy1.5) and G-quadruplexes from 25 nM-2 μM were incubated in 50 mM KGlu (Oxy1.5) or 50 mM K^+ or NaGlu (Oxy3.5 and Ea23) at 25ºC for 60 minutes in the presence of 1.4 ng of purified telomerase. * denotes the ^{32}P-labelled 113mer loading control. Figure adapted from (Oganesian *et al.*, 2006).

Table 4.3. K_m values and relative V_{max} ratios (folded/linear Ea23 control) for gel-purified *Euplotes* G-quadruplexes. DNAs were folded and stabilized in 50 mM monovalent cation and their linear counterparts. [a]K_m's of Ea23 and G-quadruplexes were determined simultaneously to account for inter-day variation. Figure adapted from (Oganesian *et al.*, 2006).

Primer	Stabilizing Cation	Conformation	$K_m \pm$ s.d. (nM)	Relative V_{max} (folded/linear)
Ea23	K^+	Linear/denatured	90 ± 20[a]	1.00 ± 0.06
Oxy3.5	K^+	Linear/denatured	100 ± 30	0.50 ± 0.07
Oxy3.5	K^+	Intramolecular	460 ± 120	0.30 ± 0.03
Ea23	Na^+	Linear/denatured	40 ± 3	1.00 ± 0.02
Oxy3.5	Na^+	Linear/denatured	47 ± 12	0.65 ± 0.03
Oxy3.5	Na^+	Intramolecular	27 ± 9	0.56 ± 0.03
Ea23	K^+	Linear/denatured	110 ± 40	1.00 ± 0.14
Oxy1.5	K^+	Linear/denatured	40 ± 7	0.67 ± 0.03
Oxy1.5	K^+	Intermolecular	74 ± 16	0.57 ± 0.04

Tetrahymena Telomerase

The Na^+-stabilized intramolecular 21GG and 24TT G-quadruplexes were readily extended by recombinant *Tetrahymena* telomerase (Figures 4.8.A and 4.9.A). These G-quadruplexes exhibited higher K_m values and equivalent or lower relative V_{max} values than their linear counterparts (Table 4.4), indicating that these structures are used less efficiently (lower k_{cat}/K_m) as substrates for telomerase. This supports the idea that the Na^+-stabilized G-quadruplex is in constant equilibrium with its linear counterpart, meaning less linear substrate is available for binding and extension by telomerase when compared to linear or denatured controls.

The K^+-stabilized intramolecular 21GG and 24TT G-quadruplexes (Figures 4.8.B and 4.9.B) served poorly as primers for telomerase. This result was unexpected due to the rapid hybridization of 32-40% of the purified G-quadruplexes in the complementary strand trap assays (Figure 4.6.A). The lack of extension by telomerase is not likely due to the absence of an accessory protein in the *in vitro* reconstituted preparation of *Tetrahymena* telomerase, as partially purified native *Tetrahymena* telomerase also failed to utilize the K^+-stabilized intramolecular 24GG G-quadruplex as a primer (data not shown).

The intermolecular 21GG, 24TT and 12GT G-quadruplexes, in contrast to their intramolecular counterparts, were excellent substrates for *Tetrahymena* telomerase (Figures 4.8.C-E and 4.9.B and C). Importantly, the extension observed was not likely due to spontaneous dissociation of the quadruplexes, as the unfolding analyses showed that only a small percentage (at most ~6%) of the G-quadruplex unfolds within the first 10 minutes of the reaction. In the extension of the 21GG intermolecular G-quadruplex (Figure 4.8.D), if spontaneous unfolding was the cause for the observed extension, then the amount of activity

observed for a given concentration of the quadruplex should be equivalent to the activity of the corresponding linear sequence at 6%. However, the amount of extension of linear 21GG at 0.09 μM (6% of 1.5 μM), for example is 3.8 fold lower than the amount of extension of the intermolecular 21GG G-quadruplex at 1.5 μM. This same trend is observed for the 24TT intermolecular G-quadruplex (Figure 4.9.C), and is even more pronounced for the intermolecular 12GT G-quadruplex, where it is extended by telomerase (Figure 4.8.E) in the absence of any detectable unfolding, 0% unfolding over 60 minutes (Figure 4.6.C).

To further characterize the K^+-stabilized intermolecular 24TT G-quadruplex as a candidate substrate for telomerase, the affinity (K_m) and rate constants (k_{cat}) for the purified quadruplex and linear control were measured. Telomerase exhibited a reduced affinity for the intermolecular G-quadruplex, with a K_m of 3160 $\pm$ 1100 nM as compared to its linear control at 450 $\pm$ 230 nM. Despite a higher k_{cat} for the G-quadruplex at 0.4 $\pm$ 0.1, as compared to 0.18 $\pm$ 0.01 for its linear counterpart, the quadruplex retains a lower k_{cat}/K_m than that of the linear control (2.1 $\pm$ 0.9 x 10^3 versus 6.7 $\pm$ 2.5 x 10^3 s^{-1} M^{-1}). Therefore, while the G-quadruplex serves as a good substrate, the linear counterpart is favored by telomerase.

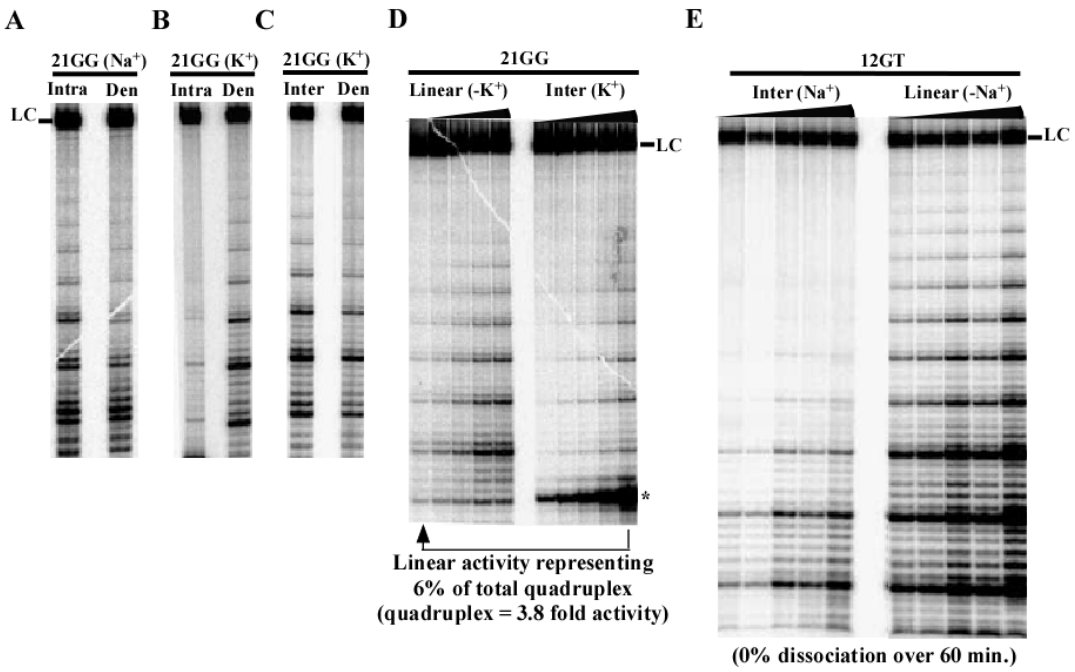

Figure 4.8. *Tetrahymena* telomerase can extend some G-quadruplexes. For all panels, LC denotes the ^{32}P-labelled 100-mer loading control; * denotes unextended ^{32}P-labeled gel-purified G-quadruplexes; Den represents denatured oligonucleotides, respectively. All assays were conducted at 25ºC for 60 min (A-C), 10 min (D), or 15 (E) min using ~ 2 nM *in vitro* reconstituted *Tetrahymena* telomerase. (A) Extension of ^{32}P-labeled intramolecular 21GG (GP; 1.8 μM; 85% purity) and unlabeled 21GG (1.8 μM) in 50 mM NaGlu. (B) Extension of ^{32}P-labeled intramolecular 21GG (1.1 μM; 78% purity) and unlabeled 21GG (1.1 μM) in 150 mM KGlu. (C) Extension of ^{32}P-labeled intermolecular 21GG (0.7 μM; 66% purity) and unlabeled 21GG (0.7 μM) in 150 mM KGlu. (D) Extension of ^{32}P-labeled intermolecular 21GG (0.9 μM; 63% purity) in 50 mM KGlu. The control is unlabeled linear 21GG over the same concentration range (-KGlu). (E) Telomerase extension of intermolecular 12GT (0.06-8 μM; 99% purity) in 100 mM NaCl. Linear 12GT (-NaCl) and denatured 12GT (+NaCl) G-quadruplex over the same concentration range were used as controls. Figure adapted from (Oganesian *et al.*, 2006).

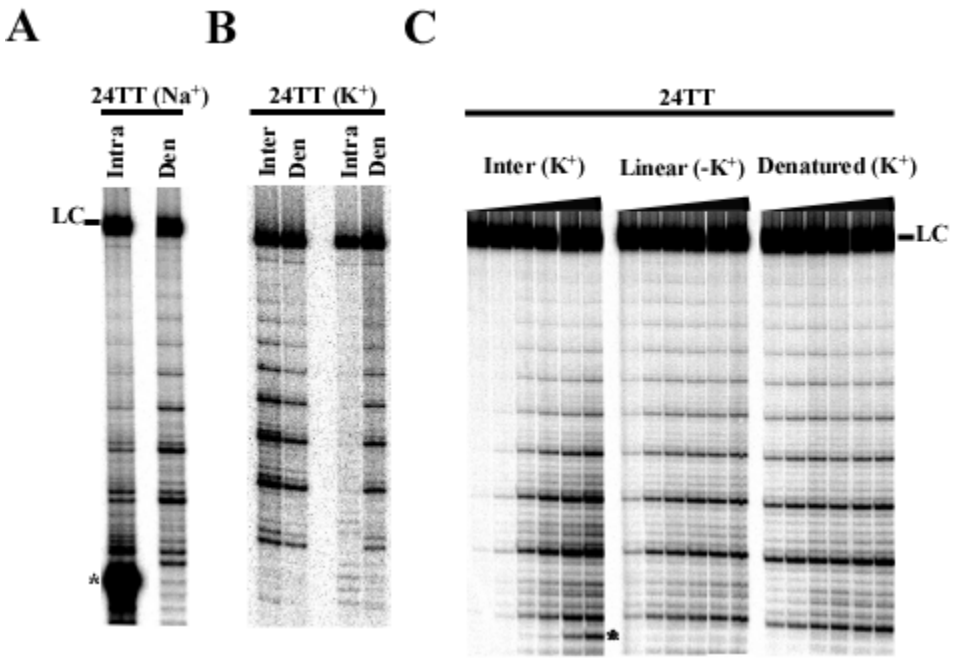

Figure 4.9. *Tetrahymena* telomerase can extend some G-quadruplexes (continued). For all panels, LC denotes the ^{32}P-labelled 100-mer loading control; * denotes unextended ^{32}P-labelled gel-purified G-quadruplexes; Den represents denatured oligonucleotides, respectively. All assays were conducted at 25ºC. (A) ^{32}P-labeled intramolecular 7.7 μM 24TT (GP Intra; 93% purity) stabilized in 50 mM NaGlu was incubated for 60 min in a telomerase activity assay. Unlabeled unpurified 24TT primer of the same concentration folded in the presence of 50 mM NaGlu was used as a control. (B) Telomerase activity assay using unlabeled inter- (7.7 μM) and intramolecular (1.3 μM) 24TT G-quadruplex stabilized in the presence of 50 mM KGlu (lanes 1 and 3 respectively). Unpurified 24TT primer was folded in the presence of 50 mM KGlu at either 7.7 μM or 1.3 μM (lanes 2 and 4 respectively) and was incubated in a 60 min telomerase activity assay. (C) Telomerase extension of increasing concentrations (0.04-18 mM) of ^{32}P-labeled intermolecular 24TT G-quadruplex (86% purity) stabilized in 50 mM KGlu. The control is unlabeled linear 24TT over the same concentration range (-KGlu). Additionally, to control for the effect of KGlu, linear 24TT (+KGlu) was denatured at 95ºC for 5 min and immediately placed on ice prior to extension. The extension was carried out for 10 min. Figure adapted from (Oganesian *et al.*, 2006).

Table 4.4. K_m values and relative V_{max} ratios (G-quadruplex/linear DNA) for gel-purified intramolecular *Tetrahymena* G-quadruplexes. Figure adapted from (Oganesian *et al.*, 2006).

Primer	Conformation	K_m + s.d. (nM)	Relative V_{max} (folded/linear)
24TT	Intramolecular	1240 ± 750	0.34 ± 0.09
24TT	Linear	560 ± 60	
24GG	Intramolecular	880 ± 420	1.19 ± 0.4
24GG	Linear	160 ± 50	

Snake Venom Phosphodiesterase I Digestion of G-quadruplexes

To further support the observation that extension of *Euplotes* and *Tetrahymena* intermolecular G-quadruplexes was not due to dissociation related to the equilibrium of these structures with their linear counterparts, or the possibility that 3' overhangs may exist which telomerase could exploit (Figure 4.10.A), G-quadruplexes were subjected to enzymes that are known to act on single-stranded DNA. Snake venom phosphodiesterase I (SVPI), an enzyme that cleaves single-stranded DNA exonucleolytically from the 3' end, efficiently digested a majority of linear single-stranded control DNA (Figure 4.10.B-E). However, approximately 100% of the intermolecular Oxy1.5, 24TT, and 12GT G-quadruplexes were resistant to SVPI treatment. Furthermore, the intramolecular G-quadruplexes were more prone to digestion than the intermolecular G-quadruplexes, consistent with their faster rates of unfolding and in contrast to their decreased extension by telomerase (Figure 4.10.C and E). Approximately 13% of the intermolecular 21GG G-quadruplex was digested, however it was likely attributed to the approximate 35% contaminating intramolecular 21GG quadruplex. As expected, the terminal two 3' residues on the intermolecular 24TT G-quadruplex were digested, however none of the other G-quadruplexes showed digestion of terminal nucleotides, indicating that these structures do not contain 3' overhangs which potentially could be extended.

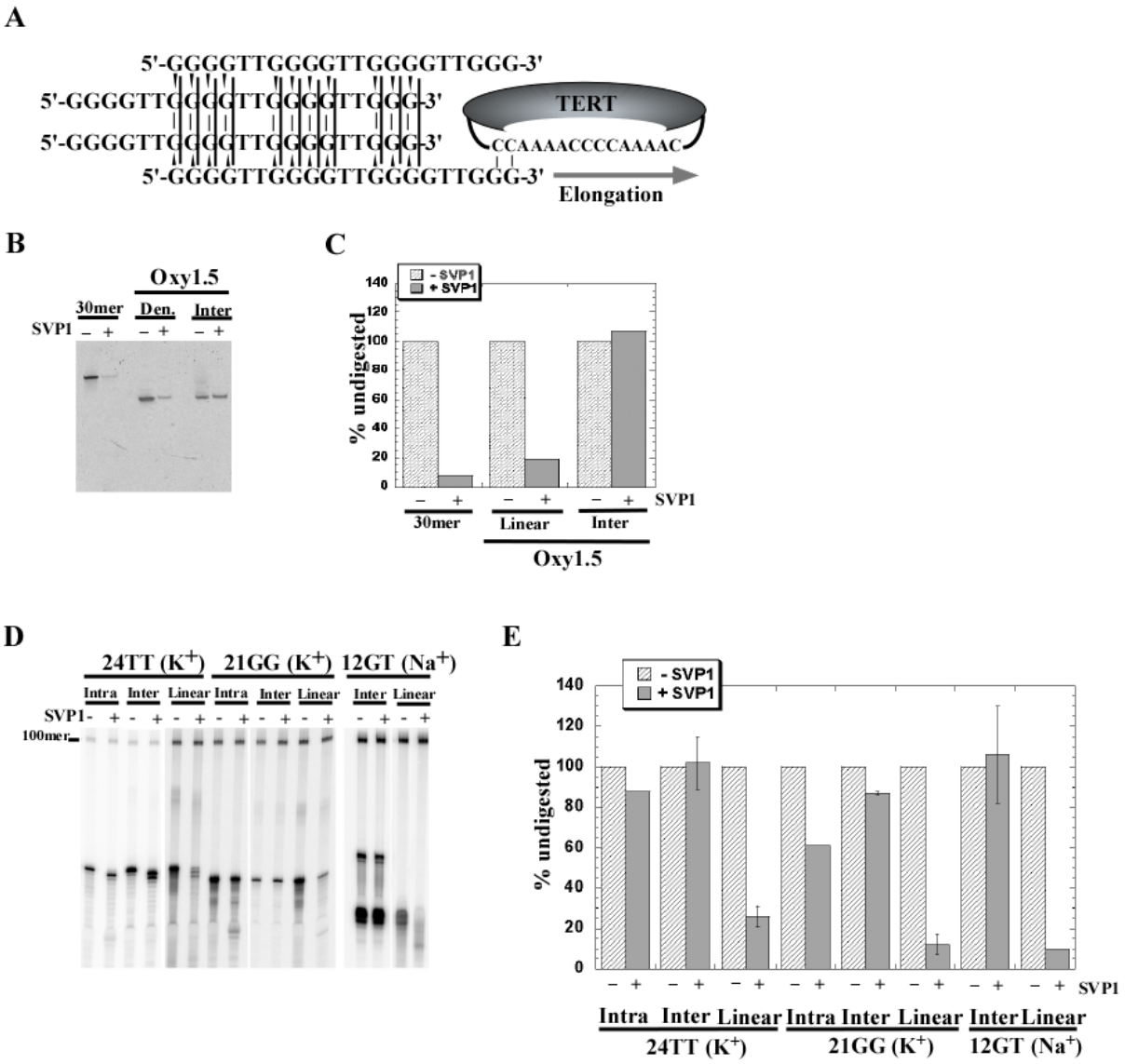

Figure 4.10. Snake venom phosphodiesterase I (SVPI) digestions of G-quadruplexes from the *Euplotes* and *Tetrahymena* telomeric sequence. (A) 200 ng of intermolecular (K^+) Oxy1.5 G-quadruplex, denatured (Den.) Oxy1.5, and nontelomeric 30mer control were incubated with or without SVPI for 25 min at 25ºC. The proportion of undigested DNA, as a percentage of the –SVPI control, is represented in (B). (C) 21GG and 24TT intra- (~73% and 94% purities; 0.7 and 1.5 μM respectively) and intermolecular (~64% and 88% purities; 12 and 3 μM respectively) K^+-stabilized G-quadruplexes, intermolecular (Na^+) 12GT G-quadruplex (~99% purity; 95 μM), and linear controls were incubated with or without SVPI for 10 min at 25ºC. The proportion of undigested DNA, as a percentage of the –SVPI control, is represented in (D). Figure adapted from (Oganesian *et al.*, 2006).

Terminal Deoxytransferase Extension of G-quadruplexes

Just as the previous experiment probed G-quadruplexes for dissociation and overhangs by examining susceptibility to degradation, the reverse experiment was employed to validate the previous results by detecting for extension of G-quadruplexes using a different single-stranded DNA processing enzyme. The enzyme terminal deoxytransferase (TdT), which adds nucleotides to 3' overhangs or double-stranded DNA, was used to probe intermolecular G-quadruplexes for 3' overhangs or dissociation to linear forms. While TdT efficiently extended the linear controls, the intermolecular Oxy1.5 and 12GT G-quadruplexes showed only minimal extension by this enzyme (Figure 4.11.A-C).

The SVPI and TdT assays demonstrate that the intermolecular G-quadruplexes are not efficient substrates for either of these nucleic acid processing enzymes. Therefore, it is unlikely that telomerase-catalyzed extension of this subset of G-quadruplexes is due to the presence of linear DNA and highlights an apparently unique ability of telomerase to process G-quadruplex DNA.

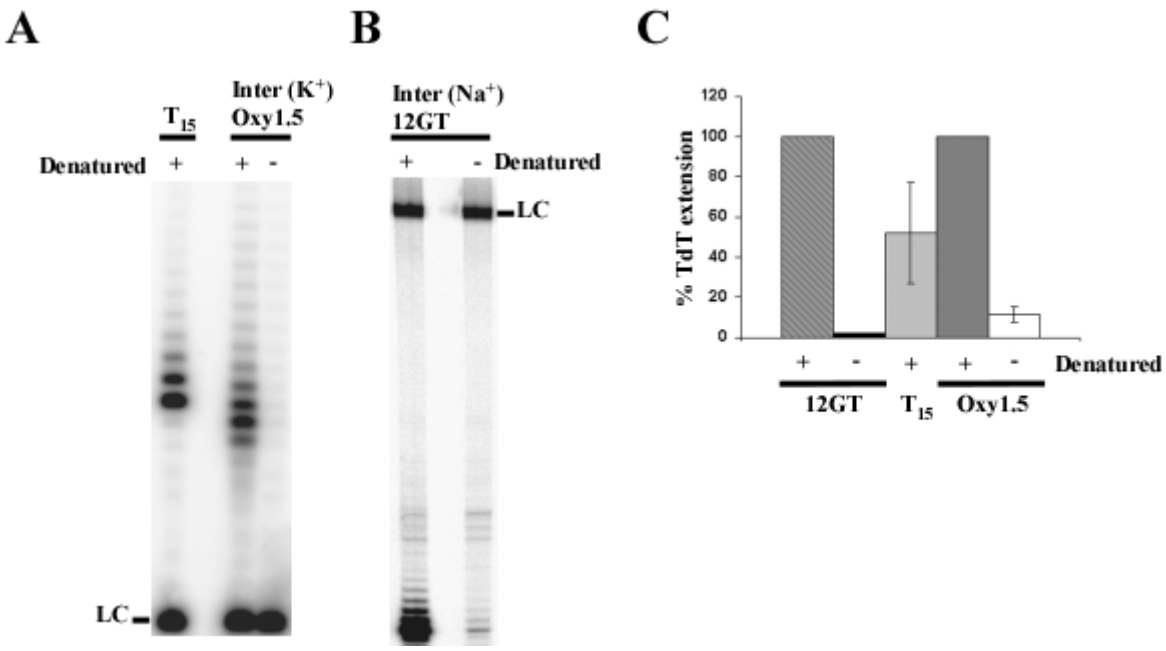

Figure 4.11. Terminal deoxytransferase (TdT) extension of intermolecular *Euplotes* Oxy1.5 and *Tetrahymena* 12GT G-quadruplexes. LC denotes loading controls. (A) 2 pmols of intermolecular K^+-stabilized Oxy1.5 G-quadruplex, denatured Oxy1.5, and T_{15} control primer were incubated with TdT for 60 min at 25ºC. (B) Intermolecular Na^+-stabilized 12GT G-quadruplex (~99% purity; 17 μM) and denatured 12GT were incubated with TdT for 10 min at 25ºC. (C) Graphical representation of the percentage of TdT extension of DNA, normalized to denatured quadruplex extension. Figure adapted from (Oganesian *et al.*, 2006).

Direct Binding of *Tetrahymena* TERT to G-quadruplex DNA

To determine whether the extension of parallel intermolecular G-quadruplexes is related to their ability to directly interact with recombinant *Tetrahymena* telomerase, DNA-protein immunoprecipitation studies were conducted. Biotinylated 21GG and 24TT oligonucleotides were gel-purified as linear DNA, intramolecular G-quadruplexes, and intermolecular G-quadruplexes, and were individually preincubated with *in vitro* reconstituted, ^{35}S-labeled immunopurified *Tetrahymena* telomerase protein (TERT). Any protein bound to the structured or unstructured DNA was then recovered using NeutrAvidin coated beads and the amount of protein was visualized on an SDS-PAGE gel.

The biotinylated 21GG (Biot-21GG) and 24TT (Biot-24TT) intermolecular G-quadruplexes (Figure 4.12.B and D) captured comparable levels of TERT protein to their linear counterparts (Figure 4.12.A and C). Both of these G-quadruplexes bind TERT with higher K_d values than their linear forms, reflecting the trend observed for their K_m values. The K^+-stabilized Biot-21GG and Biot-24TT intramolecular G-quadruplexes displayed negligible interaction with TERT (Figure 4.12.B and D). The intramolecular Biot-21GG appears to bind TERT to a greater extent than the intramolecular Biot-24TT; however the former contains an intermolecular G-quadruplex contaminant of up to 26% of the total DNA.

Together these results show that TERT has a strong binding affinity for the K^+-stabilized parallel intermolecular G-quadruplexes, but has a poor affinity for the K^+-stabilized antiparallel intramolecular G-quadruplex counterparts.

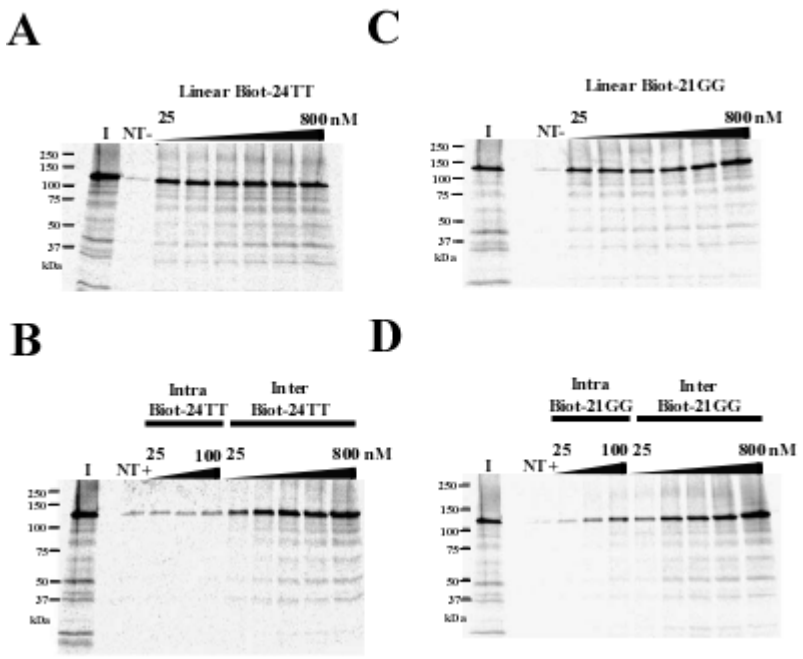

Figure 4.12. Primer pull-down assays of *in vitro* reconstituted immunopurified recombinant *Tetrahymena* telomerase using biotinylated G-quadruplexes. Biot-BPR, a nontelomeric (NT) control oligonucleotide (800 nM), in the presence (NT+) or absence (NT-) of KGlu. 'I' represents input telomerase (25%). Gel-purified intra- and intermolecular Biot-24TT G-quadruplexes (B), or a linear Biot-24TT control (A), were used in pull-down assays at the indicated concentrations, in the presence or absence of 50 mM KGlu, respectively. Gel-purified intra- and intermolecular Biot-21GG G-quadruplexes (D), or a linear Biot-21GG control (C), were used in pull-down assays at the indicated concentrations, in the presence or absence of 50 mM KGlu, respectively. Figure adapted from (Oganesian *et al.*, 2006).

Discussion

Ciliate Telomerase Extends Parallel Intermolecular G-quadruplexes

Currently, the consensus in G-quadruplex literature is that G-rich DNA is sequestered into stable G-quadruplex structures that are unavailable for enzymes such as telomerase to utilize as substrates. In this study, a subclass of G-quadruplexes that can be extended by telomerase was identified. Here in, it was demonstrated that parallel intermolecular G-quadruplexes are robust substrates for both *Euplotes* and *Tetrahymena* telomerase, to an extent exceeding that predicted from their stability. As partial resolution of the G-quadruplex structure is necessary for the required base pairing to the telomerase RNA template, we propose that telomerase itself has inherent G-quadruplex resolvase activity, specific for this particular class of G-quadruplexes.

The extension of parallel intermolecular G-quadruplexes by telomerase, as mediated through spontaneous dissociation of the quadruplex, has been discounted by a battery of experiments that interrogated the integrity of these quadruplexes. In thermal denaturation studies, the parallel intermolecular G-quadruplexes collectively exhibited the highest melting temperatures, with T_m values greater than 77°C. Furthermore, in complementary strand trap assays, only 0-7% of the *Tetrahymena* intermolecular G-quadruplexes hybridized over 60 minutes, which was an insufficient amount of DNA to account for the observed telomerase activity. Supporting this, K^+-stabilized intramolecular G-quadruplexes exhibited faster unfolding than their intermolecular counterparts, and yet were barely extended by telomerase, providing additional evidence that the amount of G-quadruplex unfolding during these time frames is not in direct correlation with the telomerase activity observed. The parallel intermolecular G-quadruplexes were also resistant to single-stranded specific

nuclease degradation (SVPI) or extension (TdT), indicating that there is insufficient single-stranded linear DNA to account for the robust extension by telomerase.

Furthermore, the *Tetrahymena* parallel intermolecular G-quadruplexes were able to directly interact with the protein component (TERT) of recombinant *Tetrahymena* telomerase, thus reinforcing the specificity of this higher order structure as a telomerase substrate. At present, we have been unable to discern whether the intermolecular or parallel property, or both properties of these G-quadruplexes is important for binding and extension by telomerase. Future studies aimed at elucidating this issue will be needed. Presently, the solution structures for parallel intermolecular G-quadruplexes assembled from 21GG, 24TT, or 12GT have not been solved; similarly, that of the *Euplotes* parallel intermolecular Oxy1.5 G-quadruplex structure is not known. The crosslinking experiments in this study support the formation of a four-stranded structure for 12GT. The migration of the remaining G-quadruplexes on native gels suggests that Oxy1.5 is a tetramer, while 21GG and 24TT are dimers. The later *Tetrahymena* quadruplexes likely have a 'propeller-like' folded structure (Parkinson *et al.*, 2002), however a four-stranded structure can not be ruled out.

Because native *Euplotes* and recombinant *Tetrahymena* telomerase are both able to utilize parallel intermolecular G-quadruplexes as substrates, we propose that the core telomerase complex, consisting of TERT protein and telomerase RNA, possesses a G-quadruplex resolvase capacity. Although we can not rule out that a contribution from contaminating protein(s) may assist in telomerase processing a structured primer, co-purification of such protein(s) in two different systems is unlikely.

Extension of Antiparallel Intramolecular G-quadruplexes Correlates with their Stability

Within this study, the previous observations made by Zahler *et al* (1991) were also confirmed in the class of antiparallel intramolecular G-quadruplexes. Na^+-stabilized G-quadruplexes of antiparallel intramolecular conformation were readily extended by telomerase. These quadruplexes have quick dissociation rates and are likely in rapid equilibrium with their linear forms, which provides an explanation for their ability to be extended by telomerase. This is consistent with the results found in this study and with previous reports, whereby lower melting points and faster unfolding kinetics have been observed for Na^+-stabilized G-quadruplexes compared to their K^+-stabilized counterparts (Balagurumoorthy and Brahmachari, 1994; Dominick and Jarstfer, 2004; Hardin *et al.*, 1991; Raghuraman and Cech, 1990; Risitano and Fox, 2003).

In agreement with this, the more stable K^+-stabilized, antiparallel, intramolecular G-quadruplexes showed two distinct phases of unfolding, rather than one as observed in the Na^+-stabilized intramolecular G-quadruplexes, a rapid phase and a slow phase, as previously reported (Raghuraman and Cech, 1990). This implies that these G-quadruplexes contain two subpopulations, one that is readily hybridizable with a complementary strand corresponding to a half-life of less than a minute, and another which shows slow dissociation corresponding to a half-life of several hours. However neither of these subpopulations is extended by telomerase nor interacts with the telomerase protein (TERT). This suggests that the simple ability of telomerase to hybridize with a complementary DNA or RNA is not the basis for telomerase extension of a G-quadruplex. Therefore, the ability of ciliate telomerase to utilize

antiparallel intramolecular G-quadruplexes as substrates is directly influenced by the relative stability of the G-quadruplex, which is dictated by the identity of the stabilizing cation.

In vivo Relevance

Although the presence of parallel intermolecular G-quadruplexes in ciliated protozoa has not been directly observed *in vivo*, the potential for their formation does exist. The single-stranded lengths of telomeres in *Euplotes* are exactly 14 nucleotides (Klobutcher *et al.*, 1981) and in *Tetrahymena* are 14-15 or 20-21 nucleotides (Jacob *et al.*, 2001), suggesting that G-quadruplex formation at the ends of these telomeres would be mediated by an antiparallel dimeric structure or a parallel dimeric or tetrameric structure. Currently, *in vivo* evidence for the formation of G-quadruplexes at the telomeres in another ciliate, *Stylonychia lemnae* (Paeschke *et al.*, 2005; Schaffitzel *et al.*, 2001), support the existence of antiparallel dimeric G-quadruplexes, however it does not rule out the formation of parallel G-quadruplexes at the telomeres, in other organisms, or at other stages in the life cycle.

As previously demonstrated *in vitro*, Na^+/K^+ concentrations can affect the balance between antiparallel and parallel G-quadruplexes, with K^+ favoring parallel conformations (Miura *et al.*, 1995; Sen and Gilbert, 1990). Ca^+ has also demonstrated the ability to induce a transition in G-quadruplexes from antiparallel to parallel (Miyoshi *et al.*, 2003). As cellular systems are dynamic, it is conceivable that under different conditions *in vivo*, one or another G-quadruplex conformation may be favored, thus influencing whether telomerase can interact with telomeric DNA. Furthermore, in *Oxytricha* and *Tetrahymena* but not human, *in vitro* molecular crowding conditions can induce a transition from antiparallel to parallel G-quadruplexes, which may more closely mimic the *in vivo* environment (Miyoshi *et al.*, 2005; Miyoshi *et al.*, 2004).

The formation of intermolecular G-quadruplexes involving telomeres from adjacent chromosomes may facilitate telomere-telomere interactions; in particular, the association of

four parallel telomeric strands could be involved the alignment of four sister chromatids during meiosis (Sen and Gilbert, 1988). The clustering of telomeres in a meiotic bouquet arrangement has been observed in almost all organisms, including ciliates (Harper *et al.*, 2004; Loidl and Scherthan, 2004); while HOP1, a component of the meiosis specific synaptonemal complex in *Saccharomyces cerevisiae*, demonstrated the ability to promote pairing of double-stranded DNA helices via G-quartet formation, and thus implicated intermolecular G-quadruplexes as the force behind chromosomal synapsis during meiotic prophase (Anuradha and Muniyappa, 2004). The TGP1 (*Tetrahymena* G-DNA binding protein 1), which has demonstrated the ability to bind intermolecular G-quadruplexes formed by the 5'-$(T_2G_4)_4$-3' sequence, may act as a stabilizing protein in such G-quadruplex intermolecular assemblies (Lu *et al.*, 1998). Potentially, telomerase's resolvase activity could allow for the dissociation of interchromosomal complexes, via parallel intermolecular G-quadruplex unwinding, and subsequently the synthesis of telomeric DNA.

Acknowledgements

I would like to thank Liana Oganesian, Ph.D. and Tracy Bryan, Ph.D. for their work with the *Tetrahymena* model for this study.

Experimental Procedures

Oligonucleotide Preparation

DNA oligonucleotides (Table I) were purchased from Sigma Genosys (*Tetrahymena*) or Integrated DNA Technologies (*Euplotes*) in desalted form. All oligonucleotides with the exception of 12GT were purified by electrophoresis on denaturing 20% polyacrylamide/8M urea gels in 1x TBE buffer (89 mM Tris, 89 mM Borate, 2 mM EDTA) and the major band was excised, eluted by crushing and soaking in TEN (10 mM Tris-HCl pH 7.5-8.0, 1 mM EDTA, 100-250 mM NaCl) and ethanol precipitated. In some experiments, the oligonucleotides were 5' end-labeled with [γ^{32}P] ATP (Perkin Elmer) using T4 polynucleotide kinase (New England Biolabs) for 30 min at 37°C. Labeled DNA was purified on either "Mini Quick Spin columns for Oligos" (Roche) or MicroSpin Sephadex G-25 TE columns (Amersham Biosciences) to eliminate unincorporated radioactive nucleotides. Purified labeled and unlabeled *Tetrahymena* oligonucleotides were dialyzed for 12-16 hours at 4°C against Milli Q water to further desalt them.

The RNA oligonucleotides EaTR and 30AA (Table I) were purchased from Dharmacon (Lafayette, CO), stored in their protected forms, and deprotected following the protocol described by the manufacturer before use.

Radiolabeling of Oligonucleotides

10 pmol of DNA was 5'end-labeled with [γ^{32}P]-ATP (Perkin Elmer) using 5-10 U of T4 poly nucleotide kinase (Promega) for 30 min at 37ºC. Labeled DNA was purified on either "Mini-Quick Spin columns for Oligos" (Roche) or MicroSpin Sephadex G-25 TE columns (Amersham Biosciences) to eliminate unincorporated radioactive nucleotides.

G-quadruplex Formation, Electrophoresis and Purification

Euplotes oligonucleotides. 200 μM Oxy 1.5 and 1 μM Oxy 3.5 in 1X *Euplotes* folding buffer (20mM TrisOAc pH 7.5, 10 mM $MgCl_2$, 1 mM DTT, and 50 mM K^+ or NaGlu) were heated to 95°C for 5 min and allowed to slowly cool (~2° C/min) to 25°C. Folded DNA was electrophoresed on 20% nondenaturing gels (50 mM K^+ or NaOAc) for 3.5 hr at 100 V at 4°C using a running buffer of 50 mM K^+ or NaOAc in 1X TBE. DNA was visualized by phosphorimaging (^{32}P-labeled DNA) or UV shadowing (unlabeled DNA), isolated by crush and soak method into 1X TEK (10 mM Tris-HCl pH 8.0, 1 mM EDTA, 100 mM KCl) or TEN buffer, and concentrated by ethanol precipitation. Samples were resuspended in the corresponding 1X *Euplotes* folding buffer, and quantified by scintillation counting (labeled DNA) or UV absorbance at 260 nm (unlabeled DNA; see Supplementary Table I for extinction coefficients) (Oganesian *et al.*, 2006). The integrity of the recovered structures was confirmed by native gel electrophoresis followed by phosphorimaging. Radiolabeled structures were used for solution hybridization studies, whereas unlabeled G-quadruplexes were used for telomerase assays and CD analysis.

Tetrahymena oligonucleotides. Oligonucleotides of *Tetrahymena thermophila* telomeric sequence spiked with 5,000-10,000 c.p.m. of radiolabeled oligonucleotide of the same sequence were heat denatured in 1x Tetrahymena Telomerase buffer (50 mM Tris-HCl pH 8.3, 1.25 mM $MgCl_2$, 5 mM dithiothreitol (DTT)) and either 50 mM sodium glutamate (NaGlu) or 50 or 150 mM potassium glutamate (KGlu) at 95°C for 5-10 min, then allowed to equilibrate at 23°C for 30 min. The folded DNA was added to 6X native gel loading buffer (0.25% bromophenol blue, 0.25% xylene cyanol and 30% glycerol) and electrophoresed on a nondenaturing 12% polyacrylamide gel for 3.5-5 hr at 10 W at 23°C. Both buffer and gel contained the same constituents as those in

which the DNA was folded with the exception of DTT. The gel was dried for 60 min at 80°C and exposed to a PhosphorImager screen (Molecular Dynamics) for 12-16 hr.

To gel purify particular G-quadruplex conformations from 21GG, 24GG and 24TT, DNA was folded as described above either in 0.1 ml of relevant salt buffer at 100 μM final concentration or 1 ml of buffer at 2-4 μM concentration for inter- and intramolecular conformations, respectively. To isolate an intermolecular form of 12GT, 1 mM DNA was heat denatured as above and incubated at 25-37ºC for 2-3 days in the presence of 1X Telomerase buffer and 100 mM NaCl. The folded DNA was electrophoresed on a native gel as described above. The gel was exposed to BioMax Kodak film for 1 hr to determine the location of the radiolabeled oligonucleotide. Comigration of this band with the bulk of the unlabeled DNA was confirmed by UV shadowing. The band of interest was excised and crushed in 250 mM KGlu/NaGlu or NaCl, 10 mM Tris-HCl pH 8.3, 1 mM EDTA and incubated for 12-16 hr at 23°C with rotation. The supernatant was filtered with a 0.22 μm filter and the DNA precipitated with 2 volumes of absolute ethanol for 4-16 hr at -20°C. The precipitated product was resuspended in the original folding buffer. DNA concentrations were determined by UV absorbance at 260 nm (see Supplementary Table I for extinction coefficients) (Oganesian *et al.*, 2006). An aliquot of the gel purified G-quadruplex was electrophoresed on a second native gel in the presence of the relevant salt to determine its purity using ImageQuant software. The remainder of the gel purified G-quadruplex was stored at 4°C in its folding buffer.

Growth of *Euplotes aediculatus* and Preparation of Native *Euplotes* Telomerase

Euplotes aediculatus was grown as previously described under non-sterile conditions using Chlorogonium as the food source (Swanton *et al.*, 1980). Cultures were grown in continuously aerated 5 gallon glass carboys. Nuclei were isolated by sucrose cushion centrifugation from 10-20 gram cell pellets, and nuclear extract was prepared by Dounce homogenization as previously

described (Lingner *et al.*, 1994). Telomerase from the *Euplotes aediculatus* nuclear extracts (isolated from ~35 grams of cells) was further purified as described (Lingner and Cech, 1996).

Preparation of Native *Tetrahymena* Telomerase

Tetrahymena thermophila vegetative cells from B2086.1 strain were grown to logarithmic phase in 2% Proteose peptone (Difco) and 0.03 mg/ml Sequestrene (Ciba-Geigy) SPP medium for 12-16 hr at 30ºC. An S100 extract was prepared (Greider and Blackburn, 1987) and telomerase was partially purified by chromatography on a DEAE (BioRad) column as described (Bryan *et al.*, 2003). The partially purified extract was dialyzed for 12-16 hr at 4ºC against TMG (10 mM Tris-acetate pH 8.0, 1mM $MgCl_2$ and 10%glycerol) with 5 mM β-mercaptoethanol and 0.1 mM phenyl-methyl-sulfonyl-fluoride (PMSF).

Preparation of *in vitro* Reconstituted Tetrahymena Telomerase

Tetrahymena telomerase was reconstituted by translation of a plasmid encoding a synthetic TERT gene with an N-terminal FLAG tag (pFLAG-TERT) (Bryan *et al.*, 2003) in the presence of *in vitro* transcribed *Tetrahymena* telomeric RNA (Bryan *et al.*, 2003) in rabbit reticulocyte lysates (TnT T7 Quick for PCR kit; Promega). 400 μL reconstitution reactions contained 320 μL of ^{35}S-methionine (Perkin Elmer; 1175 Ci/mmol), 8 μg of pFLAG-TERT plasmid and 50 nM RNA template. Translation was carried out at 30ºC for 60 min. Reconstituted enzyme was snap frozen in liquid nitrogen and stored at -80ºC or immunopurified.

Immunoprecipitation of *in vitro* translated FLAG-TERT and RNA complex was achieved using Anti-FLAG M2 affinity gel beads (Sigma) as described (Bryan *et al.*, 2000). Telomerase-bound beads were resuspended in an equal volume of TMG. The final concentration of active enzyme was determined by dot blotting and aliquot of the enzyme along with a dilution series of *Tetrahymena* telomeric RNA onto a Hybond N^+ membrane (Amersham) and detecting the RNA in

the telomerase complex by hybridizing the membrane with a radioactive probe complementary to *Tetrahymena* telomerase RNA (5'-TATCAGCACTAGATTTTTGGGGTTGAATG-3'). The average final concentration of 1:1 slurry of bead-bound telomerase was 2-5 nM.

For binding studies the immunopurified telomerase was eluted from the Anti-FLAG M2 beads. 320 μL of 1:1 immunoprecipitated bead slurry was washed once with 20 mM Tris-Acetate pH 7.5, 10% glycerol, 1 mM EDTA, 5 mM $MgCl_2$ and 0.1 mM DTT. Subsequently, 0.5 mg/ml of BSA was added to the beads to prevent the protein from sticking to the tubes and the telomerase complex was eluted by competition with 3 x FLAG peptide (Sigma) at a final concentration of 0.75 mg/ml with rotation at 4ºC for 1 hr. The supernatant containing the eluted telomerase was transferred to Protein LoBind tubes (Eppendorf) and snap frozen.

Direct Telomerase Activity Assays

Euplotes telomerase assays. Primer extension assays contained varying amounts of DNA primer (25 nM to 2 μM, as indicated), 1.4 ng of purified *Euplotes* telomerase, 20 mM Tris-Acetate, 10 mM MgCl2, 50mM NaGlu or KGlu, 1 mM DTT, 80 μM dTTP, 1.5 μM dGTP, and 0.5 μl [α-^{32}P]-dGTP (3000 Ci/mmol). Reactions were incubated at 25ºC for 1 hr. Reactions were stopped by adding 50 μl of quench buffer (10 mM Tris-HCl pH 7.5, 10 mM EDTA, 1% SDS, 4 μg Proteinase K, 10 μg glycogen, and 5000 cpm of a ^{32}P-labelled 114mer loading control). DNA was recovered by phenol/chloroform extraction followed by ethanol precipitation. DNA pellets were air dried and resuspended in 10 μl of formamide loading dye (90% deionized formamide, 0.1% bromophenol blue, 0.1% xylene cyanol in 1X TBE buffer). 5 μl of telomerase extension products (the other 5 μl was stored at -20ºC if another gel was needed) were resolved on 8% denaturing polyacrylamide sequencing gels that were electrophoresed at 2000V for 1.5 hr. Gels were dried at 80ºC for 20 minutes, exposed to a Molecular Dynamics PhosphorImager screen and analyzed

using ImageQuant software. The extension products in each lane were normalized to loading controls.

Tetrahymena telomerase assays. Assays were performed using either *in vitro* reconstituted and immunopurified *Tetrahymena* telomerase or native cell extract-derived *Tetrahymena* telomerase. Various concentrations of primer in its linear of G-quadruplex conformation were incubated at 25ºC for 10-60 minutes in the presence of 1X *Tetrahymena* telomerase buffer (50 mM Tris-HCL pH 8.3, 1.25 mM $MgCl_2$, 5 mM dithiothreitol (DTT)) with or without 50/150 mM KGlu, 50 mM NaGlu or 100 mM NaCl, 10 μM dTTP (Roche), 10 μM [α-^{32}P]-dGTP at 80 Ci/mmol (0.4 μl nonradioactive dGTP [Roche] at 487 μM and 1.6 μl [α-^{32}P]-dGTP [Perkin Elmer] at 10 μCi/μl, 3000 Ci/mmol) and 5.6 μl of either 1:1 slurry of *in vitro* synthesized and immunopurified telomerase of native *Tetrahymena* telomerase in a 20 ml reaction. The reaction was terminated by adding 80 μl of TES (50 mM Tris-HCl pH 8.3, 20 mM EDTA and 0.2% SDS). 5000 cpm of a ^{32}P-labelled 100mer oligonucleotide was added as a recovery and loading control. The reaction products were phenol/chloroform extracted and ethanol precipitated. The pellet was resuspended in 5 μL of formamide loading dye (90% deionized formamide, 0.1% bromophenol blue, 0.1% xylene cyanol in 1X TBE buffer) and ½ of each reaction was electrophoresed on a denaturing 10-12% polyacrylamide/8 M urea sequencing-type gel for 1.5 hr at 80 W. The gel was dried for 1 hr at 80ºC, exposed to a Molecular Dynamics PhosphorImager screen and analyzed using ImageQuant software.

Kinetic Analyses

Measurements of the rate constant (k_{cat}) were carried out by performing telomerase extension assays using gel purified intermolecular G-quadruplexes and their linear counterparts, as described above. Reactions were carried out for 10 minutes, which was within the linear phase of the

reaction. The rate constant for the first round of repeat addition (*Tetrahymena*) was measured by inclusion of 100 μM ddTTP in place of dTTP. Dilutions of the ^{32}P-labeled 100mer loading control were loaded onto the same gel so that a standard curve for radioactive intensity could be established. From this standard curve phosphorimager units (PIU) could be converted to counts per minute (CPM). CPM were converted to Ci using the formula 1 Ci = 2.22 x 10^{12} CMP. The specific activity of each product (corrected for the number of radioactive dGTPs added) was used to convert Ci to fmol of product. The loading control was used to correct for loss of DNA during the extraction and precipitation. Thus the value for k_{cat} was determined by using the formula k_{cat} (min^{-1}) = V_{max} (fmol/min) ÷ fmol of enzyme.

Affinity constant (K_m) measurements were also carried out by performing telomerase extension assays within the linear phase of the reaction. Total intensity of extension products at each substrate concentration was normalized against the intensity of the ^{32}P-labeled 100mer loading control. Increasing substrate concentrations were then plotted against PIU intensity and expressed as percentage of maximum intensity at the highest primer concentration. This was fitted to a Michaelis-Menten kinetics equation to yield K_m. The specificity constant is defined as the k_{cat}/K_m $s^{-1}M^{-1}$ value.

Complementary Strand Trap Method (Unfolding Assays)

Euplotes trap assays. This method was modified from (Raghuraman and Cech, 1990). A ^{32}P-labeled gel-purified *Euplotes* G-quadruplex of the desired conformation was incubated in the presence of 1 or 100 equivalents of a 15 nucleotide RNA molecule resembling the *Euplotes* telomerase RNA template (EaTR) in 50 mM K^+ or Na^+ reaction buffer (*Euplotes* telomerase assay buffer without nucleotides) at 25ºC for 1 minute or 30 minute time intervals. Aliquots of each reaction were run on 20% non-denaturing polyacrylamide gels containing either 50 mM K^+ or Na^+

at 4ºC at 100 V. Gels were dried, analyzed by phosphorimaging, and quantified using ImageQuant.

Tetrahymena trap assays. Similar unfolding assays were carried out with the *Tetrahymena* G-quadruplexes, except that the complementary trap was a 48 nucleotide DNA molecule. G-quadruplexes were incubated in the presence of 20 fold excess of the 48CC complementary strand at 23ºC. Aliquots of this hybridization reaction were removed at regular time intervals and loaded onto a native 12% polyacrylamide gel containing either 50 mM KGlu or NaGlu. Electrophoresis was conducted as previously described. The gel was dried, exposed to a Phosphorimager screen and analyzed using ImageQuant software.

Unfolding rates were determined by plotting the percentage of folded G-quadruplex that remained intact as a function of time. Where the reaction followed a biphasic mode of unfolding the curve was fit to a double exponential equation: $y = ae^{-k1t} + be^{-k2t}$. Monophasic rates of unfolding were fit to a single exponential equation: $y = ae^{-kt}$. To calculate the half-life of each population the following equation was applied: $t_{1/2} = 0.693/k$.

UV Crosslinking

Irradiation of ^{32}P labeled intermolecular 12GT G-quadruplex and linear control were performed in a Stratalinker® UV crosslinker 1800 (Stratagene) at 254 nm in conical 0.2 ml PCR tubes with no lids at a distance of about 6 cm from light source for the indicated times at 25ºC in a total volume of 5 µl. An equal volume of formamide loading dye was added and the cross-linked products were run on a denaturing 14% polyacrylamide gel. The gel was fixed in 25% isopropanol, 10% acetic acid and 20% glycerol for 30 minutes, dried and analyzed by phosphorimaging.

Snake Venom Phosphodiesterase I (SVPI) Digestion

Euplotes SVPI digestion. 200 ng of G-quadruplex, denatured counterpart and linear non-telomeric 30mer DNA (in 1X telomerase reaction buffer or dH_2O) were incubated with 1 μl of 1 mg/ml SVPI (Amersham Biosciences) at 25ºC for 25 minutes in a total reaction volume of 5 μl. The reaction was terminated by addition of 1 μl of 500 mM EDTA. An equal volume of 2X formamide loading dye was added, the samples were heat denatured at 95ºC for 3 minutes and loaded onto a 20% acrylamide denaturing gel. The gel was electrophoresed for 1.5 hr at 200 V and stained with Sybr Green I® for 20 minutes.

Tetrahymena SVPI digestion. G-quadruplexes and linear (- salt) controls containing a ^{32}P end label were incubated with 2 μl of 1 mg/ml SVP1 (Amersham Biosciences; resuspended in 1X Telomerase buffer without DTT + 50% glycerol) at various DNA concentrations for 10 minutes at 25ºC in a total reaction volume of 20 μl. The reaction was terminated with 80 μl of TES (50 mM Tris-HCL pH 8.3, 20 mM EDTA and 0.2% SDS). From this point onwards the samples were treated in the same manner as "telomerase activity assay" reactions (see above).

Terminal Deoxytransferase (TdT) Extension

Euplotes TdT extension. 2 pmol of intermolecular Oxy1.5 G-quadruplex in 50 mM KGlu, its denatured control (+KGlu) and a non-telomeric linear control 30mer were incubated in the presence of 30 U of TdT (Promega) and 16 μCi of [α-^{32}P]-dTTP (3000 Ci/mmol) for 60 minutes at 25°C in a total reaction volume of 10 μl. TdT extension products were phenol/chloroform extracted, ethanol precipitated and electrophoresed on an 8% polyacrylamide denaturing sequencing gel.

Tetrahymena TdT extension. Intermolecular 12GT in 100 mM NaCl and its denatured control (12GT quadruplex denatured for 5 minutes at 95°C then placed on ice) at 17 μM concentration

were incubated with 2.5 U of TdT (Roche), 100 mM NaCl and 0.2 mM dGTP (8.2 μl non-radioactive dGTP [Roche] at 487 μM and 1.6 μl [α-^{32}P]-dGTP [Perkin Elmer] at 10 μCi/μl, 3000 Ci/mmol) for 10 minutes at 25°C in a total reaction volume of 20 μl. The reaction was stopped by addition of 80 μl of TES and the samples were treated in the same manner as the SVPI digested samples (see above).

Biotinylated Primer Pull-down Assays (Binding Studies)

Binding studies were conducted by immobilizing biotinylated *Tetrahymena* G-quadruplex DNA on NeutrAvidin beads (Pierce Biotechnology) in the presence of radiolabeled recombinant *Tetrahymena* telomerase. Nonradioactive biotinylated oligonucleotides 24TT and 21GG were folded and gel purified (as described above). Each biotin-conjugated G-quadruplex (10 μL) or its linear counterpart was incubated with 10 μl of eluted ^{35}S-labelled recombinant telomerase in 1X Tetrahymena Telomerase buffer (see above) with or without 50 mM KGlu at 25°C for 10 min. NeutrAvidin beads (10 μL per reaction) were washed 4 times with 1X Telomerase buffer with 10% glycerol. The beads were blocked twice for 15 min at 4°C in the same buffer with the addition of 0.75 mg/ml BSA, 0.15 mg/ml glycogen and 0.15 mg/ml yeast RNA. NeutrAvidin beads that were to be used for G-quadruplex samples included 50 mM KGlu in the wash and blocking steps to preserve the folded conformation. Blocked beads were resuspended in 1 volume of blocking buffer. Blocked bead slurry (20 μl) was added to the DNA-telomerase reaction mix and the samples were rotated at 4°C for 15 min. The beads were washed 4 times with 1X Telomerase buffer with 10% glycerol and 300 mM LiOAC for linear DNA or 300 mM KGlu for G-quadruplex DNA. The beads were resuspended in 1 volume of the corresponding salt buffer. Half of each reaction was added to an equal volume of 2X Laemmli's loading buffer (125 mM Tris-HCl pH 6.8, 4% SDS, 0.005% bromophenol blue, 20% glycerol and 0.72 M β-

mercaptoethanol) plus 300 mM KGlu, denatured at 95°C for 3 min, loaded onto a 4-20% SDS-PAGE gel (Novex) and electrophoresed for 1.5 hr at 120 V. The gel was fixed in 25% isopropanol and 10% acetic acid for 20 min, dried at 80°C for 1 hr then exposed to a PhosphorImager screen for 12-16 hr.

Circular Dichroism (CD)

CD spectra were recorded on a Jasco J-810 spectrophotometer at 23ºC (*Tetrahymena*) or a Pistar 180 circular dichroism spectrophotometer equipped with a MTCA series Melcor temperature controller at 25ºC (*Euplotes*). Samples of gel-purified G-quadruplex of the desired conformation were prepared at 3-20 μM final concentration in buffer in which the DNA was originally folded. For each sample three to five spectral scans were accumulated over a wavelength range of 200-400 nm in a 0.1 cm path length cell at a scanning rate of 20-100 nm/min. The scan of the buffer alone was subtracted from the average scan for each sample. CD spectra were collected in millidegrees, normalized to the total species concentrations and expressed as molar ellipticity units (deg x cm^2/dmol).

CHAPTER V

RETROSPECTIVE

Telomerase Oligomerization

As a majority of the literature supports telomerase oligomerization in most the organisms studied (Aigner *et al.*, 2003; Beattie *et al.*, 2001; Cohen *et al.*, 2007; Fouche *et al.*, 2006; Prescott and Blackburn, 1997; Wang *et al.*, 2002; Wenz *et al.*, 2001), one may ask for what reason is this necessary and what goal does it achieve? While monomeric telomerase is capable of extending telomeric DNA efficiently (Bryan *et al.*, 2003; Lingner and Cech, 1996), research has supported that telomerase activity is much more processive when telomerase oligomerizes (Wenz *et al.*, 2001). Therefore, the question arises, "How would a dimer or oligomer of telomerase benefit the cell over lone acting monomers?" It may be that telomerase oligomerization is a means to boost and/or regulate telomerase activity (including all the known and unknown activities associated with telomerase). When considering telomeric DNA extension by telomerase, an oligomer of telomerase places a higher concentration of enzyme at the telomere, further promoting the elongation of one or more telomere(s). From a regulatory standpoint, a cell may limit the expression of telomerase, resulting in a more dilute enzyme concentration, thus promoting more monomeric telomerase complexes, rather than the more processive and concentrated oligomer. Other activities of telomerase within the cell may be regulated in this manner, if they are proven to be as dependent on telomerase oligomerization as telomerase catalyzed extension of telomeric

DNA. The answers to these questions have yet to be elucidated and further research aimed at identifying factors that promote telomerase oligomerization is required.

Telomerase Interacts with Parallel Intermolecular G-quadruplexes

Since the completion of this work, a follow-up study conducted by collaborators Oganesian *et al.* has further probed the novel interaction between ciliate *Tetrahymena* telomerase and parallel intermolecular G-quadruplexes (Oganesian *et al.*, 2007). Using electrospray ionization mass spectrometry, the Na^+-stabilized parallel intermolecular 12GT G-quadruplex used in this work (Oganesian *et al.*, 2006), which was characterized as a tetrameric structure by native gel migration and UV crosslinking studies, was confirmed to be a four-stranded quadruplex. Using biotinylated DNA pull down experiments, as documented in Chapter IV, the tetrameric 12GT G-quadruplex recovered comparable amounts of *t*TERT, regardless of the presence or absence of *t*TR, as the denatured biotinylated 12GT DNA. Upon probing for domains in *t*TERT that directly bind to the 12GT G-quadruplex, it was observed that the N- and C- terminal domains (N1-519 and C520-1127) of truncated *t*TERT mutants bound specifically (micromolar affinity) and independently to the quadruplex. Point mutation studies of the TERT subunit aimed at identifying amino acids important for extension of G-quadruplex structures, revealed that a single lysine to alanine point mutation at amino acid 538 (K538A) in motif 1 of tTERT reduced extension of the quadruplex, but not extension of linear 12GT DNA, yet retained wild type binding affinity for the quadruplex. Collectively the data supports a telomerase model where the active site undergoes a conformational change to specifically bind and extend parallel intermolecular G-quadruplexes, therefore recognizing this subset of G-quadruplex structures as distinct substrates.

Cellular environments where telomerase may encounter parallel intermolecular telomeric G-quadruplex DNA include the clustering of telomeres in the formation of the meiotic

bouquet (Anuradha and Muniyappa, 2004; Harper *et al.*, 2004; Loidl and Scherthan, 2004; Sen and Gilbert, 1988) and the tethering of telomeres that results in chromosomal organization and positional stability (Chuang *et al.*, 2004; Lipps, 1980; Lipps *et al.*, 1982; Luderus *et al.*, 1996; Nagele *et al.*, 2001; Paeschke *et al.*, 2005). Telomerase may assist in resolving these higher order telomeric structures, following the event with extension of telomeric DNA.

REFERENCES

Ahmed, S., and Hodgkin, J. (2000). MRT-2 checkpoint protein is required for germline immortality and telomere replication in C. elegans. Nature *403*, 159-164.

Aigner, S., and Cech, T. R. (2004). The Euplotes telomerase subunit p43 stimulates enzymatic activity and processivity in vitro. RNA *10*, 1108-1118.

Aigner, S., Lingner, J., Goodrich, K. J., Grosshans, C. A., Shevchenko, A., Mann, M., and Cech, T. R. (2000). Euplotes telomerase contains an La motif protein produced by apparent translational frameshifting. EMBO J *19*, 6230-6239.

Aigner, S., Postberg, J., Lipps, H. J., and Cech, T. R. (2003). The Euplotes La motif protein p43 has properties of a telomerase-specific subunit. Biochemistry *42*, 5736-5747.

Alberti, P., Bourdoncle, A., Sacca, B., Lacroix, L., and Mergny, J. L. (2006). DNA nanomachines and nanostructures involving quadruplexes. Org Biomol Chem *4*, 3383-3391.

Allen, D. J., Makhov, A., Grilley, M., Taylor, J., Thresher, R., Modrich, P., and Griffith, J. D. (1997). MutS mediates heteroduplex loop formation by a translocation mechanism. EMBO J *16*, 4467-4476.

Ambrus, A., Chen, D., Dai, J., Bialis, T., Jones, R. A., and Yang, D. (2006). Human telomeric sequence forms a hybrid-type intramolecular G-quadruplex structure with mixed parallel/antiparallel strands in potassium solution. Nucleic Acids Res *34*, 2723-2735.

Anuradha, S., and Muniyappa, K. (2004). Meiosis-specific yeast Hop1 protein promotes synapsis of double-stranded DNA helices via the formation of guanine quartets. Nucleic Acids Res *32*, 2378-2385.

Arimondo, P. B., Riou, J. F., Mergny, J. L., Tazi, J., Sun, J. S., Garestier, T., and Helene, C. (2000). Interaction of human DNA topoisomerase I with G-quartet structures. Nucleic Acids Res *28*, 4832-4838.

Autexier, C., and Lue, N. F. (2006). The Structure and Function of Telomerase Reverse Transcriptase. Annu Rev Biochem *75*, 493-517.

Balagurumoorthy, P., and Brahmachari, S. K. (1994). Structure and stability of human telomeric sequence. J Biol Chem *269*, 21858-21869.

Baran, N., Pucshansky, L., Marco, Y., Benjamin, S., and Manor, H. (1997). The SV40 large T-antigen helicase can unwind four stranded DNA structures linked by G-quartets. Nucleic Acids Res *25*, 297-303.

Beattie, T. L., Zhou, W., Robinson, M. O., and Harrington, L. (2001). Functional multimerization of the human telomerase reverse transcriptase. Mol Cell Biol *21*, 6151-6160.

Bednenko, J., Melek, M., Greene, E. C., and Shippen, D. E. (1997). Developmentally regulated initiation of DNA synthesis by telomerase: evidence for factor-assisted de novo telomere formation. EMBO J *16*, 2507-2518.

Bekaert, S., Derradji, H., and Baatout, S. (2004). Telomere biology in mammalian germ cells and during development. Dev Biol *274*, 15-30.

Blasco, M. A. (2005). Telomeres and human disease: ageing, cancer and beyond. Nat Rev Genet *6*, 611-622.

Bryan, T. M., Goodrich, K. J., and Cech, T. R. (2000). A mutant of Tetrahymena telomerase reverse transcriptase with increased processivity. J Biol Chem *275*, 24199-24207.

Bryan, T. M., Goodrich, K. J., and Cech, T. R. (2003). Tetrahymena telomerase is active as a monomer. Mol Biol Cell *14*, 4794-4804.

Cairns, D., Anderson, R. J., Perry, P. J., and Jenkins, T. C. (2002). Design of telomerase inhibitors for the treatment of cancer. Curr Pharm Des *8*, 2491-2504.

Cesare, A. J., Quinney, N., Willcox, S., Subramanian, D., and Griffith, J. D. (2003). Telomere looping in P. sativum (common garden pea). Plant J *36*, 271-279.

Chai, W., Du, Q., Shay, J. W., and Wright, W. E. (2006). Human telomeres have different overhang sizes at leading versus lagging strands. Mol Cell *21*, 427-435.

Chang, C. C., Kuo, I. C., Ling, I. F., Chen, C. T., Chen, H. C., Lou, P. J., Lin, J. J., and Chang, T. C. (2004). Detection of quadruplex DNA structures in human telomeres by a fluorescent carbazole derivative. Anal Chem *76*, 4490-4494.

Chapon, C., Cech, T. R., and Zaug, A. J. (1997). Polyadenylation of telomerase RNA in budding yeast. RNA *3*, 1337-1351.

Chen, J.-L., Blasco, M. A., and Greider, C. W. (2000). Secondary structure of vertebrate telomerase RNA. Cell *100*, 503-514.

Chikashige, Y., and Hiraoka, Y. (2001). Telomere binding of the Rap1 protein is required for meiosis in fission yeast. Curr Biol *11*, 1618-1623.

Chuang, T. C., Moshir, S., Garini, Y., Chuang, A. Y., Young, I. T., Vermolen, B., van den Doel, R., Mougey, V., Perrin, M., Braun, M.*, et al.* (2004). The three-dimensional organization of telomeres in the nucleus of mammalian cells. BMC Biol *2*, 12.

Cogoi, S., and Xodo, L. E. (2006). G-quadruplex formation within the promoter of the KRAS proto-oncogene and its effect on transcription. Nucleic Acids Res *34*, 2536-2549.

Cohen, S. B., Graham, M. E., Lovrecz, G. O., Bache, N., Robinson, P. J., and Reddel, R. R. (2007). Protein composition of catalytically active human telomerase from immortal cells. Science *315*, 1850-1853.

Cohn, M., and Blackburn, E. H. (1995). Telomerase in yeast. Science *269*, 396-400.

Collins, K. (2006). The biogenesis and regulation of telomerase holoenzymes. Nat Mol Cell Biol *7*.

Collins, K., and Gandhi, L. (1998). The reverse transcriptase component of the *Tetrahymena* telomerase ribonucleoprotein complex. Proceedings of the National Academy of Science USA *95*, 8485-8490.

Collins, K., and Greider, C. W. (1993). *Tetrahymena* telomerase catalyzes nucleolytic cleavage and nonprocessive elongation. Genes and Development *7*, 1364-1376.

Collins, K., and Greider, C. W. (1995). Utilization of ribonucleotides and RNA primers by *Tetrahymena* telomerase. EMBO J *14*, 5422-5432.

Collins, K., and Mitchell, J. R. (2002). Telomerase in the human organism. Oncogene *21*, 564-579.

Connor, A. C., Frederick, K. A., Morgan, E. J., and McGown, L. B. (2006). Insulin capture by an insulin-linked polymorphic region G-quadruplex DNA oligonucleotide. J Am Chem Soc *128*, 4986-4991.

Cooper, J. P., Watanabe, Y., and Nurse, P. (1998). Fission yeast Taz1 protein is required for meiotic telomere clustering and recombination. Nature *392*, 828-831.

Counter, C. M., Hahn, W. C., Wei, W., Caddle, S. D., Beijersbergen, R. L., Lansdorp, P. M., Sedivy, J. M., and Weinberg, R. A. (1998). Dissociation among *in vitro* telomerase activity, telomere maintenance, and cellular immortalization. Proceedings of the National Academy of Science USA *95*, 14723-14728.

Crabbe, L., Verdun, R. E., Haggblom, C. I., and Karlseder, J. (2004). Defective telomere lagging strand synthesis in cells lacking WRN helicase activity. Science *306*, 1951-1953.

de Lange, T. (2002). Protection of mammalian telomeres. Oncogene *21*, 532-540.

de Lange, T. (2005). Shelterin: the protein complex that shapes and safeguards human telomeres. Genes Dev *19*, 2100-2110.

Dominick, P. K., and Jarstfer, M. B. (2004). A conformationally constrained nucleotide analogue controls the folding topology of a DNA g-quadruplex. J Am Chem Soc *126*, 5050-5051.

Dragon, F., Pogacic, V., and Filipowicz, W. (2000). In vitro assembly of human H/ACA small nucleolar RNPs reveals unique features of U17 and telomerase RNAs. Mol Cell Biol *20*, 3037-3048.

Enokizono, Y., Konishi, Y., Nagata, K., Ouhashi, K., Uesugi, S., Ishikawa, F., and Katahira, M. (2005). Structure of hnRNP D complexed with single-stranded telomere DNA and unfolding of the quadruplex by heterogeneous nuclear ribonucleoprotein D. J Biol Chem *280*, 18862-18870.

Etheridge, K. T., Banik, S. S., Armbruster, B. N., Zhu, Y., Terns, R. M., Terns, M. P., and Counter, C. M. (2002). The nucleolar localization domain of the catalytic subunit of human telomerase. J Biol Chem *277*, 24764-24770.

Fan, X., and Price, C. M. (1997). Coordinate regulation of G- and C strand length during new telomere synthesis. Mol Biol Cell *8*, 2145-2155.

Fang, G., and Cech, T. R. (1993). The beta subunit of Oxytricha telomere-binding protein promotes G-quartet formation by telomeric DNA. Cell *74*, 875-885.

Feng, J., Funk, W. D., Wang, S. S., Weinrich, S. L., Avilion, A. A., Chiu, C. P., Adams, R. R., Chang, E., Allsopp, R. C., Yu, J., and et al. (1995). The RNA component of human telomerase. Science *269*, 1236-1241.

Forstemann, K., and Lingner, J. (2005). Telomerase limits the extent of base pairing between template RNA and telomeric DNA. EMBO Rep *6*, 361-366.

Fouché, N., Moon, I. K., Keppler, B. R., Griffith, J. D., and Jarstfer, M. B. (2006). Electron Microscopic Visualization of Telomerase from Euplotes aediculatus Bound to a Model Telomere DNA. Biochemistry *45*, 9624-9631.

Fu, D., and Collins, K. (2003). Distinct biogenesis pathways for human telomerase RNA and H/ACA small nucleolar RNAs. Mol Cell *11*, 1361-1372.

Fu, D., and Collins, K. (2006). Human telomerase and Cajal body ribonucleoproteins share a unique specificity of Sm protein association. Genes Dev *20*, 531-536.

Fukuda, H., Katahira, M., Tsuchiya, N., Enokizono, Y., Sugimura, T., Nagao, M., and Nakagama, H. (2002). Unfolding of quadruplex structure in the G-rich strand of the minisatellite repeat by the binding protein UP1. Proc Natl Acad Sci U S A *99*, 12685-12690.

Garcia-Cao, M., O'Sullivan, R., Peters, A. H., Jenuwein, T., and Blasco, M. A. (2004). Epigenetic regulation of telomere length in mammalian cells by the Suv39h1 and Suv39h2 histone methyltransferases. Nat Genet *36*, 94-99.

Geserick, C., and Blasco, M. A. (2006). Novel roles for telomerase in aging. Mech Ageing Dev *127*, 579-583.

Giraldo, R., and Rhodes, D. (1994). The yeast telomere-binding protein RAP1 binds to and promotes the formation of DNA quadruplexes in telomeric DNA. EMBO J *13*, 2411-2420.

Giraldo, R., Suzuki, M., Chapman, L., and Rhodes, D. (1994). Promotion of parallel DNA quadruplexes by a yeast telomere binding protein: a circular dichroism study. Proc Natl Acad Sci U S A *91*, 7658-7662.

Golubovskaya, I. N., Harper, L. C., Pawlowski, W. P., Schichnes, D., and Cande, W. Z. (2002). The pam1 gene is required for meiotic bouquet formation and efficient homologous synapsis in maize (Zea mays L.). Genetics *162*, 1979-1993.

Gomez, D., O'Donohue, M. F., Wenner, T., Douarre, C., Macadre, J., Koebel, P., Giraud-Panis, M. J., Kaplan, H., Kolkes, A., Shin-ya, K., and Riou, J. F. (2006). The G-quadruplex ligand telomestatin inhibits POT1 binding to telomeric sequences in vitro and induces GFP-POT1 dissociation from telomeres in human cells. Cancer Res *66*, 6908-6912.

Granotier, C., Pennarun, G., Riou, L., Hoffschir, F., Gauthier, L. R., De Cian, A., Gomez, D., Mandine, E., Riou, J. F., Mergny, J. L., *et al.* (2005). Preferential binding of a G-quadruplex ligand to human chromosome ends. Nucleic Acids Res *33*, 4182-4190.

Greene, E. C., and Shippen, D. E. (1998). Developmentally programmed assembly of higher order telomerase complexes with distinct biochemical and structural properties. Genes Dev *12*, 2921-2931.

Greider, C. (1991). Telomerase is processive. Mol Cell Biol *11*, 4572-4580.

Greider, C. (1996). Telomere length regulation. Annu Rev Biochem *65*, 337-365.

Greider, C. W., and Blackburn, E. H. (1985). Identification of a specific telomere terminal transferase activity in Tetrahymena extracts. Cell *43*, 405-413.

Greider, C. W., and Blackburn, E. H. (1987). The telomere terminal transferase of Tetrahymena is a ribonucleoprotin enzyme with two kinds of primer specificity. Cell *51*, 887-898.

Griffith, J., Bianchi, A., and de Lange, T. (1998). TRF1 promotes parallel pairing of telomeric tracts in vitro. J Mol Biol *278*, 79-88.

Griffith, J. D., and Christiansen, G. (1978). Electron microscope visualization of chromatin and other DNA-protein complexes. Annu Rev Biophys Bioeng *7*, 19-35.

Griffith, J. D., Comeau, L., Rosenfield, S., Stansel, R. M., Bianchi, A., Moss, H., and de Lange, T. (1999). Mammalian telomeres end in a large duplex loop. Cell *97*, 503-514.

Haider, S., Parkinson, G. N., and Neidle, S. (2002). Crystal structure of the potassium form of an Oxytricha nova G-quadruplex. J Mol Biol *320*, 189-200.

Hammond, P. W., and Cech, T. R. (1997). dGTP-dependent processivity and possible template switching of euplotes telomerase. Nucleic Acids Res *25*, 3698-3704.

Hammond, P. W., and Cech, T. R. (1998). Euplotes telomerase: evidence for limited base-pairing during primer elongation and dGTP as an effector of translocation. Biochemistry *37*, 5162-5172.

Hammond, P. W., Lively, T. N., and Cech, T. R. (1997). The anchor site of telomerase from Euplotes aediculatus revealed by photo-cross-linking to single- and double-stranded DNA primers. Mol Cell Biol *17*, 296-308.

Hardin, C. C., Henderson, E., Watson, T., and Prosser, J. K. (1991). Monovalent cation induced structural transitions in telomeric DNAs: G-DNA folding intermediates. Biochemistry *30*, 4460-4472.

Hardy, C. D., Schultz, C. S., and Collins, K. (2001). Requirements for the dGTP-dependent repeat addition processivity of recombinant *Tetrahymena* telomerase. J Biol Chem *276*, 4863-4871.

Harper, L., Golubovskaya, I., and Cande, W. Z. (2004). A bouquet of chromosomes. J Cell Sci *117*, 4025-4032.

Harrington, C., Lan, Y., and Akman, S. A. (1997). The identification and characterization of a G4-DNA resolvase activity. J Biol Chem *272*, 24631-24636.

Harrington, L. A., and Greider, C. W. (1991). Telomerase primer specificity and chromosome healing. Nature *353*, 451-454.

Hayflick, L. (1965). The limited in vitro lifetime of human diploid cell strains. Exp Cell Res *37*, 614-636.

He, F., Tang, Y., Wang, S., Li, Y., and Zhu, D. (2005). Fluorescent amplifying recognition for DNA G-quadruplex folding with a cationic conjugated polymer: a platform for homogeneous potassium detection. J Am Chem Soc *127*, 12343-12346.

Hockemeyer, D., Sfeir, A. J., Shay, J. W., Wright, W. E., and de Lange, T. (2005). POT1 protects telomeres from a transient DNA damage response and determines how human chromosomes end. EMBO J *24*, 2667-2678.

Holt, S. E., Aisner, D. L., Baur, J., Tesmer, V. M., Dy, M., Ouellette, M., Trager, J. B., Morin, G. B., Toft, D. O., Shay, J. W., *et al.* (1999). Functional requirement of p23 and Hsp90 in telomerase complexes. Genes and Development *13*, 817-826.

Horvath, M. P., and Schultz, S. C. (2001). DNA G-quartets in a 1.86 A resolution structure of an Oxytricha nova telomeric protein-DNA complex. J Mol Biol *310*, 367-377.

Huard, S., and Autexier, C. (2004). Human telomerase catalyzes nucleolytic primer cleavage. Nucleic Acids Res *32*, 2171-2180.

Huffman, K. E., Levene, S. D., Tesmer, V. M., Shay, J. W., and Wright, W. E. (2000). Telomere shortening is proportional to the size of the G-rich telomeric 3'-overhang. J Biol Chem *275*, 19719-19722.

Huppert, J. L., and Balasubramanian, S. (2007). G-quadruplexes in promoters throughout the human genome. Nucleic Acids Res *35*, 406-413.

Hurley, L. H., Wheelhouse, R. T., Sun, D., Kerwin, S. M., Salazar, M., Fedoroff, O. Y., Han, F. X., Han, H., Izbicka, E., and Von Hoff, D. D. (2000). G-quadruplexes as targets for drug design. Pharmacology and Therapeutics *85*, 151-158.

Ishikawa, F., and Naito, T. (1999). Why do we have linear chromosomes? A matter of Adam and Eve. Mutat Res *434*, 99-107.

Jacob, N. K., Kirk, K. E., and Price, C. M. (2003). Generation of telomeric G strand overhangs involves both G and C strand cleavage. Mol Cell *11*, 1021-1032.

Jacob, N. K., Skopp, R., and Price, C. M. (2001). G-overhang dynamics at Tetrahymena telomeres. EMBO J *20*, 4299-4308.

Jady, B. E., Bertrand, E., and Kiss, T. (2004). Human telomerase RNA and box H/ACA scaRNAs share a common Cajal body-specific localization signal. J Cell Biol *164*, 647-652.

Jarstfer, M. B., and Cech, T. R. (2002). Effects of nucleotide analogues on Euplotes aediculatus telomerase processivity: evidence for product-assisted translocation. Biochemistry *41*, 151-161.

Jordan, P. (2006). Initiation of homologous chromosome pairing during meiosis. Biochem Soc Trans *34*, 545-549.

Kang, C., Zhang, X., Ratliff, R., Moyzis, R., and Rich, A. (1992). Crystal structure of four-stranded Oxytricha telomeric DNA. Nature *356*, 126-131.

Kelleher, C., Teixeira, M. T., Forstemann, K., and Lingner, J. (2002). Telomerase: biochemical considerations for enzyme and substrate. Trends Biochem Sci *27*, 572-579.

Keniry, M. (2000). Quadruplex structures in nucleic acids. Biopolymers *56*, 123-146.

Klobutcher, L. A., Swanton, M. T., Donini, P., and Prescott, D. M. (1981). All gene-sized DNA molecules in four species of hypotrichs have the same terminal sequence and an unusual 3' terminus. Proc Natl Acad Sci U S A *78*, 3015-3019.

LaBranche, H., Dupuis, S., Ben-David, Y., Bani, M. R., Wellinger, R. J., and Chabot, B. (1998). Telomere elongation by hnRNP A1 and a derivative that interacts with telomeric repeats and telomerase. Nat Genet *19*, 199-202.

Lee, H. W., Blasco, M. A., Gottlieb, G. J., Horner, J. W., 2nd, Greider, C. W., and DePinho, R. A. (1998). Essential role of mouse telomerase in highly proliferative organs. Nature *392*, 569-574.

Lillard-Wetherell, K., Machwe, A., Langland, G. T., Combs, K. A., Behbehani, G. K., Schonberg, S. A., German, J., Turchi, J. J., Orren, D. K., and Groden, J. (2004). Association and regulation of the BLM helicase by the telomere proteins TRF1 and TRF2. Hum Mol Genet *13*, 1919-1932.

Lingner, J., and Cech, T. R. (1996). Purification of telomerase from *Euplotes aediculatus*: Requirement of a primer 3' overhang. Proc Natl Acad Sci U S A *93*, 10712-10717.

Lingner, J., Cooper, J. P., and Cech, T. R. (1995). Telomerase and DNA end replication: no longer a lagging strand problem? Science *269*, 1533-1534.

Lingner, J., Hendrick, L. L., and Cech, T. R. (1994). Telomerase RNAs of different ciliates have a common secondary structure and a permuted template. Genes Dev *8*, 1984-1998.

Lipps, H. (1980). In vitro aggregation of the gene-sized DNA molecules of the ciliate Stylonychia mytilus. Proc Natl Acad Sci *77*, 4104-4107.

Lipps, H. J., Gruissem, W., and Prescott, D. M. (1982). Higher order DNA structure in macronuclear chromatin of the hypotrichous ciliate Oxytricha nova. Proc Natl Acad Sci U S A *79*, 2495-2499.

Liu, Z., Frantz, J. D., Gilbert, W., and Tye, B. K. (1993). Identification and characterization of a nuclease activity specific for G4 tetrastranded DNA. Proc Natl Acad Sci U S A *90*, 3157-3161.

Loidl, J., and Scherthan, H. (2004). Organization and pairing of meiotic chromosomes in the ciliate Tetrahymena thermophila. J Cell Sci *117*, 5791-5801.

Lu, Q., Schierer, T., Kang, S. G., and Henderson, E. (1998). Purification, characterization and molecular cloning of TGP1, a novel G-DNA binding protein from Tetrahymena thermophila. Nucleic Acids Res *26*, 1613-1620.

Luderus, M. E., van Steensel, B., Chong, L., Sibon, O. C., Cremers, F. F., and de Lange, T. (1996). Structure, subnuclear distribution, and nuclear matrix association of the mammalian telomeric complex. J Cell Biol *135*, 867-881.

Lukowiak, A. A., Narayanan, A., Li, Z. H., Terns, R. M., and Terns, M. P. (2001). The snoRNA domain of vertebrate telomerase RNA functions to localize the RNA within the nucleus. RNA *7*, 1833-1844.

Luu, K. N., Phan, A. T., Kuryavyi, V., Lacroix, L., and Patel, D. J. (2006). Structure of the human telomere in K+ solution: an intramolecular (3 + 1) G-quadruplex scaffold. J Am Chem Soc *128*, 9963-9970.

Marchand, C., Pourquier, P., Laco, G. S., Jing, N., and Pommier, Y. (2002). Interaction of human nuclear topoisomerase I with guanosine quartet-forming and guanosine-rich single-stranded DNA and RNA oligonucleotides. J Biol Chem *277*, 8906-8911.

Melek, M., Greene, E. C., and Shippen, D. E. (1996). Processing of nontelomeric 3' ends by telomerase: default template alignment and endonucleolytic cleavage. Mol Cell Biol *16*, 3437-3445.

Mitchell, J. R., Cheng, J., and Collins, K. (1999). A box H/ACA small nucleolar RNA-like domain at the human telomerase RNA 3' end. Mol Cell Biol *19*, 567-576.

Miura, T., Benevides, J. M., and Thomas, G. J., Jr. (1995). A phase diagram for sodium and potassium ion control of polymorphism in telomeric DNA. J Mol Biol *248*, 233-238.

Miyoshi, D., Karimata, H., and Sugimoto, N. (2005). Drastic effect of a single base difference between human and tetrahymena telomere sequences on their structures under molecular crowding conditions. Angew Chem Int Ed Engl *44*, 3740-3744.

Miyoshi, D., Matsumura, S., Nakano, S., and Sugimoto, N. (2004). Duplex dissociation of telomere DNAs induced by molecular crowding. J Am Chem Soc *126*, 165-169.

Miyoshi, D., Nakao, A., and Sugimoto, N. (2003). Structural transition from antiparallel to parallel G-quadruplex of d(G4T4G4) induced by Ca2+. Nucleic Acids Res *31*, 1156-1163.

Mohaghegh, P., Karow, J. K., Brosh Jr, R. M., Jr., Bohr, V. A., and Hickson, I. D. (2001). The Bloom's and Werner's syndrome proteins are DNA structure-specific helicases. Nucleic Acids Res *29*, 2843-2849.

Mollenbeck, M., Postberg, J., Paeschke, K., Rossbach, M., Jonsson, F., and Lipps, H. J. (2003). The telomerase-associated protein p43 is involved in anchoring telomerase in the nucleus. J Cell Sci *116*, 1757-1761.

Moon, I. K., and Jarstfer, M. B. (2007). The human telomere and its relationship to human disease, therapy, and tissue engineering. Front Biosci *12*, 4595-4620.

Moriarty, T. J., Marie-Egyptienne, D. T., and Autexier, C. (2004). Functional organization of repeat addition processivity and DNA synthesis determinants in the human telomerase multimer. Mol Cell Biol *24*, 3720-3733.

Moriarty, T. J., Ward, R. J., Taboski, M. A., and Autexier, C. (2005). An anchor site-type defect in human telomerase that disrupts telomere length maintenance and cellular immortalization. Mol Biol Cell *16*, 3152-3161.

Morin, G. (1989). The human telomere terminal transferase enzyme is a ribonucleoprotein that synthesizes ttaggg repeats. Cell *59*, 521-529.

Munoz-Jordan, J. L., Cross, G. A., de Lange, T., and Griffith, J. D. (2001). t-loops at trypanosome telomeres. EMBO J *20*, 579-588.

Murti, K. G., and Prescott, D. M. (1999). Telomeres of polytene chromosomes in a ciliated protozoan terminate in duplex DNA loops. Proc Natl Acad Sci U S A *96*, 14436-14439.

Nagele, R. G., Velasco, A. Q., Anderson, W. J., McMahon, D. J., Thomson, Z., Fazekas, J., Wind, K., and Lee, H. (2001). Telomere associations in interphase nuclei: possible role in maintenance of interphase chromosome topology. J Cell Sci *114*, 377-388.

Neidle, S., and Read, M. A. (2001). G-quadruplexes as therapeutic targets. Biopolymers (Nucleic Acid Sci) *56*, 195-208.

Neidle, S., and Read, M. A. (2000). G-quadruplexes as therapeutic targets. Biopolymers *56*, 195-208.

Nikitina, T., and Woodcock, C. L. (2004). Closed chromatin loops at the ends of chromosomes. J Cell Biol *166*, 161-165.

Nimmo, E. R., Pidoux, A. L., Perry, P. E., and Allshire, R. C. (1998). Defective meiosis in telomere-silencing mutants of Schizosaccharomyces pombe. Nature *392*, 825-828.

Niu, H., Xia, J., and Lue, N. F. (2000). Characterization of the interaction between the nuclease and reverse transcriptase activity of the yeast telomerase complex. Mol Cell Biol *20*, 6806-6815.

Nosek, J., Kosa, P., and Tomaska, L. (2006). On the origin of telomeres: a glimpse at the pre-telomerase world. Bioessays *28*, 182-190.

O'Connor, C. M., and Collins, K. (2006). A novel RNA binding domain in tetrahymena telomerase p65 initiates hierarchical assembly of telomerase holoenzyme. Mol Cell Biol *26*, 2029-2036.

Oganesian, L., and Bryan, T. M. (2007). Physiological relevance of telomeric G-quadruplex formation: a potential drug target. Bioessays *29*, 155-165.

Oganesian, L., Graham, M. E., Robinson, P. J., and Bryan, T. M. (2007). Telomerase recognizes G-quadruplex and linear DNA as distinct substrates. Biochemistry *46*, 11279-11290.

Oganesian, L., Moon, I. K., Bryan, T. M., and Jarstfer, M. B. (2006). Extension of G-quadruplex DNA by ciliate telomerase. EMBO J *25*, 1148-1159.

Olovnikov, A. (1973). The incomplete copying of template margin in enzymatic synthesis of polynucleotides and biological significance of the phenomenon. J Theor Biol *41*, 181-190.

Opresko, P. L., Mason, P. A., Podell, E. R., Lei, M., Hickson, I. D., Cech, T. R., and Bohr, V. A. (2005). POT1 stimulates RecQ helicases WRN and BLM to unwind telomeric DNA substrates. J Biol Chem *280*, 32069-32080.

Opresko, P. L., Otterlei, M., Graakjaer, J., Bruheim, P., Dawut, L., Kolvraa, S., May, A., Seidman, M. M., and Bohr, V. A. (2004). The Werner syndrome helicase and exonuclease cooperate to resolve telomeric D loops in a manner regulated by TRF1 and TRF2. Mol Cell *14*, 763-774.

Opresko, P. L., von Kobbe, C., Laine, J. P., Harrigan, J., Hickson, I. D., and Bohr, V. A. (2002). Telomere-binding protein TRF2 binds to and stimulates the Werner and Bloom syndrome helicases. J Biol Chem *277*, 41110-41119.

Ouellette, M. M., Aisner, D. L., Savre-Train, I., Wright, W. E., and Shay, J. W. (1999). Telomerase activity does not always imply telomere maintenance. Biochem Biophys Res Commun *254*, 795-803.

Oulton, R., and Harrington, L. (2004). A Human Telomerase-associated Nuclease. Mol Biol Cell *15*, 3244-3256.

Paeschke, K., Simonsson, T., Postberg, J., Rhodes, D., and Lipps, H. J. (2005). Telomere end-binding proteins control the formation of G-quadruplex DNA structures in vivo. Nat Struct Mol Biol *12*, 847-854.

Parkinson, G. N., Lee, M. P., and Neidle, S. (2002). Crystal structure of parallel quadruplexes from human telomeric DNA. Nature *417*, 876-880.

Peersen, O. B., Ruggles, J. A., and Schultz, S. C. (2002). Dimeric structure of the Oxytricha nova telomere end-binding protein alpha-subunit bound to ssDNA. Nat Struct Biol *9*, 182-187.

Petraccone, L., Erra, E., Esposito, V., Randazzo, A., Mayol, L., Nasti, L., Barone, G., and Giancola, C. (2004). Stability and structure of telomeric DNA sequences forming quadruplexes containing four G-tetrads with different topological arrangements. Biochemistry *43*, 4877-4884.

Phan, A. T., Modi, Y. S., and Patel, D. J. (2004). Two-repeat Tetrahymena telomeric d(TGGGGTTGGGGT) Sequence interconverts between asymmetric dimeric G-quadruplexes in solution. J Mol Biol *338*, 93-102.

Phan, A. T., and Patel, D. J. (2003). Two-repeat human telomeric d(TAGGGTTAGGGT) sequence forms interconverting parallel and antiparallel G-quadruplexes in solution: distinct topologies, thermodynamic properties, and folding/unfolding kinetics. J Am Chem Soc *125*, 15021-15027.

Pogacic, V., Dragon, F., and Filipowicz, W. (2000). Human H/ACA small nucleolar RNPs and telomerase share evolutionarily conserved proteins NHP2 and NOP10. Mol Cell Biol *20*, 9028-9040.

Prathapam, R., Witkin, K. L., O'Connor, C. M., and Collins, K. (2005). A telomerase holoenzyme protein enhances telomerase RNA assembly with telomerase reverse transcriptase. Nat Struct Mol Biol *12*, 252-257.

Prescott, J. (1994). The DNA of ciliated protozoa. Microbiol Rev *58*, 233-267.

Prescott, J., and Blackburn, E. H. (1997). Functionally interacting telomerase RNAs in the yeast telomerase complex. Genes Dev *11*, 2790-2800.

Prowse, K. R., Avilion, A. A., and Greider, C. W. (1993). Identification of a nonprocessive telomerase activity from mouse cells. Proc Natl Acad Sci U S A *90*, 1493-1497.

Raghuraman, M. K., and Cech, T. R. (1990). Effect of monovalent cation-induced telomeric DNA structure on the binding of Oxytricha telomeric protein. Nucleic Acids Res *18*, 4543-4552.

Redon, S., Bombard, S., Elizondo-Riojas, M. A., and Chottard, J. C. (2001). Platination of the (T2G4)4 telomeric sequence: a structural and cross-linking study. Biochemistry *40*, 8463-8470.

Richards, R. J., Theimer, C. A., Finger, L. D., and Feigon, J. (2006). Structure of the Tetrahymena thermophila telomerase RNA helix II template boundary element. Nucleic Acids Res *34*, 816-825.

Risitano, A., and Fox, K. R. (2003). Stability of intramolecular DNA quadruplexes: comparison with DNA duplexes. Biochemistry *42*, 6507-6513.

Rivera, M. A., and Blackburn, E. H. (2004). Processive utilization of the human telomerase template: lack of a requirement for template switching. J Biol Chem *279*, 53770-53781.

Salas, T. R., Petruseva, I., Lavrik, O., Bourdoncle, A., Mergny, J. L., Favre, A., and Saintome, C. (2006). Human replication protein A unfolds telomeric G-quadruplexes. Nucleic Acids Res *34*, 4857-4865.

Schaffitzel, C., Berger, I., Postberg, J., Hanes, J., Lipps, H. J., and Pluckthun, A. (2001). In vitro generated antibodies specific for telomeric guanine-quadruplex DNA react with Stylonychia lemnae macronuclei. Proc Natl Acad Sci U S A *98*, 8572-8577.

Schultze, P., Smith, F. W., and Feigon, J. (1994). Refined solution structure of the dimeric quadruplex formed from the Oxytricha telomeric oligonucleotide d(GGGGTTTTGGGG). Structure *2*, 221-233.

Sen, D., and Gilbert, W. (1988). Formation of parallel four-stranded complexes by guanine-rich motifs in DNA and its implications for meiosis. Nature *334*, 364-366.

Sen, D., and Gilbert, W. (1990). A sodium-potassium switch in the formation of four-stranded G4-DNA. Nature *344*, 410-414.

Seto, A. G., Zaug, A. J., Sobel, S. G., Wolin, S. L., and Cech, T. R. (1999). Saccharomyces cerevisiae telomerase is an Sm small nuclear ribonucleoprotein particle. Nature *401*, 177-180.

Sfeir, A. J., Chai, W., Shay, J. W., and Wright, W. E. (2005). Telomere-end processing the terminal nucleotides of human chromosomes. Mol Cell *18*, 131-138.

Shay, J. W., and Bacchetti, S. (1997). A survey of telomerase activity in human cancer. Eur J Cancer *33*, 787-791.

Shippen-Lentz, D., and Blackburn, E. H. (1990). Functional evidence for an RNA template in telomerase. Science *247*, 546-552.

Siddiqui-Jain, A., Grand, C. L., Bearss, D. J., and Hurley, L. H. (2002). Direct evidence for a G-quadruplex in a promoter region and its targeting with a small molecule to repress c-MYC transcription. Proc Natl Acad Sci U S A *99*, 11593-11598.

Simonsson, T. (2001). G-quadruplex DNA structures--variations on a theme. Biol Chem *382*, 621-628.

Singer, M. S., and Gottschling, D. E. (1994). TLC1: template RNA component of Saccharomyces cerevisiae telomerase. Science *266*, 404-409.

Smith, F. W., and Feigon, J. (1993). Strand orientation in the DNA quadruplex formed from the Oxytricha telomere repeat oligonucleotide d(G4T4G4) in solution. Biochemistry *32*, 8682-8692.

Smith, F. W., Schultze, P., and Feigon, J. (1995). Solution structures of unimolecular quadruplexes formed by oligonucleotides containing *Oxytricha* telomere repeats. Structure *3*, 997-1008.

Smogorzewska, A., and de Lange, T. (2004). Regulation of telomerase by telomeric proteins. Annu Rev Biochem *73*, 177-208.

Stansel, R. M., de Lange, T., and Griffith, J. D. (2001). T-loop assembly in vitro involves binding of TRF2 near the 3' telomeric overhang. EMBO J *20*, 5532-5540.

Stewart, S. A., Hahn, W. C., O'Connor, B. F., Banner, E. N., Lundberg, A. S., Modha, P., Mizuno, H., Brooks, M. W., Fleming, M., Zimonjic, D. B., *et al.* (2002). Telomerase contributes to tumorigenesis by a telomere length-independent mechanism. Proc Natl Acad Sci USA *99*, 12606-12611.

Stone, M. D., Mihalusova, M., O'Connor C, M., Prathapam, R., Collins, K., and Zhuang, X. (2007). Stepwise protein-mediated RNA folding directs assembly of telomerase ribonucleoprotein. Nature *446*, 458-461.

Sun, D., Guo, K., Rusche, J. J., and Hurley, L. H. (2005). Facilitation of a structural transition in the polypurine/polypyrimidine tract within the proximal promoter region of the human VEGF gene by the presence of potassium and G-quadruplex-interactive agents. Nucleic Acids Res *33*, 6070-6080.

Sun, H., Bennett, R. J., and Maizels, N. (1999). The Saccharomyces cerevisiae Sgs1 helicase efficiently unwinds G-G paired DNAs. Nucleic Acids Res *27*, 1978-1984.

Sun, H., Karow, J. K., Hickson, I. D., and Maizels, N. (1998). The Bloom's syndrome helicase unwinds G4 DNA. J Biol Chem *273*, 27587-27592.

Sun, H., Yabuki, A., and Maizels, N. (2001). A human nuclease specific for G4 DNA. Proc Natl Acad Sci U S A *98*, 12444-12449.

Swanton, M. T., Heumann, J. M., and Prescott, D. M. (1980). Gene-sized DNA molecules of the macronuclei in three species of hypotrichs: size distributions and absence of nicks. DNA of ciliated protozoa. VIII. Chromosoma *77*, 217-227.

Tasset, D. M., Kubik, M. F., and Steiner, W. (1997). Oligonucleotide inhibitors of human thrombin that bind distinct epitopes. J Mol Biol *272*, 688-698.

Tesmer, V. M., Ford, L. P., Holt, S. E., Frank, B. C., Yi, X., Aisner, D. L., Ouellette, M., Shay, J. W., and Wright, W. E. (1999). Two inactive fragments of the integral RNA cooperate to assemble active telomerase with the human protein catalytic subunit (hTERT) in vitro. Mol Cell Biol *19*, 6207-6216.

Tomaska, L., Makhov, A. M., Griffith, J. D., and Nosek, J. (2002). t-Loops in yeast mitochondria. Mitochondrion *1*, 455-459.

Trelles-Sticken, E., Loidl, J., and Scherthan, H. (1999). Bouquet formation in budding yeast: initiation of recombination is not required for meiotic telomere clustering. J Cell Sci *112 (Pt 5)*, 651-658.

Uddin, M. K., Kato, Y., Takagi, Y., Mikuma, T., and Taira, K. (2004). Phosphorylation at 5' end of guanosine stretches inhibits dimerization of G-quadruplexes and formation of a G-quadruplex interferes with the enzymatic activities of DNA enzymes. Nucleic Acids Res *32*, 4618-4629.

Vaughn, J. P., Creacy, S. D., Routh, E. D., Joyner-Butt, C., Jenkins, G. S., Pauli, S., Nagamine, Y., and Akman, S. A. (2005). The DEXH protein product of the DHX36 gene is the major source of tetramolecular quadruplex G4-DNA resolving activity in HeLa cell lysates. J Biol Chem *280*, 38117-38120.

Wang, H., Gilley, D., and Blackburn, E. H. (1998). A novel specificity for the primer-template pairing requirement in Tetrahymena telomerase. EMBO J *17*, 1152-1160.

Wang, L., Dean, S. R., and Shippen, D. E. (2002). Oligomerization of the telomerase reverse transcriptase from Euplotes crassus. Nucleic Acids Res *30*, 4032-4039.

Wang, Y., and Patel, D. J. (1992). Guanine residues in d(T2AG3) and d(T2G4) form parallel-stranded potassium cation stabilized G-quadruplexes with anti glycosidic torsion angles in solution. Biochemistry *31*, 8112-8119.

Wang, Y., and Patel, D. J. (1994). Solution structure of the Tetrahymena telomeric repeat d(T2G4)4 G-tetraplex. Structure *2*, 1141-1156.

Wang, Y., and Patel, D. J. (1995). Solution structure of the Oxytricha telomeric repeat d[G4(T4G4)3] G-tetraplex. J Mol Biol *251*, 76-94.

Watson, J. (1972). Origin of concatemeric T7 DNA. Nat New Biol *239*, 197-201.

Wenz, C., Enenkel, B., Amacker, M., Kelleher, C., Damm, K., and Lingner, J. (2001). Human telomerase contains two cooperating telomerase RNA molecules. EMBO J *30*, 3526-3534.

Williamson, J. (1994). G-quartet structures in telomeric DNA. Annu Rev Biophys Biomol Struct *23*, 703-730.

Williamson, J. R., Raghuraman, M. K., and Cech, T. R. (1989). Monovalent cation-induced structure of telomeric DNA: the G-quartet model. Cell *59*, 871-880.

Witkin, K. L., and Collins, K. (2004). Holoenzyme proteins required for the physiological assembly and activity of telomerase. Genes Dev *18*, 1107-1118.

Wyatt, H. D., Lobb, D. A., and Beattie, T. L. (2007). Characterization of physical and functional anchor site interactions in human telomerase. Mol Cell Biol *27*, 3226-3240.

Zahler, A. M., Williamson, J. R., Cech, T. R., and Prescott, D. M. (1991). Inhibition of telomerase by G-quartet DNA structures. Nature *350*, 718-720.

Zaug, A. J., Podell, E. R., and Cech, T. R. (2005). Human POT1 disrupts telomeric G-quadruplexes allowing telomerase extension in vitro. Proc Natl Acad Sci U S A *102*, 10864-10869.

Zhang, N., Phan, A. T., and Patel, D. J. (2005). (3 + 1) Assembly of three human telomeric repeats into an asymmetric dimeric G-quadruplex. J Am Chem Soc *127*, 17277-17285.

Zhang, Q. S., Manche, L., Xu, R. M., and Krainer, A. R. (2006). hnRNP A1 associates with telomere ends and stimulates telomerase activity. RNA *12*, 1116-1128.

Zhu, Y., Tomlinson, R. L., Lukowiak, A. A., Terns, R. M., and Terns, M. P. (2004). Telomerase RNA accumulates in Cajal bodies in human cancer cells. Mol Biol Cell *15*, 81-90.